

**NOVEL BIO-INSPIRED SHIELDING DESIGN FOR DEPLOYABLE  
MICROREACTORS**

A Dissertation  
Presented to  
The Academic Faculty

By

Helen Cosner

In Partial Fulfillment  
of the Requirements for the Degree  
Masters of Science in the  
Woodruff School of Mechanical Engineering  
Nuclear and Radiological Engineering

Georgia Institute of Technology

December 2025

© Helen Cosner 2025

**NOVEL BIO-INSPIRED SHIELDING DESIGN FOR DEPLOYABLE  
MICROREACTORS**

Thesis committee:

Dr. Bojan Petrovic  
Thesis Advisor, Nuclear and Radiological  
Engineering  
*Georgia Institute of Technology*

Dr. Eric Pooser  
Thesis Co-Advisor, Senior Research Scien-  
tist  
*Georgia Tech Research Institute*

Dr. Steven Biegalski  
Chair, Nuclear and Radiological Engineering  
and Medical Physics Program  
*Georgia Institute of Technology*

Date approved: November 7, 2025

## ACKNOWLEDGMENTS

First of all, I would like to thank John Brittingham for helping me start this thesis project. Without his guidance at the beginning of this project, including developing the project and locating funding, this thesis would not have been started. Next, I want to thank Dr. Petrovic for guiding me throughout this entire project. His endless patience through guidance and continuous feedback helped me grow as a nuclear engineer, giving me the ability to write this thesis. Then, I want to thank Eric Pooser for stepping in as my co-advisor when John had to be deployed. He gave me endless guidance to help keep me focused on the goal of this thesis, and he gave me the tools to better analyze and understand the data. I also want to thank all of my committee members, Dr. Petrovic, Eric Pooser, and Dr. Biegalski, who took time out of their busy schedules to sit on my thesis committee.

I would like to thank my family for always supporting me. From my husband always listening to me talk through my coding problems to my parents giving me the work ethic that allowed me to push through the hardest of days, I would not be here without them. I would also like to thank my lab-mates, who were always able and willing to help me with issues with understanding the SCALE code or nuclear engineering topics.

This research was supported in part by the Georgia Tech Research Institute. And this research made use of the resources of the High Performance Computing Center at Idaho National Laboratory, which is supported by the Office of Nuclear Energy of the U.S. Department of Energy and the Nuclear Science User Facilities under Contract No. DE-AC07-05ID14517 [<https://inl.gov/hpc>]

The views in this thesis are those of the author and do not reflect the official policy or position of the United States Air Force, Department of Defense, or the U.S. Government.

## TABLE OF CONTENTS

<b>Acknowledgments</b> . . . . .	iii
<b>List of Tables</b> . . . . .	vi
<b>List of Figures</b> . . . . .	vii
<b>List of Acronyms</b> . . . . .	xii
<b>Summary</b> . . . . .	xiii
<b>Chapter 1: Introduction and Background</b> . . . . .	1
1.1 Nuclear Reactor Background . . . . .	1
1.2 Microreactors and Their Applications . . . . .	3
1.3 Shielding Radiation . . . . .	4
1.4 Logistical Requirements for Rapidly Deployable Microreactor . . . . .	7
1.5 Lightweight Shielding Materials . . . . .	8
1.6 Proposed Lightweight Shielding Design . . . . .	12
<b>Chapter 2: Methodology</b> . . . . .	15
2.1 Simulation Code SCALE . . . . .	15
2.1.1 CSAS . . . . .	15
2.1.2 MAVRIC . . . . .	16

2.1.3	ORIGEN . . . . .	17
2.1.4	MAVRIC USING ORIGEN GENERATED SOURCES . . . . .	17
2.2	Strength Calculation . . . . .	18
2.3	Weight Calculation . . . . .	18
2.4	Cost Calculation . . . . .	19
2.5	Optimization Approach . . . . .	19
<b>Chapter 3: Results and Discussion . . . . .</b>		<b>21</b>
3.1	Strength Calculations . . . . .	21
3.2	Radiation Calculations . . . . .	22
3.2.1	SCALE Simulation . . . . .	22
3.2.2	Radioisotopes Investigation . . . . .	33
3.2.3	High Energy Emitting Isotope Doped Soil . . . . .	40
3.2.4	Radioisotope Decay Paths . . . . .	46
3.3	Weight and Cost . . . . .	50
3.4	Decision Matrix . . . . .	51
<b>Chapter 4: Conclusion . . . . .</b>		<b>55</b>
<b>Appendices . . . . .</b>		<b>58</b>
Appendix A: Additional Plots . . . . .		59
References . . . . .		75

## LIST OF TABLES

2.1	List of costs for each material . . . . .	19
2.2	List of all shielding materials, structural materials, and basemat depths to be tested for design optimization. . . . .	20
3.1	Comparison of ultimate compressive strengths and factor of safety for each structural material. . . . .	21
3.2	List of material combinations and their respective smallest thickness that meets the NRC dose standard from 0 cm above the ground. . . . .	30
3.3	Compilation of half-life, decay mode, and the gamma rays for radioisotopes of interest. . . . .	36
3.4	List of weights for each basemat combination. . . . .	50
3.5	Total material cost for each basemat combination. . . . .	50
3.6	Decision matrix to determine the optimum material combination and basemat thickness. The shortened names are concrete (con), water (H <sub>2</sub> O), and borated polyethylene (BPE). . . . .	53

## LIST OF FIGURES

1.1	Diagram of a PWR [1] . . . . .	2
1.2	Example of proposed transportation methods for microreactors [3] . . . . .	3
1.3	Comparison of dose rates in millirem from various sources [12]. . . . .	5
1.4	Comparison of Different Radiation Interactions with Different Materials [14] . . . . .	6
1.5	Basemat individual unit design. . . . .	13
1.6	Basemat assembly design from top view. . . . .	13
1.7	Example of full simulation model with 4-foot thick basemat from side and front view. . . . .	14
2.1	Overall workflow for SCALE simulation. . . . .	16
3.1	Energy versus neutron flux plot for the 2-foot thick basemat separated by shielding material, and comparing the shielding material and its paired structural material. . . . .	23
3.2	Energy versus neutron flux plot for the 4.5-foot thick basemat separated by shielding material, and comparing the shielding material and its paired structural material. . . . .	24
3.3	Dose rate 1 year after the reactor and 2-foot basemat have been removed, separated by shielding material, and comparing the shielding material and its paired structural material. . . . .	26
3.4	Dose rate 1 year after the reactor and 3-foot basemat have been removed, separated by shielding material, and comparing the shielding material and its paired structural material. . . . .	27

3.5	Dose rate 1 year after the reactor and 4-foot basemat have been removed, separated by shielding material, and comparing the shielding material and its paired structural material. . . . .	28
3.6	Dose rate 1 year after the reactor and 4.5-foot basemat have been removed, separated by shielding material, and comparing the shielding material and its paired structural material. . . . .	29
3.7	Dose rate 1 year after the reactor and 5-foot basemat have been removed, separated by shielding material, and comparing the shielding material and its paired structural material. . . . .	29
3.8	Dose rate 1 year after the reactor and 5.5-foot basemat have been removed, separated by shielding material, and comparing the shielding material and its paired structural material. . . . .	30
3.9	Dose Rates at 1 meter above the soil in the center of the model from different times after the reactor and basemat were removed. . . . .	32
3.10	Top contributing radioisotopes to the dose rate from the 2-foot thick HDPE and water simulation over the time the reactor was running, to after the reactor and basemat were removed (where the negative days represent when the reactor was running)in Becquerels. Total represents the total decay rate of all isotopes. . . . .	34
3.11	Top contributing radioisotopes to the dose rate from the 2-foot thick HDPE and water simulation over the time the reactor was running, to after the reactor and basemat were removed (where the negative days represent when the reactor was running)in Gamma-Watts. Total represents the total decay rate of all isotopes. . . . .	35
3.12	Top radioisotopes by activity from the 2-foot thick concrete and water simulation over the time the reactor was running to after the reactor and basemat were removed (where the negative days represent when the reactor was running) in Bq. . . . .	38
3.13	Top contributing radioisotopes to the dose rate from the 2-foot thick concrete and water simulation over the time the reactor was running to after the reactor and basemat were removed (where the negative days represent when the reactor was running) in gamma-Watts. . . . .	39
3.14	Comparison of dose rates of U.S. average soil, soil dosed with 2 ppm of Eu, and soil dosed with 40 ppm of Co 1 year after the reactor and basemat have been removed. Shielding was a 2-foot thick basemat with HDPE and borated polythene. . . . .	41

3.15	Comparison of dose rates measured 1 meter above the ground of U.S. average soil, soil dosed with 2 ppm of Eu, and soil dosed with 40 ppm of Co over how long the reactor and basemat have been removed. Shielding was a 2-foot thick basemat with HDPE and borated polythene. . . . .	42
3.16	Top radioisotopes by activity from the europium-doped soil using 2-foot thick HDPE and borated polyethylene simulation over the time the reactor was running, to after the reactor and basemat were removed (where the negative days represent when the reactor was running) in Becquerels. Total represents the total decay rate of all isotopes. . . . .	43
3.17	Top contributing isotopes to the dose rate from the europium-doped soil using 2-foot thick HDPE and borated polyethylene simulation over the time the reactor was running, to after the reactor and basemat were removed (where the negative days represent when the reactor was running) in Gamma-Watts. Total represents the total decay rate of all isotopes. . . . .	44
3.18	Top contributing isotopes to the dose rate from the 2-foot thick cobalt-doped soil using HDPE and borated polyethylene simulation over the time the reactor was running, to after the reactor and basemat were removed (where the negative days represent when the reactor was running) in Becquerels. Total represents the total decay rate of all isotopes. . . . .	45
3.19	Top contributing isotopes to the dose rate from the 2-foot thick cobalt-doped soil using HDPE and borated polyethylene simulation over the time the reactor was running, to after the reactor and basemat were removed (where the negative days represent when the reactor was running) in Gamma-Watts. Total represents the total decay rate of all isotopes. . . . .	46
3.20	Decay path for sodium and aluminum based on the chart of nuclides [44]. . . . .	47
3.21	Decay path for iron, manganese, and cobalt based on the chart of nuclides [44]. . . . .	48
3.22	Decay path for europium based on the chart of nuclides [44]. . . . .	49
A.1	Energy versus neutron flux plot for the 3-foot thick basemat separated by shielding material, and comparing the shielding material and its paired structural material. . . . .	59
A.2	Energy versus neutron flux plot for the 4-foot thick basemat separated by shielding material, and comparing the shielding material and its paired structural material. . . . .	60

A.3	Energy versus neutron flux plot for the 5-foot thick basemat separated by shielding material, and comparing the shielding material and its paired structural material. . . . .	61
A.4	Energy versus neutron flux plot for the 5.5-foot thick basemat separated by shielding material, and comparing the shielding material and its paired structural material. . . . .	62
A.5	Top contributing isotopes to the dose rate from U.S. average soil using 2-feet of HDPE and borated polyethylene simulation over the time the reactor was running to after the reactor and basemat were removed (where the negative days represent when the reactor was running) in Becquerels. Total represents the total decay rate of all isotopes. . . . .	63
A.6	Top contributing isotopes to the dose rate from U.S. average soil using 2-feet of HDPE and borated polyethylene simulation over the time the reactor was running to after the reactor and basemat were removed (where the negative days represent when the reactor was running) in Gamma-Watts. Total represents the total decay rate of all isotopes. . . . .	64
A.7	Top contributing isotopes to the dose rate from U.S. average soil using 2-feet of concrete and borated polyethylene simulation over the time the reactor was running to after the reactor and basemat were removed (where the negative days represent when the reactor was running) in Becquerels. Total represents the total decay rate of all isotopes. . . . .	65
A.8	Top contributing isotopes to the dose rate from U.S. average soil using 2-feet of concrete and borated polyethylene simulation over the time the reactor was running to after the reactor and basemat were removed (where the negative days represent when the reactor was running) in Gamma-Watts. Total represents the total decay rate of all isotopes. . . . .	66
A.9	Top contributing isotopes to the dose rate from U.S. average soil using 2-feet of HDPE and concrete simulation over the time the reactor was running to after the reactor and basemat were removed (where the negative days represent when the reactor was running) in Becquerels. Total represents the total decay rate of all isotopes. . . . .	67
A.10	Top contributing isotopes to the dose rate from U.S. average soil using 2-feet of HDPE and concrete simulation over the time the reactor was running to after the reactor and basemat were removed (where the negative days represent when the reactor was running) in Gamma-Watts. Total represents the total decay rate of all isotopes. . . . .	68

A.11 Top contributing isotopes to the dose rate from U.S. average soil using 3-foot of concrete and concrete simulation over the time the reactor was running to after the reactor and basemat were removed (where the negative days represent when the reactor was running) in Becquerels. Total represents the total decay rate of all isotopes. . . . .	69
A.12 Top contributing isotopes to the dose rate from U.S. average soil using 3-foot of concrete and concrete simulation over the time the reactor was running to after the reactor and basemat were removed (where the negative days represent when the reactor was running) in Gamma-Watts. Total represents the total decay rate of all isotopes. . . . .	70
A.13 Top contributing isotopes to the dose rate from U.S. average soil using 2-foot of HDPE and WEP simulation over the time the reactor was running to after the reactor and basemat were removed (where the negative days represent when the reactor was running) in Becquerels. Total represents the total decay rate of all isotopes. . . . .	71
A.14 Top contributing isotopes to the dose rate from U.S. average soil using 2-foot of HDPE and WEP simulation over the time the reactor was running to after the reactor and basemat were removed (where the negative days represent when the reactor was running) in Gamma-Watts. Total represents the total decay rate of all isotopes. . . . .	72
A.15 Top contributing isotopes to the dose rate from U.S. average soil using 3-foot of concrete and WEP simulation over the time the reactor was running to after the reactor and basemat were removed (where the negative days represent when the reactor was running) in Becquerels. Total represents the total decay rate of all isotopes. . . . .	73
A.16 Top contributing isotopes to the dose rate from U.S. average soil using 3-foot of concrete and WEP simulation over the time the reactor was running to after the reactor and basemat were removed (where the negative days represent when the reactor was running) in Gamma-Watts. Total represents the total decay rate of all isotopes. . . . .	74

## **LIST OF ACRONYMS**

**ALARA** As Low as Reasonably Achievable

**Bq** Becquerels

**CSAS** Criticality Safety Analysis Sequences

**HALEU** High-Assay Low Enriched Uranium

**HDPE** High-Density Polyethylene

**LEU** Low Enriched Uranium

**MAVRIC** Monaco with Automated Variance Reduction using Importance Calculations

**NGSC** Nuclear-Grade Sandwich Composites

**NRC** U.S. Nuclear Regulatory Commission

**ORIGEN** Oak Ridge Isotope Generation

**PWR** Pressurized Water Reactor

**SCALE** Standardized Computer Analysis for Licensing Evaluation

**SMR** Small Modular Reactor

**WEP** Water Extended Polyester

## SUMMARY

Rapidly deployable microreactors are being considered as an effective approach to supplying power post-disaster. Concerns for rapid deployment arise when a flat, structurally adequate surface is not guaranteed. Moreover, environmental concerns are propagated when the risk of radiation exposure from nuclear energy is involved. This paper proposes a novel multifunctional design, referred to as basemat, that provides a level operating surface for a deployed reactor by capitalizing on lightweight shielding and high-strength-to-weight materials, at the same time providing shielding and reducing soil activation. This work considers a 5MWe rapidly deployable microreactor that will operate for one year and then be transported elsewhere. The objective is to reduce the radiation exposure to the soil underneath to the point where access control or additional shielding is not required after the reactor and basemat are removed after their cool-down period. The design was optimized using different materials and overall thickness. Each variation was evaluated for its ability to shield the soil underneath the reactor from activation, limiting the activation resulting dose rate, and its ability to hold the weight of a deployed microreactor. The shielding performance was simulated using the SCALE code package in a complex multi-step coupled analysis. The strength of the design was determined through simple compression strength calculations. From the simulation, the best-performing material combinations for radiation shielding are High Density Polyethylene (HDPE) and borated polyethylene, as well as HDPE and water, with a basemat thickness of 2 feet. These materials are capable of limiting the dose rate in the air to the United States Nuclear Regulatory Commission (NRC) yearly dose standards for the general population, while conservatively assuming someone is receiving the dose 24/7 for an entire year. Overall, the basemat design composed of lightweight shielding materials, such as water, HDPE, and borated polyethylene, is an effective solution for limiting the activation of the soil underneath a deployed microreactor, resulting in an overall dose that meets NRC standards, assuming continuous exposure.

# CHAPTER 1

## INTRODUCTION AND BACKGROUND

### 1.1 Nuclear Reactor Background

Nuclear reactors are a way of supplying consistent, clean energy on a large scale. All current reactors rely on a process of fission, a process in which heavy nuclei are split into lighter nuclei. In nuclear reactors, uranium-235 is the typical initial fissile material. Uranium-235 occurs naturally in 0.7% of uranium; thus, it is enriched to allow for the fission reaction chain to be maintained. Commercial nuclear reactors in the U.S. are limited to using uranium-235 enriched to 5% (so called low enriched uranium Low Enriched Uranium (LEU)), which is commercially available. The established limit for civilian use is 20%, and most advanced nuclear reactor designs explore using up to 20% (so-called high-assay low-enriched uranium, or High-Assay Low Enriched Uranium (HALEU)). With every split atom, energy is produced to make up for the loss of mass in the form of heat, which may then be converted into electricity, used for water desalination, or district heating. Various reactor designs use different methods to harness the heat. Most (about two-thirds) of the commercial reactors in the U.S. are the Pressurized Water Reactor (PWR). PWRs use water as the working fluid. Water in the primary loop is heated directly by fission occurring in the fuel rods and transfers the heat to the secondary loop. The steam from the second loop powers a turbine to power a generator [1]. Figure 1.1 shows what a typical PWR looks like.

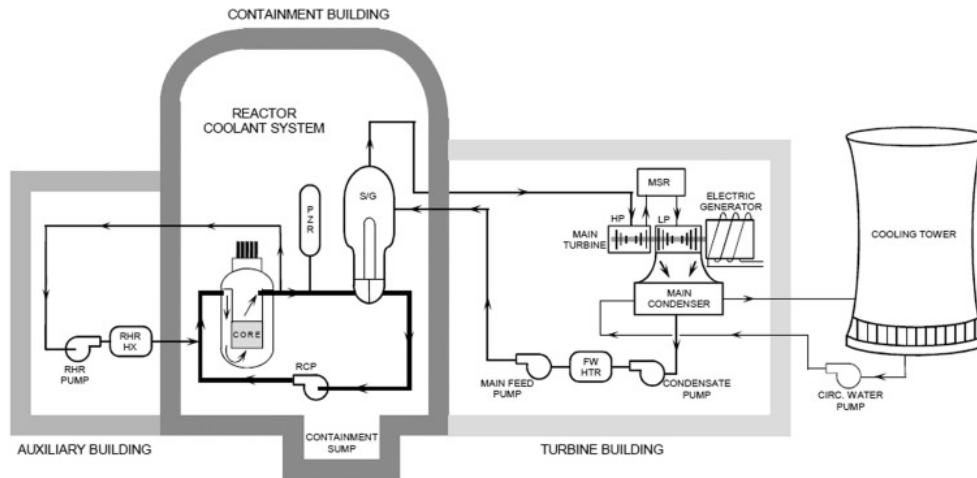
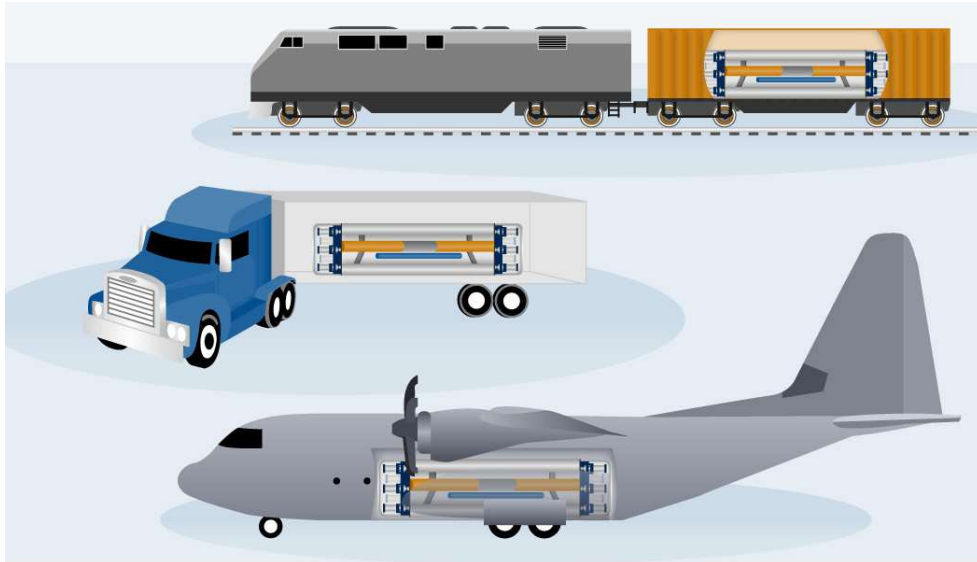


Figure 1.1: Diagram of a PWR [1]

Nuclear reactors are traditionally classified into three different categories based on their power output: Large power reactors, Small Modular Reactor (SMR), and microreactors. Large reactors produce more than 300 MW of electric energy (MWe), SMRs produce between 20 and 300 MWe. The cutoff between the SMRs and microreactors is sometimes set as high as 50 MWe; however, for the purpose of this paper, microreactors are defined to produce no more than 20 MW of thermal energy. SMRs have become popular due to their smaller size and their capability to be mass-constructed in a factory. Many have recognized the U.S.'s efficiency in factory assemblies over on-site construction, making SMRs the focus for future reactor development within the U.S [2].

Like SMRs, microreactors have garnered interest due to their small size and factory assembly, as well as transportability. Microreactors are intended to fit in a standard 20-foot shipping container, which could then be transported by train, truck, or plane, as shown in Figure 1.2. An easily transportable reactor opens up many remote applications.



Source: GAO. | GAO-20-380SP

Figure 1.2: Example of proposed transportation methods for microreactors [3]

Microreactors approach energy generation similarly to conventional large power reactors, like PWRs. Many proposed microreactor designs use the heat produced from fission to boil water and have the steam power a generator. To reduce the size, advanced reactor technologies, including cooling, heat transfer, and other technologies to maintain a nuclear reaction on a smaller scale, are being explored. Some of the advanced technologies include liquid metal, molten salt, or high temperature gas reactors, and using HALEU fuel [3]. The status of microreactor designs varies depending on the design; one of the more mature designs is the eVinci by Westinghouse. This microreactor uses heat pipes instead of a reactor coolant system to allow for a smaller overall size [4].

## 1.2 Microreactors and Their Applications

The transportability of microreactors is one of their strongest advantages, enabling applications such as powering remote locations. Remote locations typically ship diesel fuel to power generators. Consistent diesel fuel requires a significant amount of time and money, whereas a deployed microreactor can supply consistent, carbon-free energy for years before

needing to be refueled [5].

Another application for microreactors is in the recovery from natural disasters. In the U.S., 57% of infrastructure is in hazard hot spots susceptible to catastrophic events, such as hurricanes, wildfires, and tornadoes [6]. Damage to critical infrastructure from natural phenomena or hostile actions poses a significant national security risk. The duration of response times directly correlates with increased security risks. Consequently, microreactors have garnered attention due to their versatile nature and capacity to supply stable power rapidly. A 20 megawatt thermal (5 MWe) microreactor can supply a maximum of 120,000 kWh per day. The average inpatient hospital consumes 20,822 kWh per day [7]. Therefore, a microreactor exceeds the power demands of a hospital, allowing it to support other critical infrastructure, such as communication and water sectors, while emitting no carbon. Beyond power generation, the heat produced by the microreactor can be utilized for desalination, water purification, and hydrogen production [8]. With these potential applications in disaster relief, Congress recognizes the strategic relevance of rapidly deployable microreactors in the National Strategy to Utilize Microreactors for Natural Disaster Response Efforts Act, as well as ongoing research by various companies into deployable microreactors [9].

### **1.3 Shielding Radiation**

One of the most important concerns for any reactor is limiting radiation exposure to humans and the surrounding environment. Radiation is the energy emitted by a particle that, with enough energy, referred to as ionizing radiation, can break molecular bonds or displace electrons in an atom. The change in bonds and atoms is why unintentional radiation exposure is harmful to humans and the environment [10].

The amount of radiation one is exposed to is referred to as the dose. For any nuclear reactor, the goal is to limit the overall dose to As Low as Reasonably Achievable (ALARA). On top of the ALARA requirement, there are specified permissible dose rates and annual doses for the public by the U.S. Nuclear Regulatory Commission (NRC). The NRC states

that the total effective dose equivalent for the public must not exceed 0.1 rem in a year in both unrestricted and controlled areas, exclusive of natural dose. Additionally, in unrestricted areas, the dose rate must be less than 0.002 rem per hour [11]. To get a better understanding of dose rates, the NRC compiled different radiation exposures and the dose amount in millirem (1e-3 rem), shown in Figure 1.3.

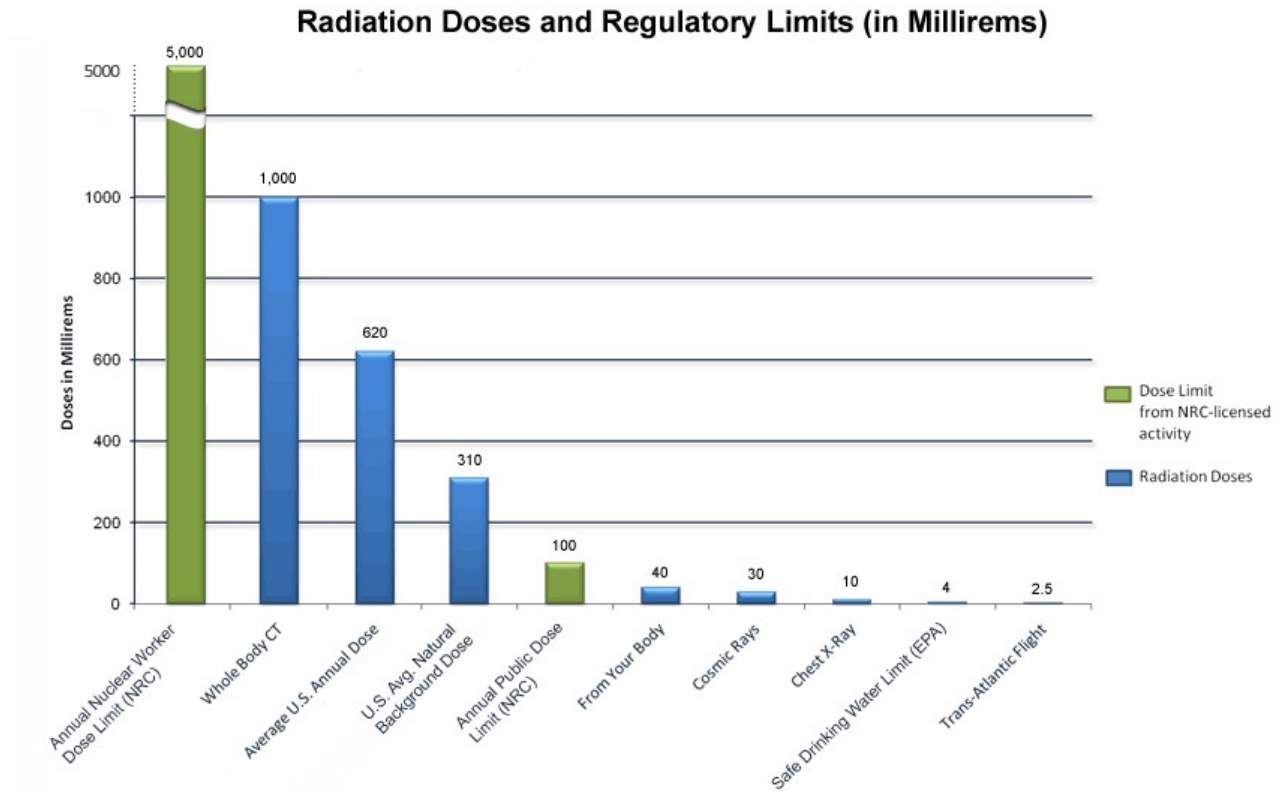


Figure 1.3: Comparison of dose rates in millirem from various sources [12].

There are four types of ionizing radiation: alpha, beta, gamma, and neutron radiation, each posing distinct hazards depending on the interaction. Alpha radiation occurs when a helium-4 nucleus is produced as a result of decay with an energy typically between 4 and 5 MeV. Beta radiation occurs when a neutron-rich nuclide decays and emits a beta particle from the nucleus. The beta particle is either negative or positive, depending on the type of decay. Gamma radiation is a result of a gamma photon being released from a nucleus in an excited state. Neutron radiation results from neutrons produced during fission. In a reactor setup, neutron radiation is the primary source of inducing radioactivity in other materials,

a process known as neutron activation. Each type of radiation has a specified penetration distance and specified materials it can be stopped by, as shown in Figure 1.4 [13]. These characteristics determine the shielding measures that need to be taken.

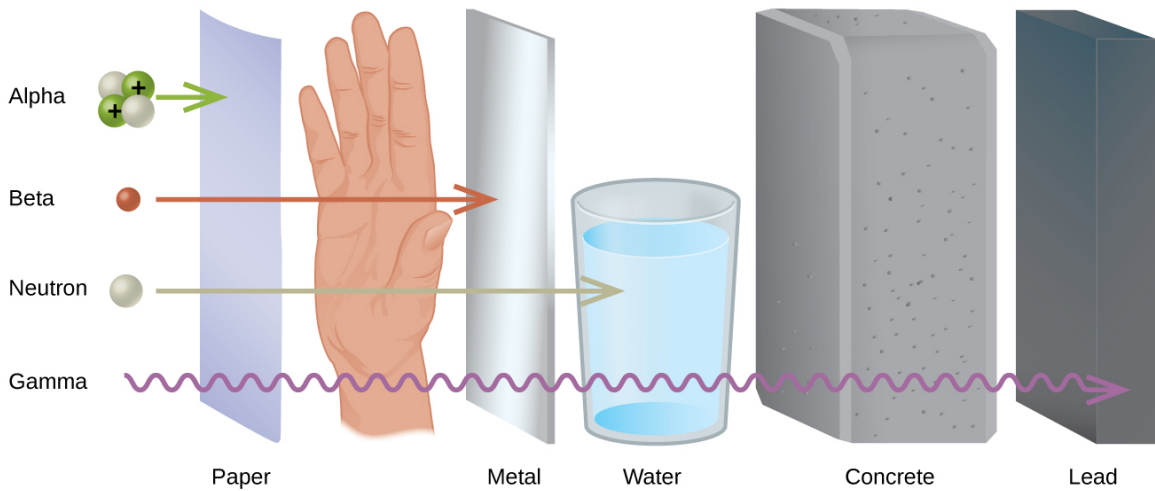


Figure 1.4: Comparison of Different Radiation Interactions with Different Materials [14]

Nuclear reactors could expose humans and the surrounding environment to external radiation. Because a thin layer of material stops alpha and beta radiation, only gamma and neutron radiation are concerns for shielding nuclear reactors. Radiation shielding incorporates time, shielding, and distance. Time relies on limiting exposure to radioactive material. Time is not an effective long-term solution, as the radioactive material can have long half-lives, ranging from thousands of years to more. The exposed area would also be quarantined for thousands of years. Distance is more reasonable, as the further one is from the source, the lower the dose one receives. Finally, shielding effectiveness depends on the shielding material, its density, and the energy of the radiation [15]. Traditional shielding designs employ materials with low atomic numbers to moderate neutrons and materials with high atomic numbers to attenuate gamma radiation. Neutron moderation refers to slowing down neutrons to thermal energy levels, thereby greatly increasing the probability of neutron absorption. The more neutrons absorbed, the better the shield [16]. Attenuation also increases in efficiency with an increase in density. Overall, a reactor is encased

by multiple layers of different shielding materials to absorb neutrons and attenuate gamma radiation.

Popular shielding materials for reactors include lead and concrete. Lead is effective at shielding, but it is costly and a toxic material to humans. Concrete is at least twice as dense as water, affordable in large quantities, and durable. And, when reinforced, concrete can bear more loads and withstand unexpected forces from natural disasters. Typical concrete used for radiation shielding consists of cement, water, and heavyweight aggregates. The cement and heavyweight aggregates attenuate the gamma photons, and the water moderates the neutrons. Studies have investigated the optimum water-to-cement ratio. When gamma radiation is the concern, a lower water-to-cement ratio is better, where a ratio of 0.38 is optimal [15]. Concrete is capable of shielding neutron and gamma radiation, demonstrating why it is so commonly used. While concrete works well for large reactors and SMRs, it contradicts the logistical requirements for rapidly deployable microreactors. This paper will explore the logistical requirements and provide a potential solution to the shielding problem.

#### **1.4 Logistical Requirements for Rapidly Deployable Microreactor**

For microreactors to serve as an effective post-disaster response unit, they must be easily deployable and incorporate adequate shielding to limit the radiological impact on the environment and humans. Deploying a microreactor entails transporting it to the site, installing the shielding, installing the reactor, and running it. Once the mission is over, the reactor is transported elsewhere. On-site, minimal installation of the reactor and the radiation shield should be required to reduce the setup timeline. Moreover, the deployed reactor must operate on a level surface, which is not guaranteed in an austere environment.

If concrete is used for radiation shielding, much of the response time and effort would be spent pouring and waiting for the layers of concrete to dry. Concrete takes at least 28 days to cure fully, after which it can support the weight of the reactor to provide the level

surface it needs to operate [17]. For post-disaster response, a month-long waiting period is entirely too long. Furthermore, concrete is difficult to work with. Ensuring the concrete is mixed correctly and poured accurately to provide a level surface on top of acting as a neutron shield introduces the risk of having to start over. An error in making the concrete shield would be detrimental to the installation timeline. Then, when the reactor is no longer needed and is moved, the irradiated concrete pad is left to be dealt with. Overall standard shielding materials contradict the logistical requirement for rapidly deploying microreactors, furthering the need for alternative shielding designs.

This thesis proposes a new shielding design that uses lightweight shielding materials that can be shipped along with the deployed microreactor. Instead of pouring concrete, the lightweight shielding apparatus is already built and just needs assembly on-site, overcoming the time issue of waiting for concrete to cure. Lightweight materials like water, borated polyethylene, and water-extended polyester can be transported more easily than concrete, as the lightweight materials are approximately half as dense as concrete. The maximum weight a standard 20-foot shipping container can hold, excluding the weight of the container, is around 21,700 kilograms. To transport alongside the microreactor, lightweight shielding materials meet the logistical requirements, and this thesis will investigate whether they meet the shielding requirements. This paper will delve into the effectiveness (in shielding ability, cost, and transportability) of various lightweight shielding materials specifically for use with rapidly deployable microreactors. Specifically, this paper focuses on reducing the activation of the soil underneath the reactor and the dose rate after the reactor and shielding have been removed. This paper does not address the shielding required for operation to reduce the dose exposure in directions beyond directly below the reactor.

## **1.5 Lightweight Shielding Materials**

Lightweight shielding materials often consist of materials with low atomic numbers, which are effective at moderating neutrons. To shield from gamma radiation, a material with a

higher atomic number is typically incorporated within the lightweight shielding design. For example, Nuclear-Grade Sandwich Composites (NGSC) are a composition of six stainless steel layers that are filled with neutron and gamma ray attenuating pellets. With the stainless steel, boron carbide was used as the low atomic number material, and tungsten tetraboride as the high atomic number material. These layers are wrapped around the reactor to act as both a pressure vessel and a radiation shield. The optimal design incorporated tungsten boride as the first couple of layers, closest to the reactor, followed by boron carbide. And, the maximum projected linear mass for this shield is  $\sim 89$  kg/cm [18]. The NGSC design was further optimized to minimize cost and the total neutron flux during operation and at the end of the microreactor's life. The optimization model included a monolithic concrete shield with a thickness of 60 cm to obtain a realistic engineering solution. The cost is driven by the number of layers of tungsten tetraboride (350 to 450 K\$/cm), which also contributes to the total neutron flux. The NGSC design is capable of reducing the dose during transport of the reactor to acceptable levels and reducing the activation of the soil below the reactor [19]. While the NGSC is a strong solution for microreactor shielding, it only investigated one combination of shielding materials, mostly relies on heavy-weight shielding, and does not address the issue of supplying a level surface area for the reactor. This paper proposes a shielding design that acts as the level surface and a radiation shield referred to as a basemat. Because the NGSC relies heavily on tungsten-tetraboride for shielding, the materials in the NGSC will not be considered for lightweight shielding materials in the basemat design.

Similar to the NGSC, tungsten carbide was explored to find a good compromise between weight and absorption, specifically for obtaining the permissible radiation dose rate for transportation after a reactor has been shut down. Carbon in tungsten carbide nuclide contributes to its moderation of fast neutrons, making it effective at shielding gamma and neutron radiation. While it was proven that tungsten carbide is a good alternative shielding material, its use is constrained by its high cost and limited amounts in large quantities [20]. The basemat design will require enough tungsten carbide to cover at least a 25-foot by 10-

foot area. The amount of tungsten carbide required to cover this area would be too costly, so it will not be considered for this paper.

Space reactor systems also require lightweight radiation shields. Research was conducted to determine which neutron attenuating material is optimal based on weight and shielding ability. In this case, the shields must maintain the dose to less than 5 rem per year. For the model, all lightweight shielding materials included a layer of tungsten, which was also varied in thickness for weight optimization. The lightweight shielding materials considered were water, borated water, lithium hydride, boron carbide, zirconium hydride, beryllium, and beryllium with 2% of boron 10. Of the materials tested, the best performing neutron dose attenuators from lightest to heaviest are: lithium hydride, water, borated water, and boron carbide. The most effective gamma radiation shielding materials from lightest to heaviest are: zirconium hydride, boron carbide, and beryllium, with 2% or boron. The zirconium hydride was so effective at gamma attenuation that it did not require a tungsten layer; however, it is too heavy and will not be considered. The borated materials were better at attenuating neutron and gamma radiation. For example, boron carbide was a strong attenuator of neutrons while also being one of the better shields for gamma dose. The borated materials required less tungsten but required more mass to meet the dose requirement, increasing by no more than 1000 kg [21]. In perspective of the maximum weight a shipping container can carry, it is an acceptable sacrifice to lower cost by utilizing less tungsten. Therefore, the basemat design will explore the utilization of water and hydrogenous and borated materials.

Composites are another viable avenue for shielding, as they can help maximize radiation shielding and minimize weight while maintaining a high compressive strength. Composites are lighter than traditional metals and can be used as a structural material [22]. Beyond their high strength-to-weight ratio, composites can combine light and heavy-weight elements to handle neutron and gamma radiation. For example, borated polyethylene combines boron, which is effective at shielding gamma radiation, and hydrogen from polyethy-

lene attenuates the neutrons [23]. One research investigated High-Density Polyethylene (HDPE), borated HDPE (by weight 30% boron carbide 70% HDPE), and borated HDPE that used samarium oxide fillers (by weight 10% samarium oxide, 20% boron carbide, and 70% HDPE). The densest material was the samarium oxide borated HDPE, at  $1.209 \text{ g/cm}^3$ , and the lightest was the HDPE at  $0.936 \text{ g/cm}^3$ . The samarium oxide micron plate was the best at shielding neutron and gamma radiation, with the borated polyethylene not far behind. To shield 95% of a californium-252 neutron source, the samarium oxide shield needed a thickness of 11.5 cm, the borated HDPE shield needed 12.9 cm, and the HDPE shield needed 15.3 cm. To shield 65% of a cesium-137 gamma source, the samarium oxide shield needed a thickness of 12 cm, the borated HDPE shield needed 13.4 cm, and the HDPE shield needed 15.4 cm [24]. All three materials are lightweight and are effective at shielding. Samarium oxide performed the best, but the other materials catch up with an increase in the thickness of the shield by a few centimeters. The cost of a more complex composite, like the samarium oxide borated HDPE, will likely increase the overall cost of a shielding design, especially for the basemat that aims to be slightly larger than the base of a 20-foot shipping container. Therefore, to keep costs down by using a simpler composite, only HDPE and borated HDPE will be considered for the basemat design.

One other polymer of interest is Water Extended Polyester (WEP). WEP consists of polyester resin and 65-70% by weight water and has an average density of  $1.1 \text{ g/cm}^3$ . In performance modeling, WEP encased the source and was studied as a single piece. The WEP model, when compared to a water shield model, performed better at shielding neutrons in terms of dose. When compared to the baseline case of no shielding, the WEP model reduces the dose by a factor of 3001, while the water shield reduces the dose by a factor of 2309 [25]. WEP is a great lightweight neutron shielding material, which is why it is considered for the basemat design.

The number of lightweight shielding materials is continuing to grow, making it difficult to account for every material in the optimization process for the basemat design. This thesis

briefly mentions a few materials it is considering or excluding. This list is not holistic to stay within a reasonable number of testing materials; only a few will be considered in the analyses. In the future, further research should be conducted utilizing other lightweight shielding materials not mentioned.

## **1.6 Proposed Lightweight Shielding Design**

For this thesis, a lightweight shielding apparatus, referred to as the basemat, was developed and optimized with different thicknesses and lightweight shielding materials. The primary requirement for the basemat is to be durable and transportable. The primary objective is to shield the environment underneath from neutrons. By shielding neutrons, there will be less activation in the soil, resulting in a lower dose rate in the air, once the reactor and the basemat are removed. A multifunctional design was approached to provide a shielding and a level operating surface. Inspiration was taken from plant xylem, which provides structural support while allowing for the storage or transport of a fluid. This direction resulted in a hexagonal mesh within a hexagon, which is repeated and arranged into the shape of a rectangular prism. The hexagonal mesh allows for two different materials, one for structural support and one for radiation shielding. The structural materials that will be investigated are HDPE and aluminum. The shielding materials that will be investigated are water, borated polyethylene, and WEP. The hexagonal shape provides structural stability in the rectangular prism to external forces beyond the reactor's weight. To maximize the shielding ability of the basemat, the shielding-material-to-structural-material ratio is 2:1. Figure 1.5 shows an individual hexagonal unit, and Figure 1.6 shows the basemat assembly as a rectangular prism.

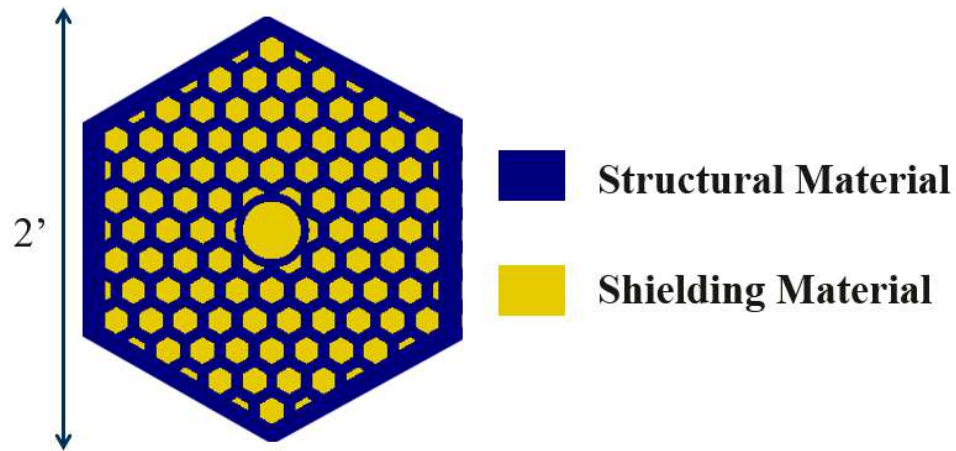


Figure 1.5: Basemat individual unit design.

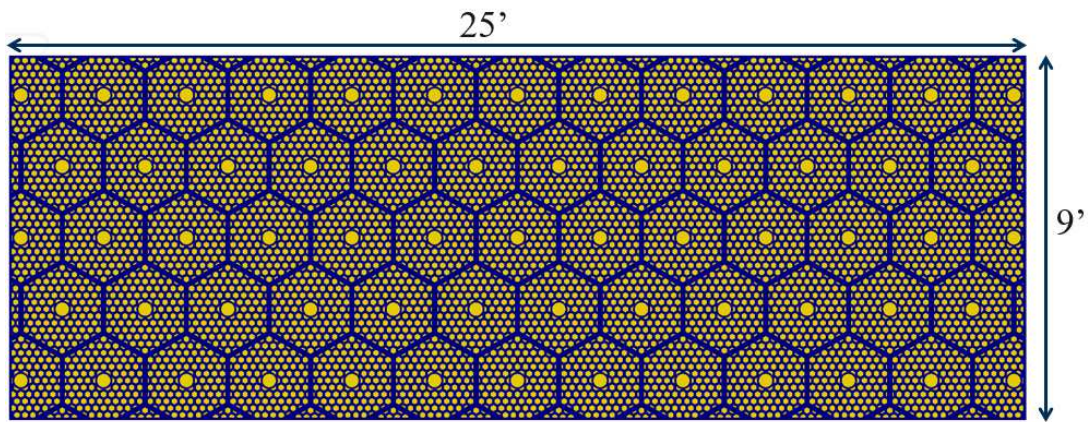


Figure 1.6: Basemat assembly design from top view.

A simplified reactor model was developed and utilized to assess the shielding performance of the basemat. The reactor is represented as a single homogenized cylindrical region (composed of, by volume, 90% graphite, 5% UO<sub>2</sub> with uranium enriched to 15%, and 5% helium), surrounded by a graphite reflector and a stainless-steel shell. Because only the leakage radiation is relevant, not its internal detailed distribution, the reactor core was simplified to a single region. The reactor was placed in a standard 20-foot container made of corten steel and is surrounded by air. Finally, underneath the basemat is 10 feet of the average composition of U.S. soil [26]. For the dose rate calculations, the soil was

sliced into 50 sections of the same composition. An example of full model geometry with a 4-foot thick basemat can be seen in Figure 1.7.

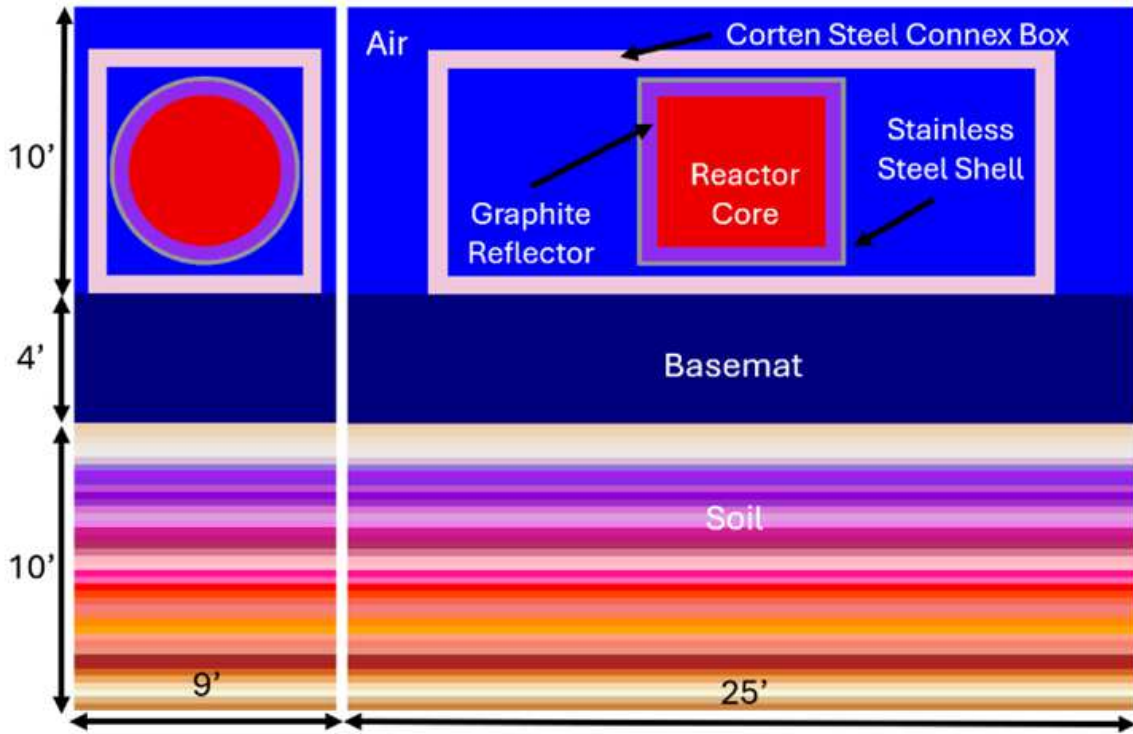


Figure 1.7: Example of full simulation model with 4-foot thick basemat from side and front view.

## CHAPTER 2

### METHODOLOGY

#### 2.1 Simulation Code SCALE

To determine how well each material combination and depth performed as a radiation shield, a sophisticated modeling tool was required. The Standardized Computer Analysis for Licensing Evaluation (SCALE) is a code developed by the Oak Ridge National Laboratory. SCALE is comprised of various verified and validated tools that are widely used for modeling and simulating multiple scenarios involving nuclear reactors. SCALE is capable of using deterministic and Monte Carlo solvers for the radiation transport equation [27]. The basemat shielding simulation used SCALE version 6.3.1. The three main tools within SCALE used were: Criticality Safety Analysis Sequences (CSAS), Monaco with Automated Variance Reduction using Importance Calculations (MAVRIC), and Oak Ridge Isotope Generation (ORIGEN). Using these modules, a series of six steps was followed to assess the effectiveness of each basemat material combination and overall thickness. The workflow followed is illustrated in Figure 2.1.

##### 2.1.1 CSAS

CSAS is used to solve criticality, the state in which fission is sustained within the reactor, primarily through Monte Carlo methods [27]. The fission source for the simplified reactor core was generated using 550 generations, with the first 50 generations skipped and 1,000,000 neutrons per generation, resulting in a total of 500 million active particle histories. The 500 million active particle histories are used in an eigenvalue calculation to determine the multiplication factor ( $k$ -eff), assessing whether the reactor has reached criticality. The  $k$ -eff for the reactor for the simulation was  $1.104354 \pm 0.000045$ . The fission

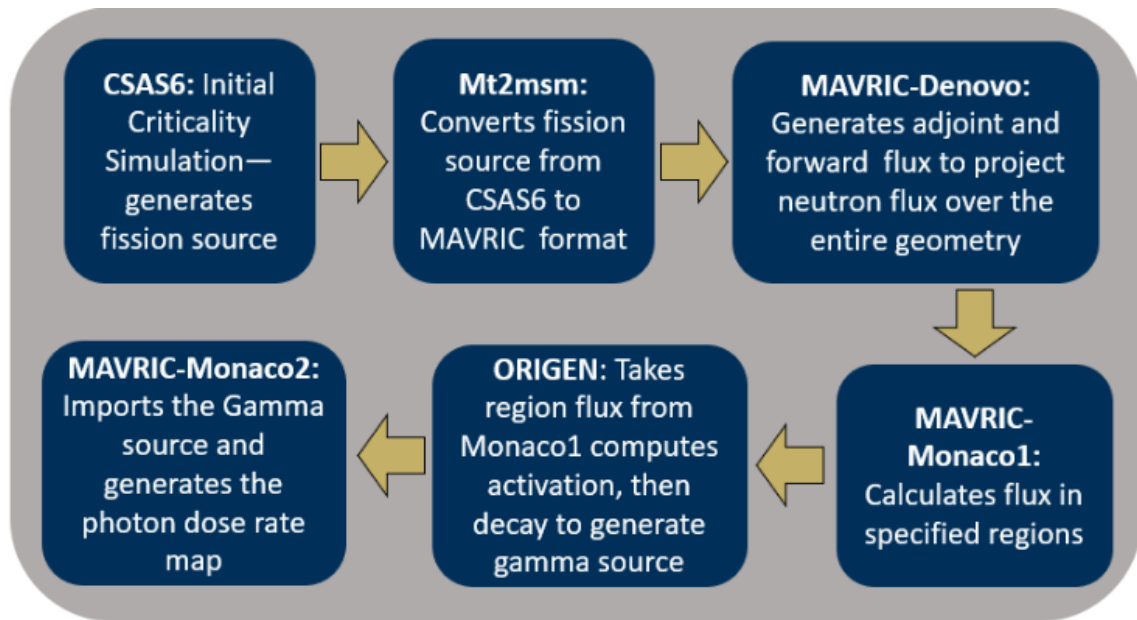


Figure 2.1: Overall workflow for SCALE simulation.

source produced needs to be converted to MAVRIC format by converting the mesh tally into a mesh source using the Mt2msm utility.

### 2.1.2 MAVRIC

MAVRIC uses CADIS and FW-CADIS methodology to prefer efficient variance reduction parameters. Denovo, a function within MAVRIC, performs discrete-ordinates calculations to generate the forward and adjoint flux using the newly converted mesh source [27]. The adjoint calculations placed importance first on the bottom of the soil and worked their way up to build an importance map for the entire model, Figure 1.7. After the variance reduction parameters were generated, the Monaco function becomes biased and performs Monte Carlo calculations to calculate the neutron tallies. For this scenario, the 10-foot block of soil was split into 50 slices to determine the neutron flux in each slice. The soil was split into 50 slices to obtain a depth-dependent distribution of activated radioisotopes. The MAVRIC module used 250 batches and a total of 250 million particles. These simulations were run on 1 CPU on the Sawtooth cluster from the Idaho National Laboratory. The maximum simulation time was 140 CPU hours. Within MAVRIC, the neutron flux was

produced with sufficient batches and particle histories per batch to maintain the relative uncertainty for each region at less than 4 percent.

### 2.1.3 ORIGEN

ORIGEN can calculate activation, radiation source terms, and time-dependent decay concentrations for most isotopes generated from a fission source. On top of that, ORIGEN can generate neutron and gamma decay emission spectra [27]. The neutron flux was parsed and used within ORIGEN to create the activation source library. For the soil activation and dose rate calculations, the reactor operated for one year. It is assumed that a temporary post-disaster microreactor deployment will last up to one year, so this is a conservative estimate. The reactor is then removed and redeployed elsewhere, together with the basemat. After removal, the radioisotopes in the activated soil will decay. ORIGEN performed the decay analysis and generated the gamma sources for the cool-down period, which ranged from a few months to 5 years.

### 2.1.4 MAVRIC USING ORIGEN GENERATED SOURCES

In the final step, MAVRIC's Monaco, a Monte Carlo code, function was used again to calculate the dose rate. Specifically, the gamma sources resulting from the activation of the soil were used to determine the dose rate in the air above the activated soil. Then, the calculated evolution of the dose rate over time was used to obtain the total dose over a specified period, e.g., the annual dose. The second round of Monaco was conducted with 200 batches and a total of 200 million particles, resulting in a relative uncertainty of less than 5 percent for each region. Overall, the six-step workflow was repeated to compare different shielding materials, structural materials, and the thickness of the basemat. The next section will explain in depth the design of experiments.

## 2.2 Strength Calculation

To ensure the basemat can hold up the weight of the reactor, compressive strength calculations were performed. Assuming the basemat's strength is reliant on the structural material, it will be the only material considered in the calculation as a conservative analysis. On top of only measuring the strength, a factor of safety of at least 3 is required. The equations used to calculate the compressive strength, the cross-sectional area, and the factor of safety are shown below. Sigma is the compressive strength, W is the maximum weight a 20-foot shipping container can hold, 30,480 kg, to be conservative. Because the ratio between shielding and structural material is 2:1, the shielding area is 2/3 of the total area.

$$\sigma_{applied} = W * g / A_{net} \quad (2.1)$$

$$A_{net} = A_{Basemat} - A_{Shielding} \quad (2.2)$$

$$A_{Shielding} = A_{Basemat} * 2/3 \quad (2.3)$$

$$F.S = \sigma_{Max Compressive} / \sigma_{applied} \quad (2.4)$$

## 2.3 Weight Calculation

Weight is a large contributor to transportability. The weight of each basemat design at its optimal shielding thickness will be compared by mass for optimization. Because the basemat is composed of a complex geometry, the ratio between shielding and structural material (2:1) will be used to determine the average density of the basemat design. The average density will then be multiplied by the volume to obtain the overall mass of the specific basemat design.

$$\rho_{average} = \rho_{shielding} * 2/3 + \rho_{structural} * 1/3 \quad (2.5)$$

$$m = \rho_{average} * V_{basemat} \quad (2.6)$$

## 2.4 Cost Calculation

The overall cost of each basemat design is an important factor in determining the optimal basemat. More expensive shielding materials may provide a stronger radiation shield, but the high cost may not be justified, depending on the performance of cheaper shielding materials. To determine cost, the ratio between the shielding and structural material (2:1) was used to estimate the price needed for each material. The cost analysis only looks at the cost for raw materials and does not delve into labor costs to make it into the basemat design. Furthermore, due to limited public information on the cost of some materials, some costs were estimated from what information was available. The estimated cost for each material is listed in Table 2.1

Table 2.1: List of costs for each material

Material	Cost
Light Water (high-purity water) [28]	0.32 \$/kg
Borated Polyethylene [29]	7.323 \$/kg
Concrete [30]	0.09\$/kg
WEP [31]	14.5 \$/kg
HDPE [32]	0.95\$/kg
Aluminum 7075 (Hex Bar) [33]	4.4 \$/kg

## 2.5 Optimization Approach

To optimize the basemat design, four different shielding materials were paired with three different structure materials, resulting in 12 different material groupings. Each pairing was evaluated at 6 different thicknesses to determine the smallest thickness the basemat can be while meeting ALARA and NRC standards. The materials and basemat thickness can be seen in Table 2.2. It should be noted that concrete was chosen as both a shielding material and a structural material due to its strength in radiation shielding and in load-bearing. While

a concrete pad takes time to cure, it can potentially be used in the basemat design. In the basemat design, the concrete can either be used as the structure or the shielding filling, either of which requires less concrete than a full concrete pad, which is easier to transport, especially if the concrete is cured in the basemat design beforehand. Ultimately, concrete was included to see if a compromise between traditional shielding and lightweight materials is another possible path toward lightweight shielding.

Table 2.2: List of all shielding materials, structural materials, and basemat depths to be tested for design optimization.

Shielding Materials	Structural Materials	Thickness
Water	High Density Polyethylene (HDPE)	2 ft
Borated Polyethylene	Concrete	3 ft
Concrete	Aluminum 7075-O	4 ft
Water Extended Polyester (WEP)		4.5 ft
		5 ft
		5.5 ft

Optimization of the basemat will be based on weight, cost, and shielding capability. Shielding capability is the first analysis. If a basemat composition and thickness result in a dose rate higher than the standards set by the NRC, it will not be considered. Specifically, the dose rate that is evaluated is the dose one year after the reactor and basemat have been removed. One year is a generous amount of recovery time for many isotopes to decay away. Suppose a basemat design cannot reach an acceptable dose after one year. In that case, it will most likely take several years, counteracting the benefits of using a microreactor to recover from a natural disaster. Then, each material combination will be compared at the smallest thickness that meets the dose exposure requirements.

## CHAPTER 3

### RESULTS AND DISCUSSION

#### 3.1 Strength Calculations

Each structural material was evaluated to ensure it is strong enough to hold the weight of the reactor. For a conservative analysis, the surface area undergoing compression was reduced to the surface area with only structural material. The total basemat area is  $68.58 \text{ m}^2$ , which is reduced to  $22.86 \text{ m}^2$  for the structural surface area. For a 20-foot shipping container with a maximum weight, equation 2.1 establishes the compressive stress as 13.08 kPa. The ultimate compressive strengths for HDPE and Concrete can be found in Table 3.1 [34] [35]. The ultimate compressive strength of Aluminum 7075-O is not specified in public documents, so its maximum yield strength was approximated as its ultimate compressive strength [36]. The factor of safety for each structural material exceeds the set goal of a factor of safety of 3. Ultimately, each structural material can hold the weight of any deployable microreactor that is under the maximum weight allowed in a 20-foot shipping container (30,480 kg).

Table 3.1: Comparison of ultimate compressive strengths and factor of safety for each structural material.

Structural Materials	HDPE	Concrete	Aluminum 7075-O
Ultimate Compressive Strength (MPa)	3.447	17	145
Factor of Safety (unit-less)	263	1299	11085

## 3.2 Radiation Calculations

### 3.2.1 SCALE Simulation

As discussed in the methodology, 72 different material combinations were tested to determine the optimal material combination and overall basemat thickness, which are dependent on the radiation shielding ability, weight, and cost. In the process of obtaining the dose rate, the neutron flux is calculated in the first round using MAVRIC's Monaco function. The neutron flux can indicate how well the basemat shields neutrons at different energy levels. Figure 3.1 demonstrates the flux for each material combination of the 2-foot thick basemat, with the shielding material separated into different plots. These plots indicate that the HDPE material is the best pairing for all shielding materials. At the same time, concrete is close behind, meaning that a combination of pre-cured concrete and a lightweight shielding material is another potential solution for a rapidly deployable radiation shield. On the other hand, aluminum performs poorly as a radiation shield. When paired with water or concrete, the no shielding case is slightly better at attenuating the thermal neutrons, indicating that aluminum will likely perform the worst when limiting dose.

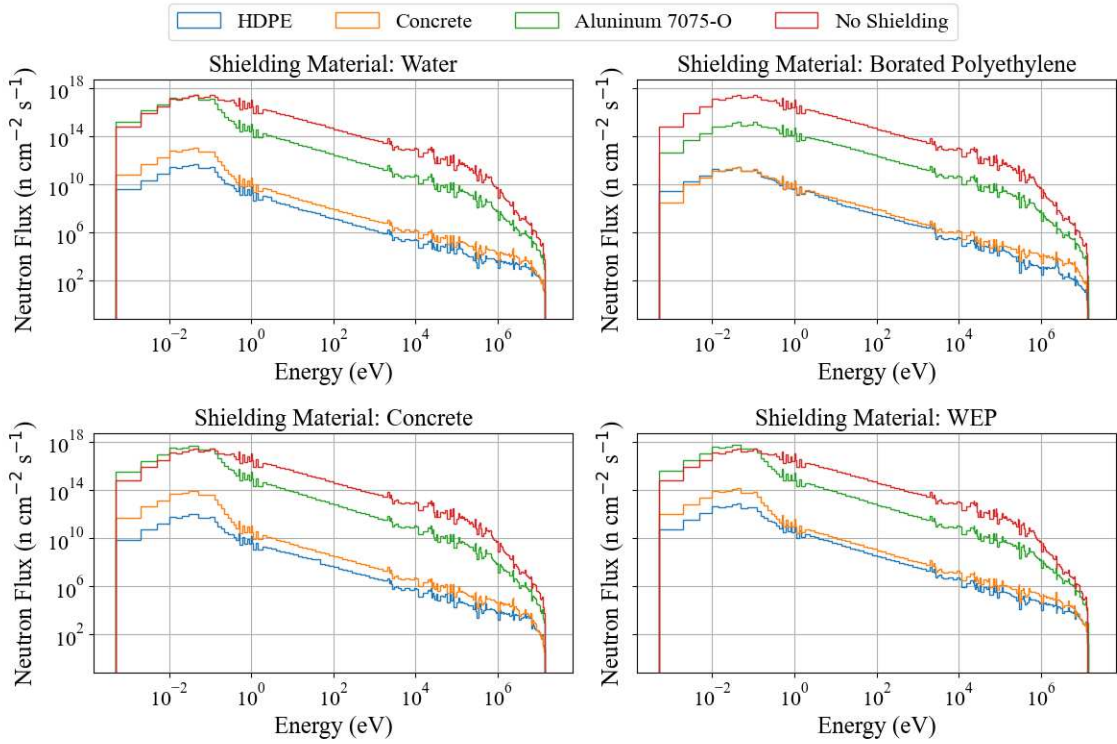


Figure 3.1: Energy versus neutron flux plot for the 2-foot thick basemat separated by shielding material, and comparing the shielding material and its paired structural material.

The 3-foot and 4-foot basemat energy versus neutron flux plots are similar to Figure 3.1 and can be found in Appendix A. The 4.5-foot basemat energy versus neutron flux plot shows an interesting divergence in the concrete and HDPE material combinations. The plot can be found in Figure 3.2.

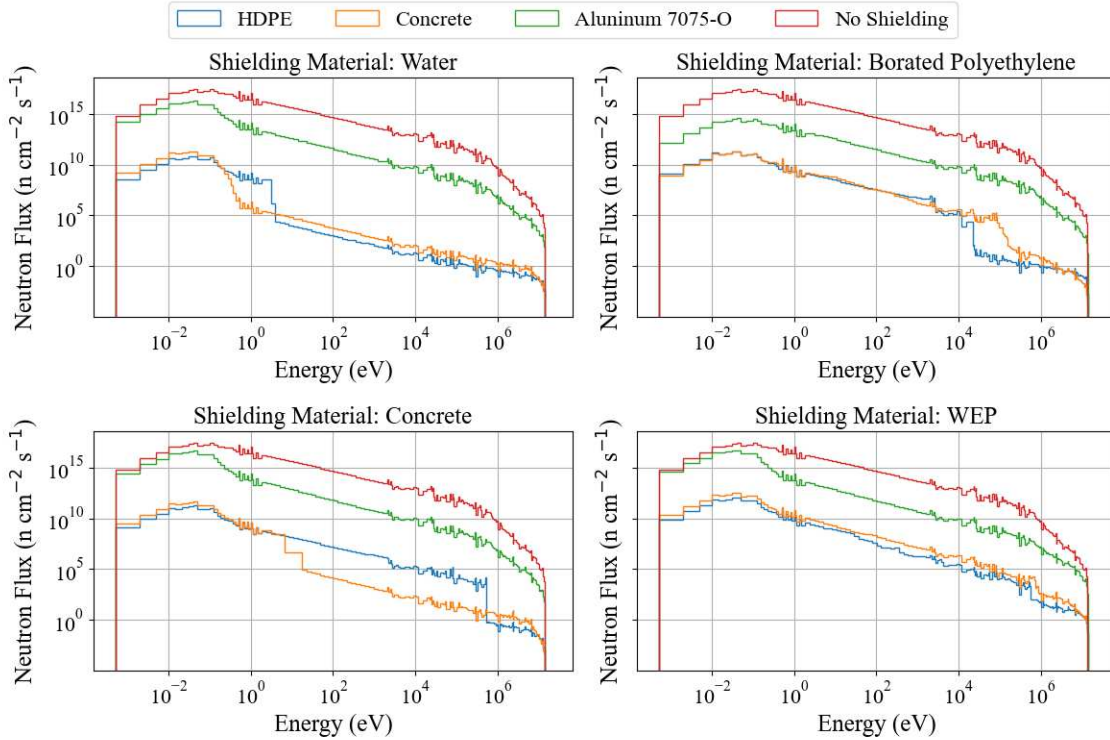


Figure 3.2: Energy versus neutron flux plot for the 4.5-foot thick basemat separated by shielding material, and comparing the shielding material and its paired structural material.

Unlike Figure 3.1, HDPE performs worse than concrete at attenuating the neutron flux around the eV range when paired with water. When HDPE and concrete are paired with concrete, their performance diverges starting around the eV range. And when paired with borated polyethylene, HDPE is much better at shielding in the 10 keV to the MeV range. These differences indicate that at 4.5 feet, concrete can outperform HDPE in certain eV ranges. The 5-foot and 5.5-foot thick basemat follow a similar trend to Figure 3.2 and can be seen in Appendix A.

The first shielding requirement was the yearly dose standard for the general population set by the NRC (0.1 rem per year) [11]. For a conservative safety approach, it is assumed that a general population member remains in the proximity of the irradiated area 24/7 all year long. This additional assumption reduces the annual dose limit to the dose rate of

about  $1 \times 10^5$  rem/hr, as shown in the equation below.

$$0.1 \text{ rem/year} * \text{year}/365 \text{ days} * \text{day}/24 \text{ hours} = 1.14 * 10^{-5} \text{ rem/hr} \quad (3.1)$$

Each shielding combination was tested one year after the reactor and basemat were removed. For better comparison, the material combinations were divided into six different basemat thicknesses and further categorized by shielding material to compare their performance with each structural material. For simplicity, the dose rate was averaged across the x and y directions and calculated in 5 cm increments in the z direction. As established by a separate analysis that considered a detailed radial activation rate distribution, the impact of averaging is to underestimate the peak dose rate by approximately 22.4%. Because a majority of dose rates for the cases of interest are on a millirem ( $1e-6$ ) scale, a 22.4% underestimate may be easily accommodated.

Figure 3.3 shows the dose rate after the two-foot basemat is removed, for each shielding material grouping, in air above the irradiated soil, with 0 meters representing the closest distance to the soil and 300 meters representing the farthest distance considered. It also displays the NRC limit based on continuous exposure and the dose rate without any shielding.

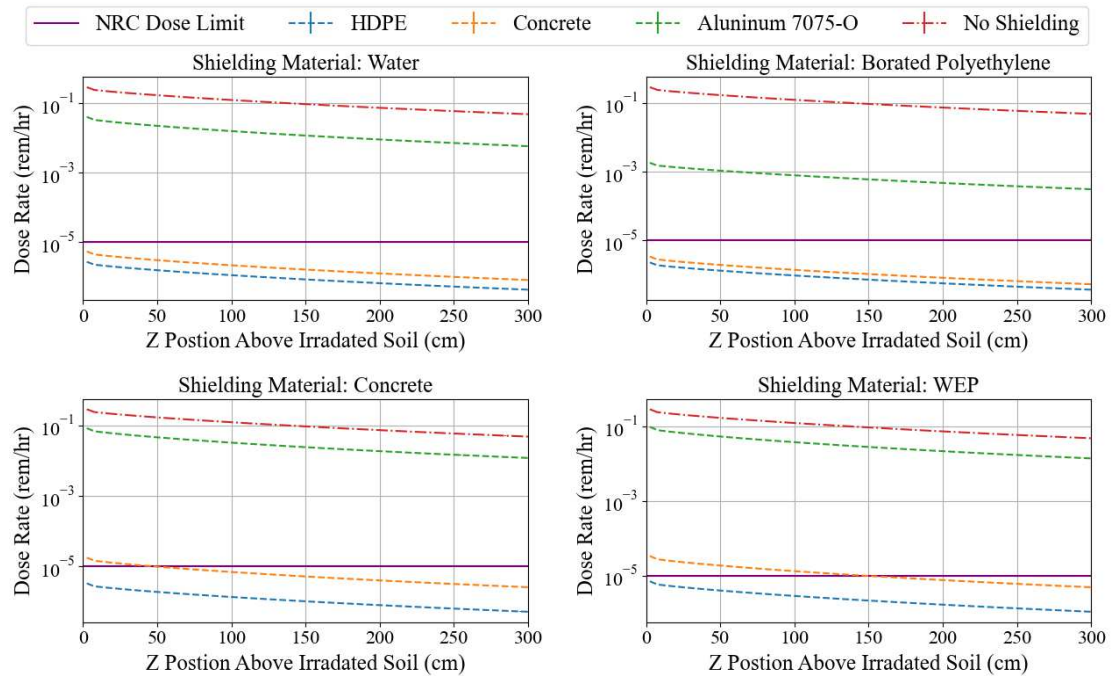


Figure 3.3: Dose rate 1 year after the reactor and 2-foot basemat have been removed, separated by shielding material, and comparing the shielding material and its paired structural material.

For all shielding materials, the HDPE reduces the dose rate to comply with the established NRC standard. This is due to the high weight percentage of hydrogen (14%). Hydrogen is a strong moderator by effectively slowing fast neutrons to thermal energies, which are easier to absorb. The next best structural material to also meet the NRC standard in most cases is concrete, despite only having 0.62% by weight of hydrogen. Concrete's strong shielding ability comes from the aggregates that have higher atomic numbers, which are effective at absorbing gamma radiation. For a 2-foot thick basemat, Aluminum 7075-O did not perform well. When paired with water, concrete, and WEP, it performed similarly to the no-shielding case. When paired with borated polyethylene, the dose is lower than with the other materials. This is most likely a result of the boron-10 in the borated polyethylene absorbing more of the neutrons. HDPE outperforms concrete with a 2-foot thick basemat, effectively showing the strength of lightweight shielding.

Continuing with the next basemat thickness, Figure 3.4 shows the dose rate of a 3-

foot thick basemat in the same organization, done for Figure 3.3. Like the 2-foot basemat, HDPE and concrete material pairings met the NRC standard, while Aluminum did not. The combinations with either HDPE or concrete produced very similar dose rates, encouraging the idea that these material combinations are close to reaching the lowest dose rate that is reasonably achievable, i.e., ALARA. The thicker aluminum slightly lowered the dose rate when compared to the 2-foot basemat, but the dose is still too high.

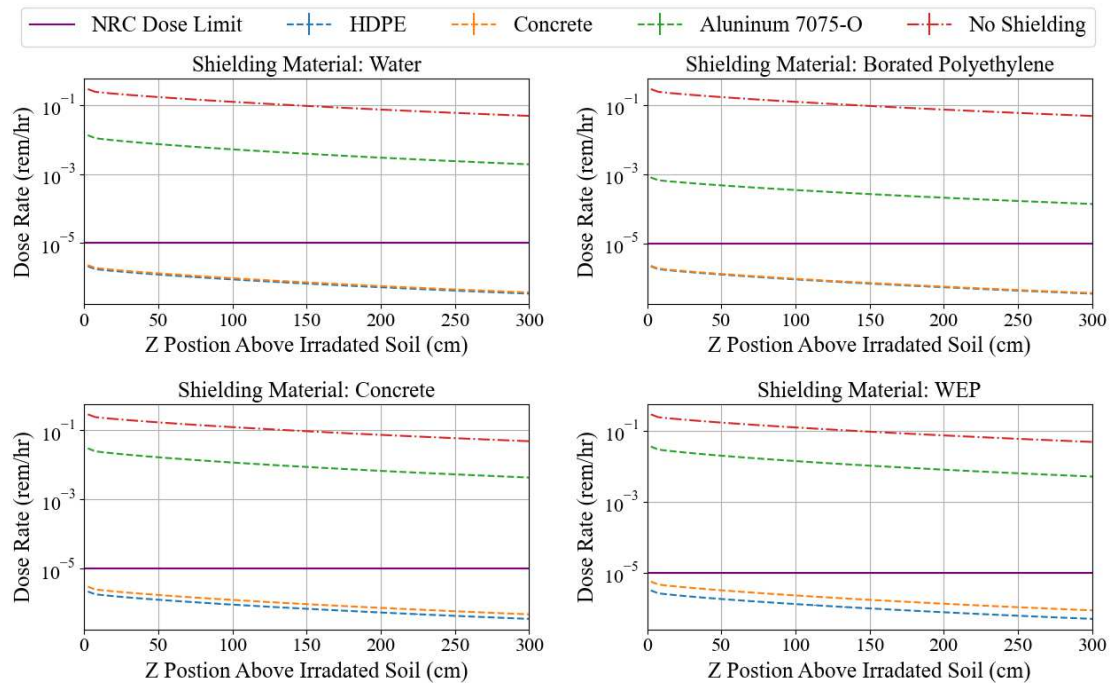


Figure 3.4: Dose rate 1 year after the reactor and 3-foot basemat have been removed, separated by shielding material, and comparing the shielding material and its paired structural material.

The 4-foot thick basemat follows the trend set by the 2-foot and 3-foot thick basemat as seen in Figure 3.5. At 4 feet thick, the HDPE and concrete material combinations are essentially producing the same dose rate. Additionally, the aluminum combination continues the trend of decreasing the dose rate, but not by enough to meet the set NRC requirement.

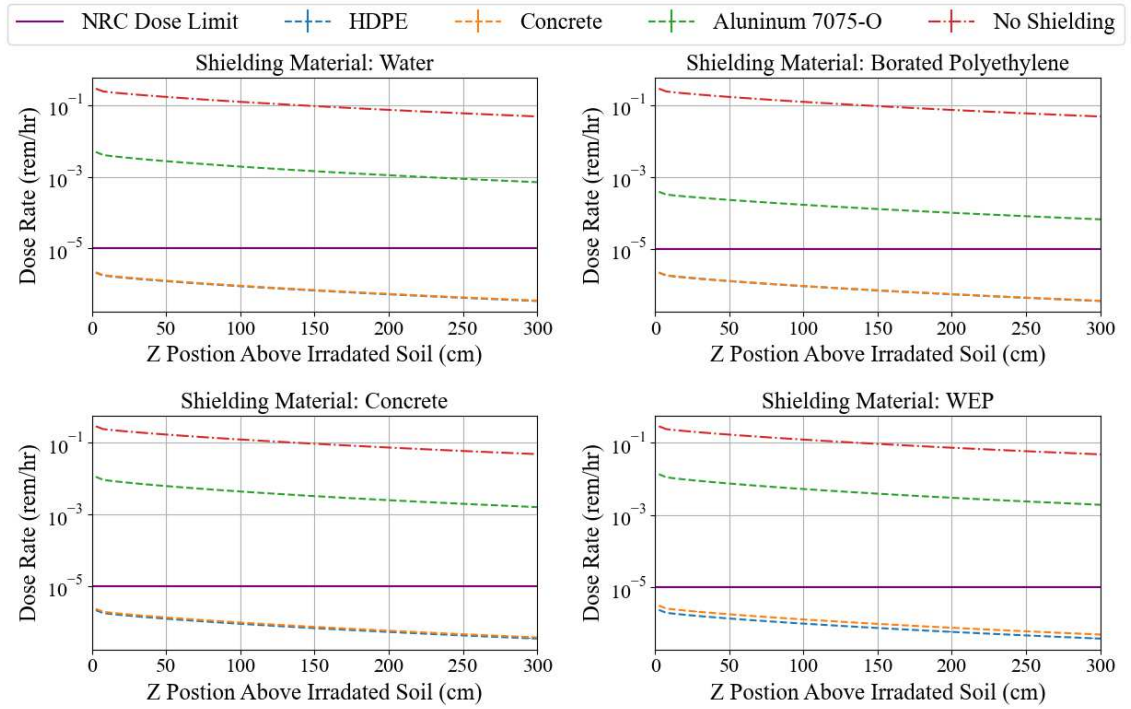


Figure 3.5: Dose rate 1 year after the reactor and 4-foot basemat have been removed, separated by shielding material, and comparing the shielding material and its paired structural material.

The basemats thicker than 4 feet continue the established trend for each material. Figure 3.6, Figure 3.7, and Figure 3.8 show that HDPE and concrete are the only structural materials that can be paired with shielding material to limit the dose rate in the air to NRC standards with a reasonable amount of material. The aluminum and borated polyethylene get close to the dose standard in the 5.5-foot basemat, and with an extra couple of feet, it would reach the dose standard. However, 5.5 feet is already a substantial amount of material, especially when HDPE and concrete limit the dose rate to below the dose limit, given a thickness of 2 feet. Therefore, any basemat thickness exceeding 5.5 feet is unreasonable and will not be considered.

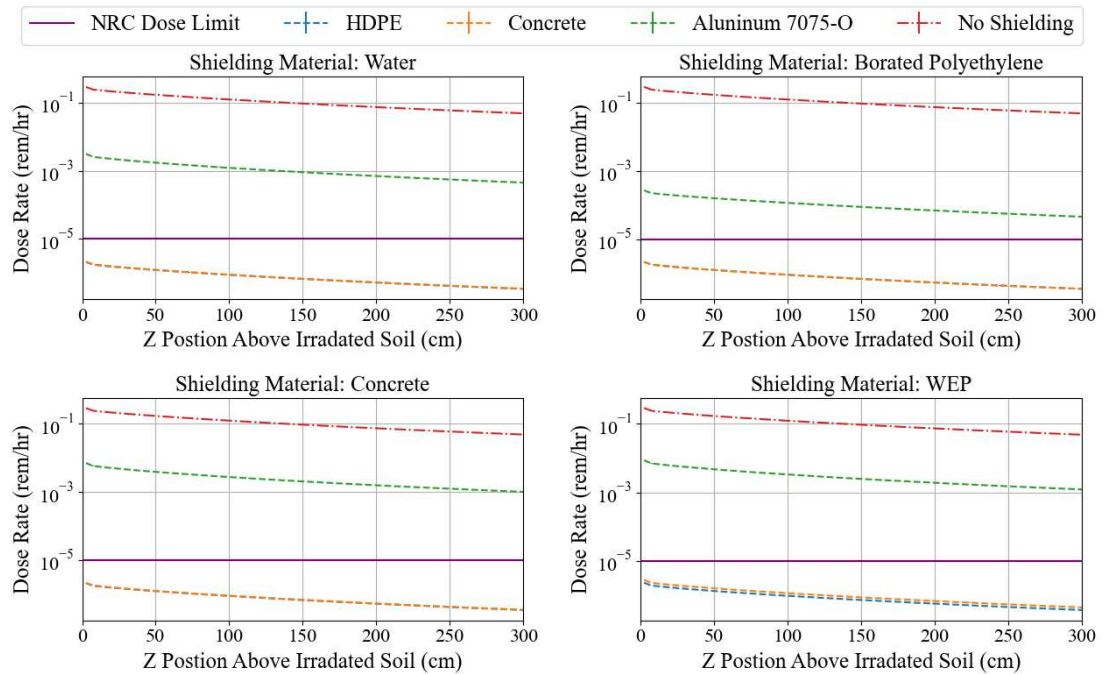


Figure 3.6: Dose rate 1 year after the reactor and 4.5-foot basemat have been removed, separated by shielding material, and comparing the shielding material and its paired structural material.

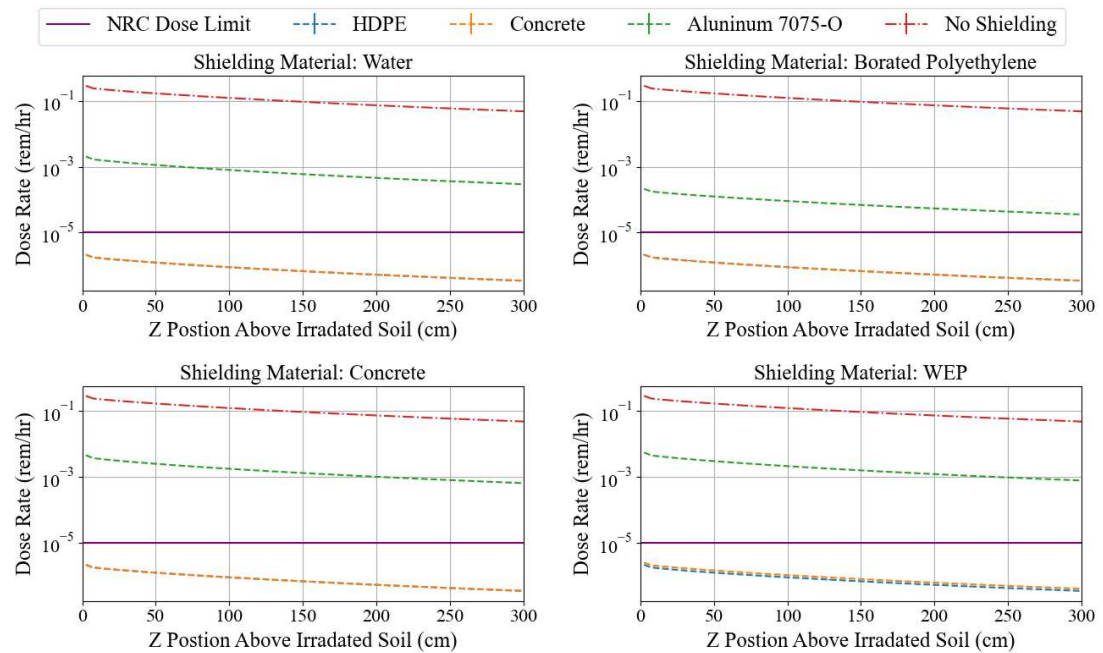


Figure 3.7: Dose rate 1 year after the reactor and 5-foot basemat have been removed, separated by shielding material, and comparing the shielding material and its paired structural material.

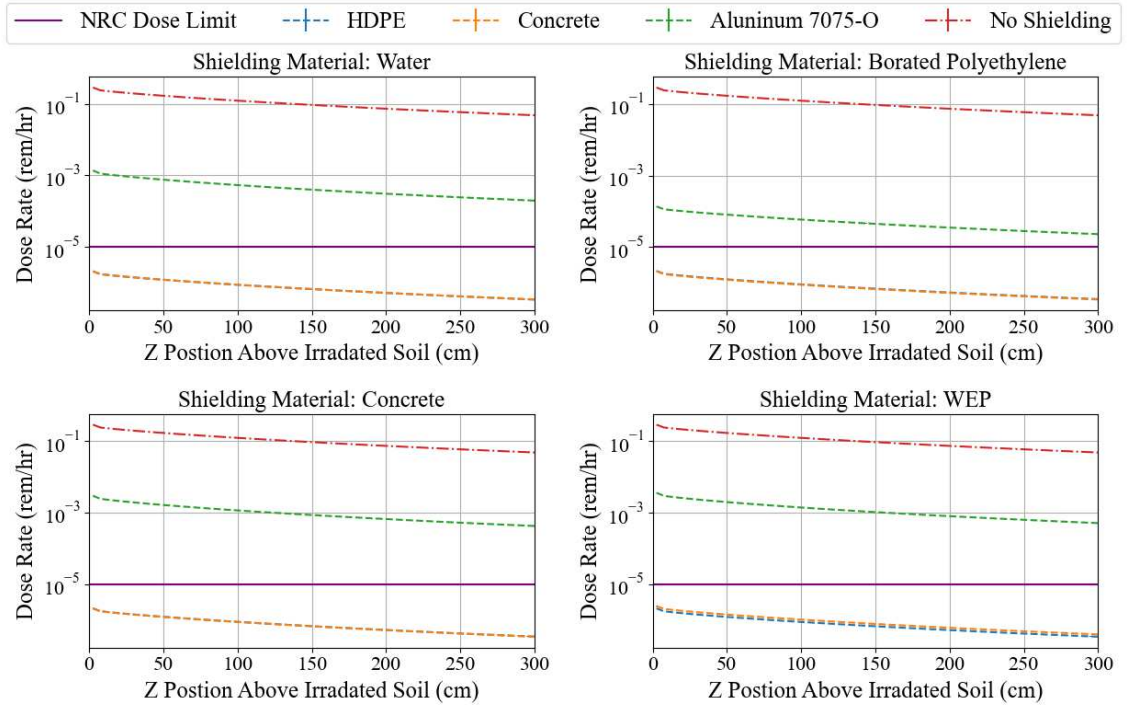


Figure 3.8: Dose rate 1 year after the reactor and 5.5-foot basemat have been removed, separated by shielding material, and comparing the shielding material and its paired structural material.

Each material combination with the smallest basemat thickness that met the NRC dose limit at 0 cm above the ground was considered a viable solution and will be explored further. The material combinations and basemat thickness that met the requirement can be found in Table 3.2.

Table 3.2: List of material combinations and their respective smallest thickness that meets the NRC dose standard from 0 cm above the ground.

Material Combination (Structural Material & Shielding Material)	Basemat Thickness
HDPE & Water	2 ft
Concrete & Water	2 ft
HDPE & Borated Polyethylene	2 ft
Concrete & Borated Polyethylene	2 ft
HDPE & Concrete	2 ft
Concrete & Concrete	3 ft
HDPE & WEP	2 ft
Concrete & WEP	3 ft

These 8 material combinations met the NRC dose standard one year after the reactor and

basemat combination were removed. Further exploring the radiation shielding effectiveness of these material combinations, the dose rate from 1 meter above the ground and in the center of the model was plotted against five time steps: 30 days, 90 days, 180 days, 1 year, and 5 years, compiled in Figure 3.9. One meter above the ground was chosen as it represents the central point of the human body, where vital organs are most susceptible to damage from gamma radiation [37].

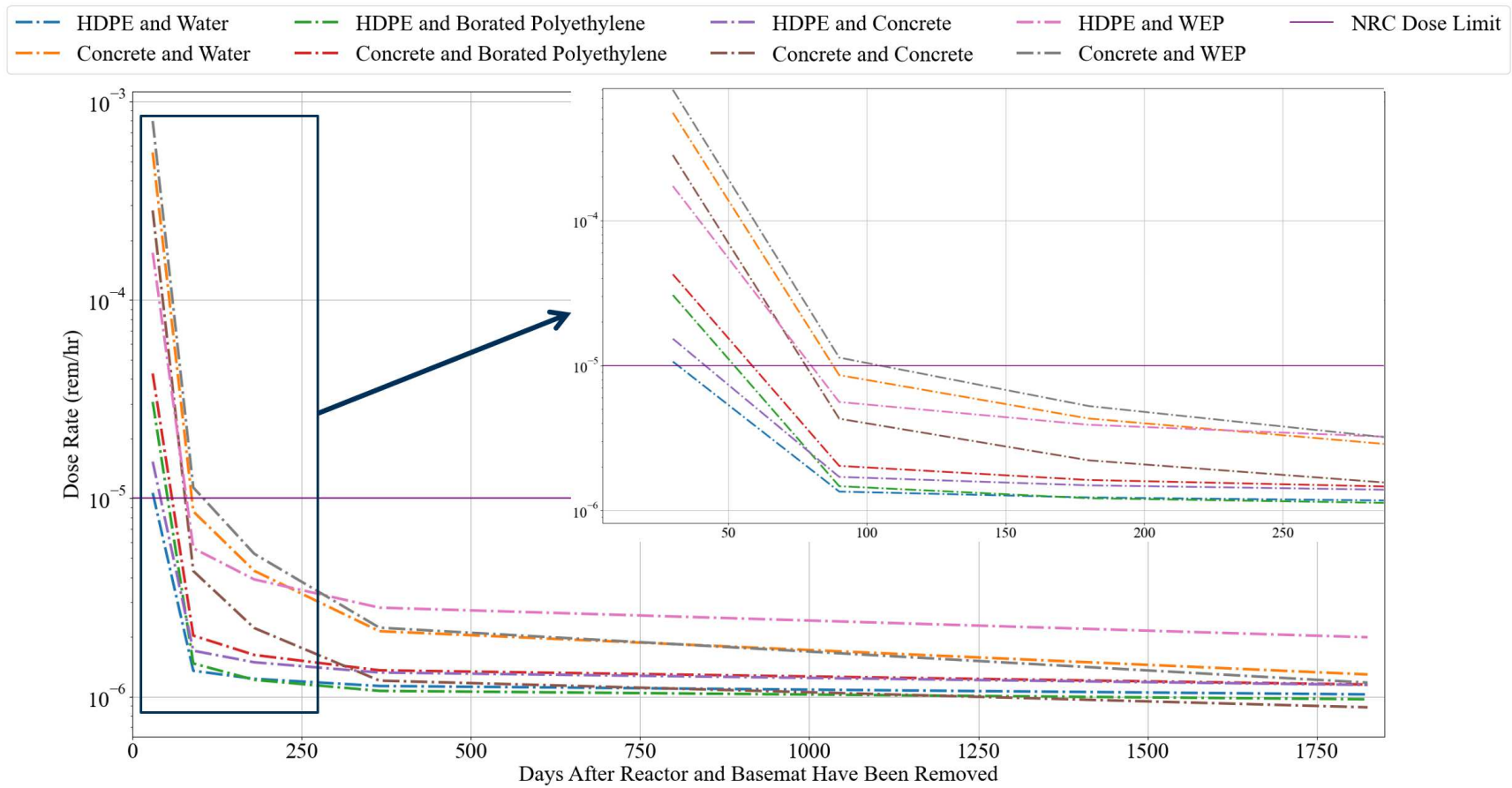


Figure 3.9: Dose Rates at 1 meter above the soil in the center of the model from different times after the reactor and basemat were removed.

The top-performing material combinations are HDPE and water, HDPE and concrete, and HDPE and borated polyethylene. The HDPE and water require approximately 33 days to meet the NRC standard, HDPE and concrete require approximately 43 days, and HDPE and borated polyethylene require approximately 52 days. Beyond the top performers, the maximum needed cool-down period is approximately 108 days. Quarantining the microreactor's working area for at most a third of the year is reasonable, especially when a deployed reactor will require no more than a couple of acres of land. Therefore, all 8 material combinations will be considered in the final decision matrix, and these combinations will be the only materials considered in the future analyses in this work.

### 3.2.2 Radioisotopes Investigation

In Figure 3.9, the rate of total decay changes over time. The difference in the total decay slopes can be attributed to the varying half-life for each isotope. The initial slope represents isotopes with a large decay rate but a short half-life. As time progresses, the final slope approaches zero, indicating that the decay rate is dependent on the isotope that has a half-life longer than 5 years. To understand which isotopes are in action, Figure 3.10 and Figure 3.11 displays the top contributing isotopes to the dose rate, from the HDPE and water simulation's top soil layer, starting from when the reactor was running (represented in the negative side of the x-axis) to the days after the reactor and basemat were removed (starting at day 0). There are two plots to show the decay for each isotope, one in Becquerels (Bq), which is equivalent to one radioactive disintegration per second, and one in Gamma-Watts to show the radioisotopes account for the total energy released by all photons due to gamma decay.

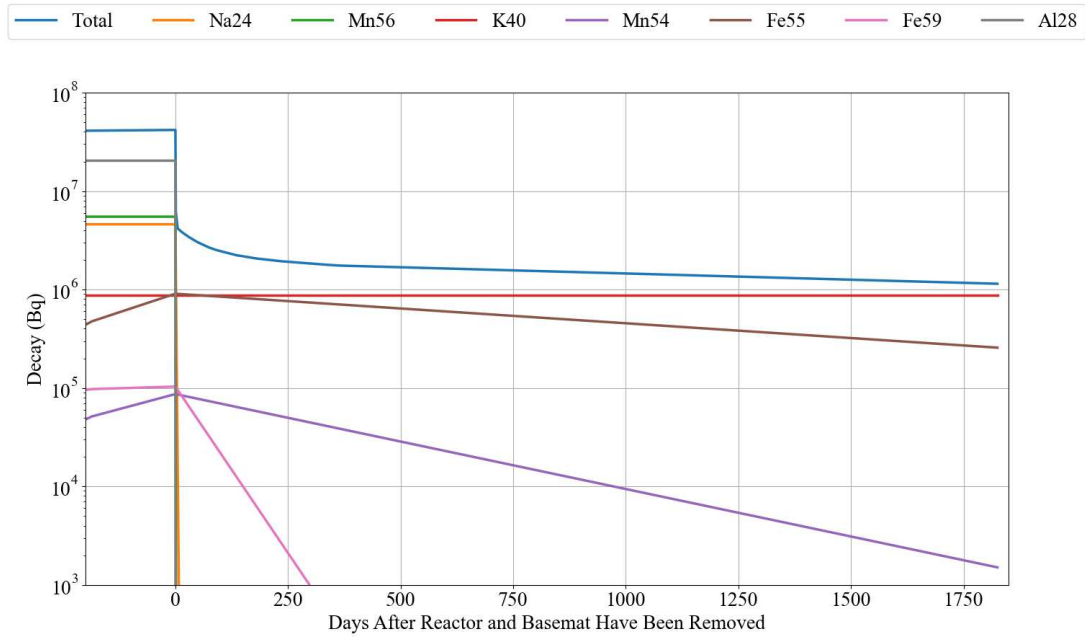


Figure 3.10: Top contributing radioisotopes to the dose rate from the 2-foot thick HDPE and water simulation over the time the reactor was running, to after the reactor and basemat were removed (where the negative days represent when the reactor was running) in Becquerels. Total represents the total decay rate of all isotopes.

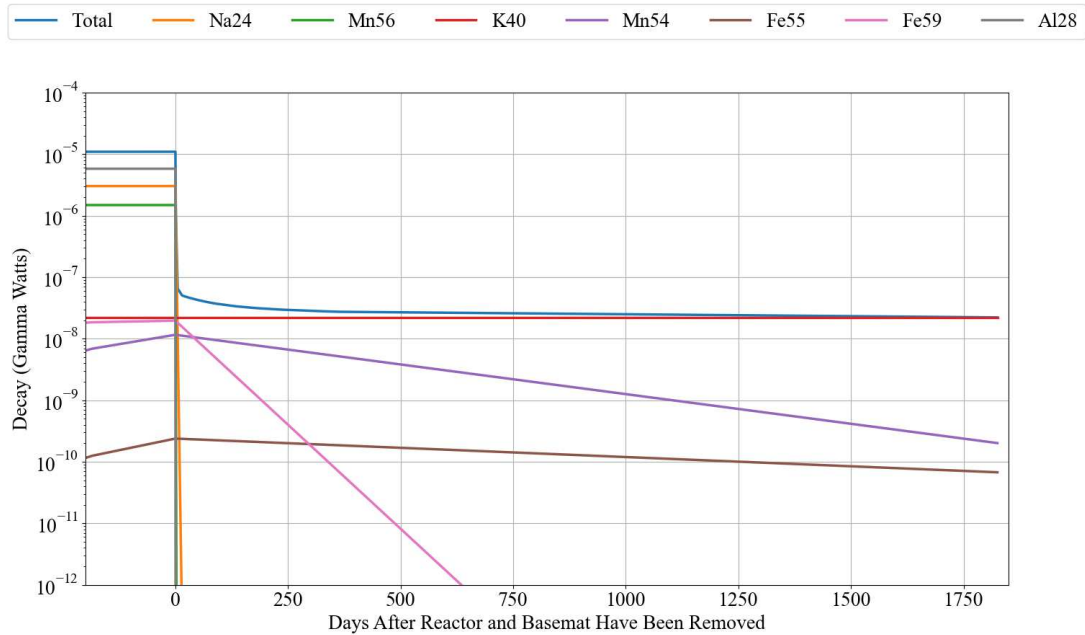


Figure 3.11: Top contributing radioisotopes to the dose rate from the 2-foot thick HDPE and water simulation over the time the reactor was running, to after the reactor and basemat were removed (where the negative days represent when the reactor was running) in Gamma-Watts. Total represents the total decay rate of all isotopes.

To understand the impact of the main contributing radioisotopes and the differences between Figure 3.10 and Figure 3.11, the half-life, decay mode, and released gamma rays can be found for radioisotopes of interest in Table 3.3.

Table 3.3: Compilation of half-life, decay mode, and the gamma rays for radioisotopes of interest.

Radioisotope	Half-Life [38]	Decay Mode [38]	Highest Probability Gamma Rays (keV) [39]
Na-24	14.997 hours	$-\beta$	1368.625, 2754.008
Al-28	2.24 minutes	$-\beta$	1778.987
K-40	1.25 billion years	$-\beta$ (89.28%), $\varepsilon$ (10.72%)	1460.820
Fe-55	2.744 years	$\varepsilon$	126.0
Fe-59	44.495 days	$-\beta$	1099.245, 1291.590, 192.343
Mn-54	312.12 days	$\varepsilon$	834.848
Co-60	1925.28 days	$-\beta$	1332.492, 1173.228
Eu-152	13.528 years	$\varepsilon$ (72.1%), $-\beta$ (27.9%)	1408.013, 1112.076, 1085.837, 964.057, 121.7817
Eu-154	8.601 years	$-\beta$	1274.429, 1004.76, 723.3014, 123.0706

The first slope of the total decay from Figure 3.10 is steep due to the large energy and short half-life of sodium-24 and aluminum-28. Within an hour for aluminum-24 and a couple of days for sodium-24, they have decayed by several orders of magnitude, driving the sharp decrease in the total decay in the first couple of days after the reactor and basement were removed. Therefore, aluminum-28 and sodium-24 drive the initial total decay, impacting how many days it takes to reduce the dose from reactor operation levels. One main difference between Figure 3.10 and Figure 3.11 is the position of iron-55. In Becquerels, iron-55 drives the total decay rate with potassium-40. In gamma watts, iron-55 is three orders of magnitude less than the total decay, meaning it has minimal impact. The difference in importance to the total decay can be explained by the gamma rays that are released by iron-55. Iron-55 only releases gamma rays with 126 keV, which is significantly lower than the other radioisotopes as seen in Table 3.3. At the same time, manganese-54 is not a large contributor in terms of Becquerels, but due to its higher gamma ray energy, it has a larger impact in terms of gamma-watts. After approximately 40 days, the total decay in Figure 3.10 and Figure 3.11 is predominantly defined by potassium-40. Because its half-life is so long, it is considered background radiation, explaining why the HDPE and water case has a dose rate essentially at the NRC limit at the 30-day mark. After 100 days, the other contributors, such as iron-59 and manganese-54, have decayed to the point where total decay is solely dependent on potassium-40, and the dose rate is under the NRC dose limit by almost an order of magnitude.

Figure 3.10 represent the material combinations: HDPE and water, HDPE and borated polyethylene, HDPE and concrete, and concrete and borated polyethylene. These material combinations followed a similar trend in the change in dose rate as seen in Figure 3.9. The dose rate of these material combinations was initially driven by sodium-24 and aluminum-28 and then by potassium-40 (the respective plots for the HDPE and borated polyethylene, HDPE and concrete, and concrete and borated polyethylene can be found in Appendix A). The 4 other material combinations of concrete and concrete, concrete and WEP, HDPE and

WEP, and concrete and water follow a different trend, so a separate analysis was conducted. Figure 3.12 and Figure 3.13 display the top contributing isotopes in the same manner as Figure 3.10 for the concrete and water simulation.

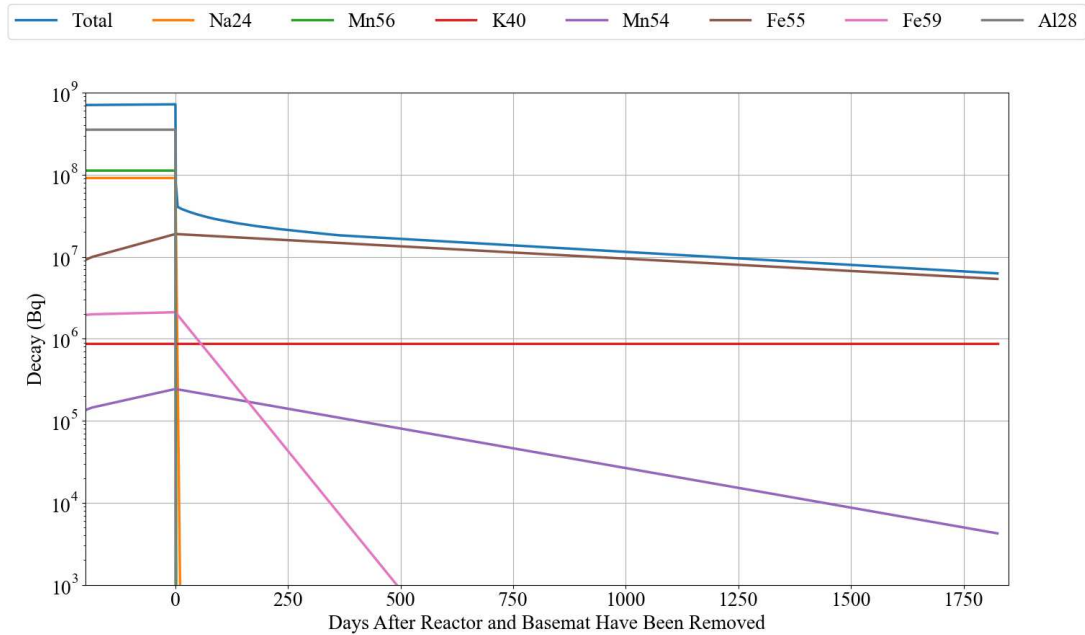


Figure 3.12: Top radioisotopes by activity from the 2-foot thick concrete and water simulation over the time the reactor was running to after the reactor and basemat were removed (where the negative days represent when the reactor was running) in Bq.

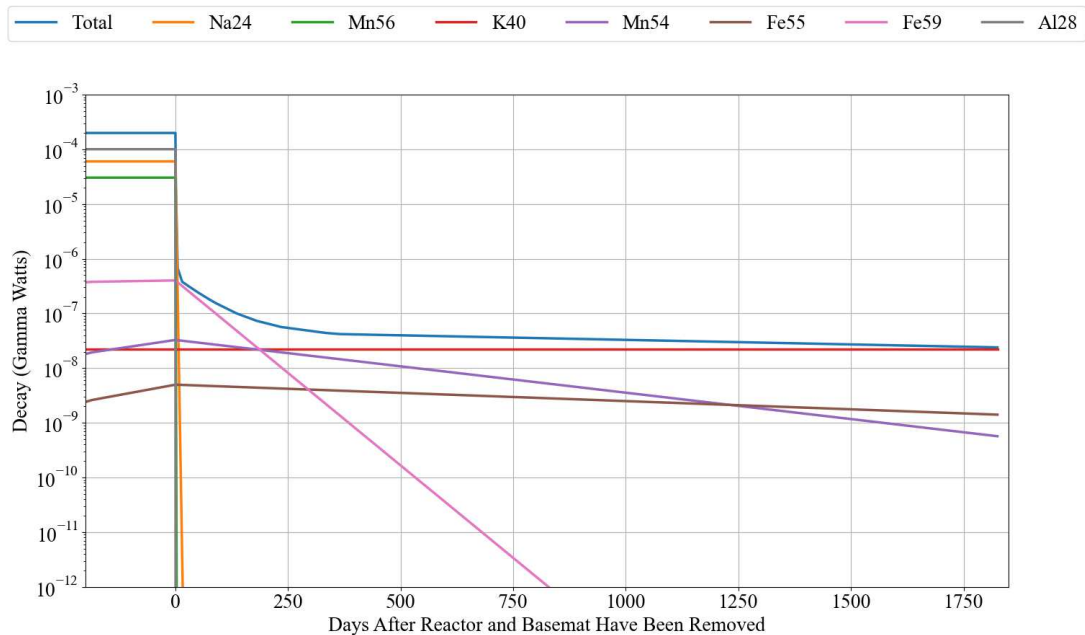


Figure 3.13: Top contributing radioisotopes to the dose rate from the 2-foot thick concrete and water simulation over the time the reactor was running to after the reactor and basemat were removed (where the negative days represent when the reactor was running) in gamma-Watts.

The total decay in Figure 3.12 starts at a higher Becquerel value than in Figure 3.10, indicating the concrete and water basemat acting as a less efficient radiation shield. Here, iron-55 is the main contributor to the decay rate after sodium-24 and aluminum-28 decay away in the first couple of days (first couple of hours for aluminum-28). In reference to how much energy is being deposited, Figure 3.13 also starts at a higher decay value than in Figure 3.11. In this plot, iron-59 is the main contributor to the dose rate until it transitions to potassium-40 around the 190-day mark. The higher total decay value at the beginning of the timeline explains the high dose rate at the 30-day mark for concrete and water, and the higher decay value of iron-59 explains why a longer period is needed for the concrete and water combination to meet the NRC dose limit. Concrete and concrete, concrete and WEP, HDPE and WEP, and concrete and water also follow the same trend, and each respective plot can be found in Appendix A. The material combinations, concrete

and concrete, concrete and WEP, HDPE and WEP, and concrete and water, are similar to the other four material combinations that are represented by Figure 3.10 except for overall higher total decay, and iron-59 dominating the total decay value for a longer period. This difference suggests that concrete and WEP have difficulty in shielding against producing the iron-59 isotope when compared to materials containing water and borated polyethylene. This may be a result of the difference in the amount of boron or hydrogen, which are more effective at attenuation. In particular, boron significantly reduces thermal flux, which is primarily responsible for activation through capture. Overall, all eight of the down-selected material combinations attenuate the neutron flux to where the activity is mostly driven by the potassium-40 background radiation after 190 days or less. Background radiation is the lowest a shield can achieve. Therefore, all eight basemat material combinations meet the ALARA requirement.

### 3.2.3 High Energy Emitting Isotope Doped Soil

The simulations above utilized the average composition of U.S. soil. This soil composition was effective in understanding how each basemat composition would generally perform. However, the soil composition lacked elements such as Europium and Cobalt, which have high-energy-emitting isotopes with relatively long half-lives, impacting the long-term dose rate. One basemat composition was tested to determine how europium and cobalt impact the dose rate with a unit of soil containing europium and a unit of soil containing cobalt. Europium has a concentration of 1.8 ppm in the Earth's crust, and in natural soil, the europium concentration ranges from 0.1 to 2.2 ppm [40] [41]. For a conservative analysis, a europium composition of 2 ppm was used for the europium-dosed soil. Cobalt has approximately 25 ppm in Earth's crust, and most soils contain between 1 and 40 ppm of cobalt, with the average in the U.S. being 7.2 ppm. For a conservative analysis, 40 ppm was used for the cobalt-dosed soil [42] [43].

The first analysis on the cobalt and europium soils compared the dose rates 1 year after

the reactor and basemat were removed. Figure 3.14 shows that Europium and Cobalt both increase the dose, but the HDPE and borated polyethylene basemat is effective in shielding radiation to maintain the dose below the NRC dose limit. Furthermore, the increase in the dose rate is linear with the amount of europium or cobalt added to the soil. In the europium case, the dose rate will increase approximately by a factor of 0.680 for every 1 ppm of europium added. For cobalt, the dose rate will increase by a factor of 0.0623 for every 1 ppm of cobalt added.

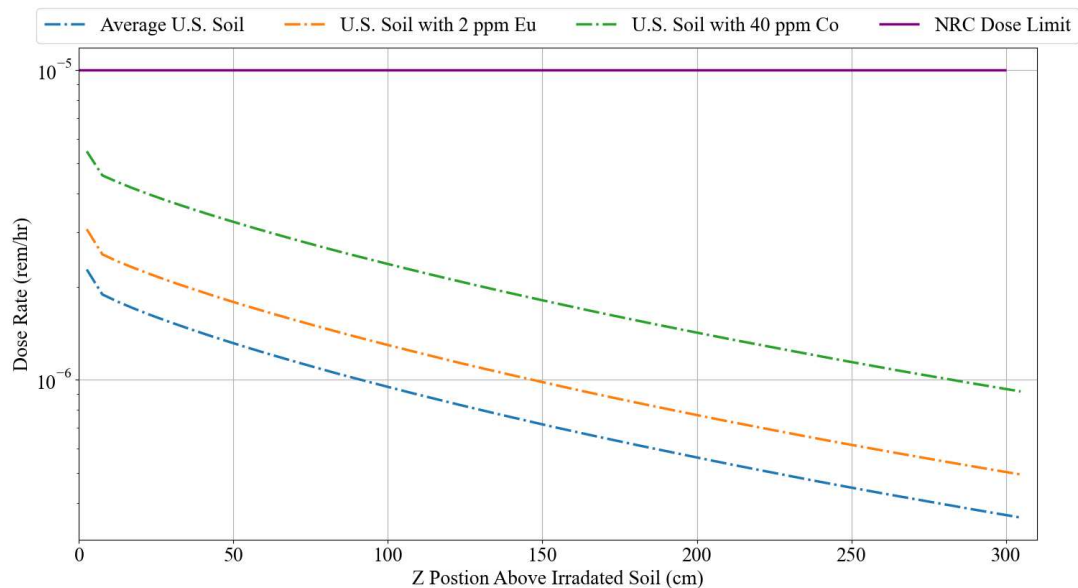


Figure 3.14: Comparison of dose rates of U.S. average soil, soil dosed with 2 ppm of Eu, and soil dosed with 40 ppm of Co 1 year after the reactor and basemat have been removed. Shielding was a 2-foot thick basemat with HDPE and borated polythene.

To see how the dose rate changes over time, Figure 3.15 displays the change in dose rate measured from 1 meter above the ground over how many days the reactor and basemat have been removed. It takes approximately 50 to 60 days for all soil compositions to meet the NRC standard. In the first sharp decay slope, the isotopes with the shorter half-lives are reduced. The relatively flat slope that starts around 90 days after the reactor and basemat were removed is dependent on the isotopes that have a half-life longer than 5 years.

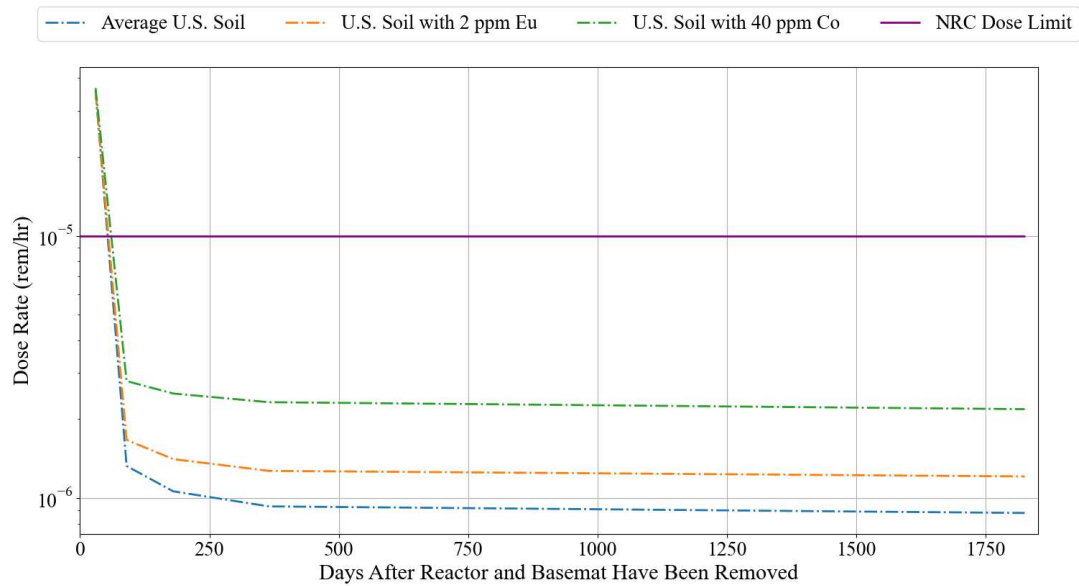


Figure 3.15: Comparison of dose rates measured 1 meter above the ground of U.S. average soil, soil dosed with 2 ppm of Eu, and soil dosed with 40 ppm of Co over how long the reactor and basemat have been removed. Shielding was a 2-foot thick basemat with HDPE and borated polythene.

Similar to the simulations run with average U.S. soil, the dose rate in the europium and cobalt-dosed soil changed at different rates over time, which can be explained by investigating the isotopes that are contributing most to the total decay in both Becquerels and Gamma-Watts. In Figure 3.16, potassium-40 is the main contribution, with the europium isotopes not contributing much, showing that in Becquerels, 2 ppm of europium in the soil has less activity, meaning it has less impact on the total decay in terms of Becquerels. On the other hand, Figure 3.17 shows that beyond sodium-24 and aluminum-28 acting as main contributors to the decay in gamma watts for the first couple of days, the europium radioisotopes play a strong role with potassium-40. The higher energy photons released by both europium radioisotopes, as seen in Table 3.3, give them a higher impact on the total decay, and ultimately the dose. The addition of europium increases the total decay consistently for a longer time period when compared to Figure 3.10 and Figure 3.12. At the same time, the decay energy of europium-154 is less than potassium-40, so once it decays out, the

main contributor remaining to the dose rate will be mostly background radiation. From Table 3.3, Europium-154 has a half-life of 8.601 years, so within two decades, Potassium-40 will remain as the main source for the total decay. The addition of europium increased the total decay for a long period of time (greater than 5 years), which correlates to the higher dose rate than the U.S. average soil simulation as seen in Figure 3.15.

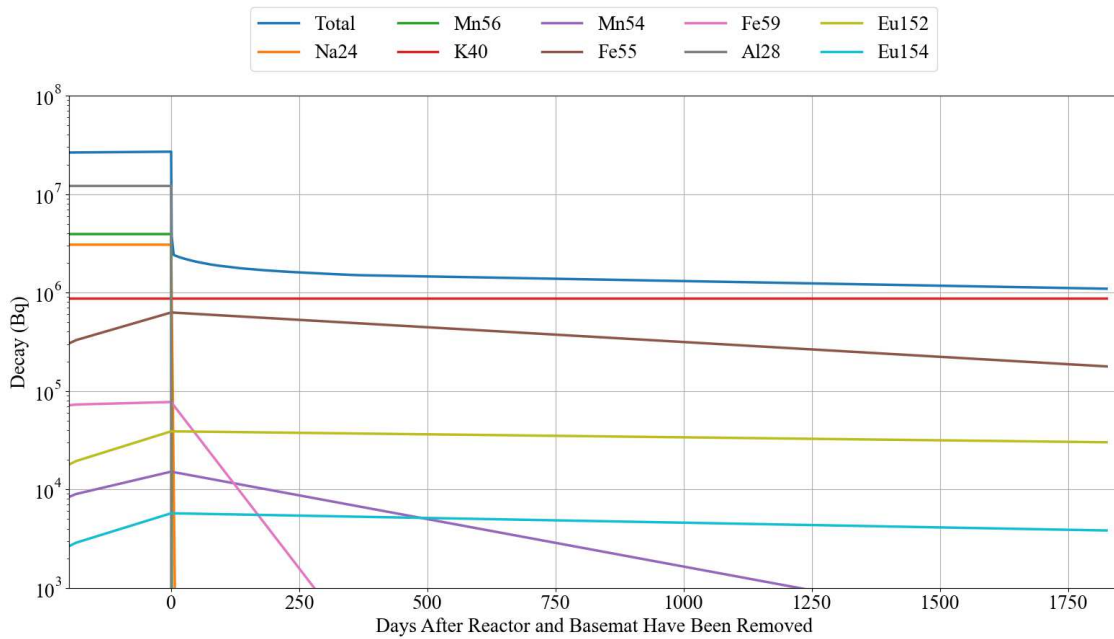


Figure 3.16: Top radioisotopes by activity from the europium-doped soil using 2-foot thick HDPE and borated polyethylene simulation over the time the reactor was running, to after the reactor and basemat were removed (where the negative days represent when the reactor was running) in Becquerels. Total represents the total decay rate of all isotopes.

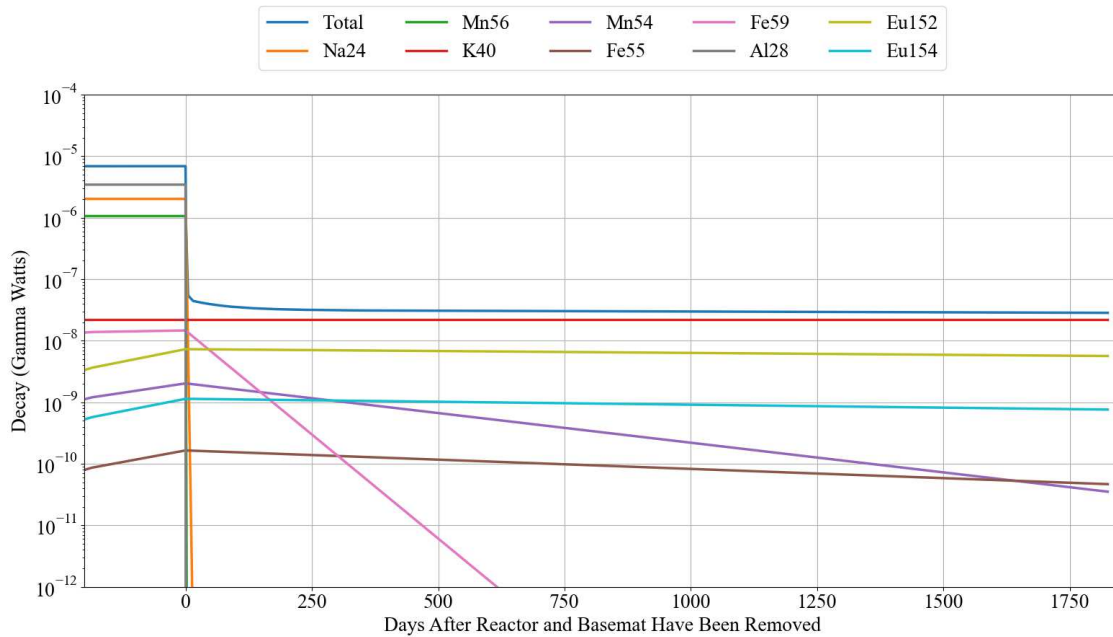


Figure 3.17: Top contributing isotopes to the dose rate from the europium-doped soil using 2-foot thick HDPE and borated polyethylene simulation over the time the reactor was running, to after the reactor and basemat were removed (where the negative days represent when the reactor was running) in Gamma-Watts. Total represents the total decay rate of all isotopes.

The Becquerel plot for the cobalt dose soil is similar to the europium case, as the cobalt-60 has little impact on the total decay rate, as seen in Figure 3.18. In the Gamma-Watts plot, the main isotopes contributing to the dose beyond sodium-24 and aluminum-28 were cobalt-60 and potassium-40, all of which have higher energy photons being released, as shown in Figure 3.19. Table 3.3 shows that cobalt-60 has a half-life of 1925.28 days, so it will contribute more to the total decay than potassium-40 for many years. Eventually, the cobalt decays to a lower energy and potassium-40 takes over. The addition of cobalt to the soil increased the total decay for several decades, which explains the overall higher dose seen in Figure 3.15.

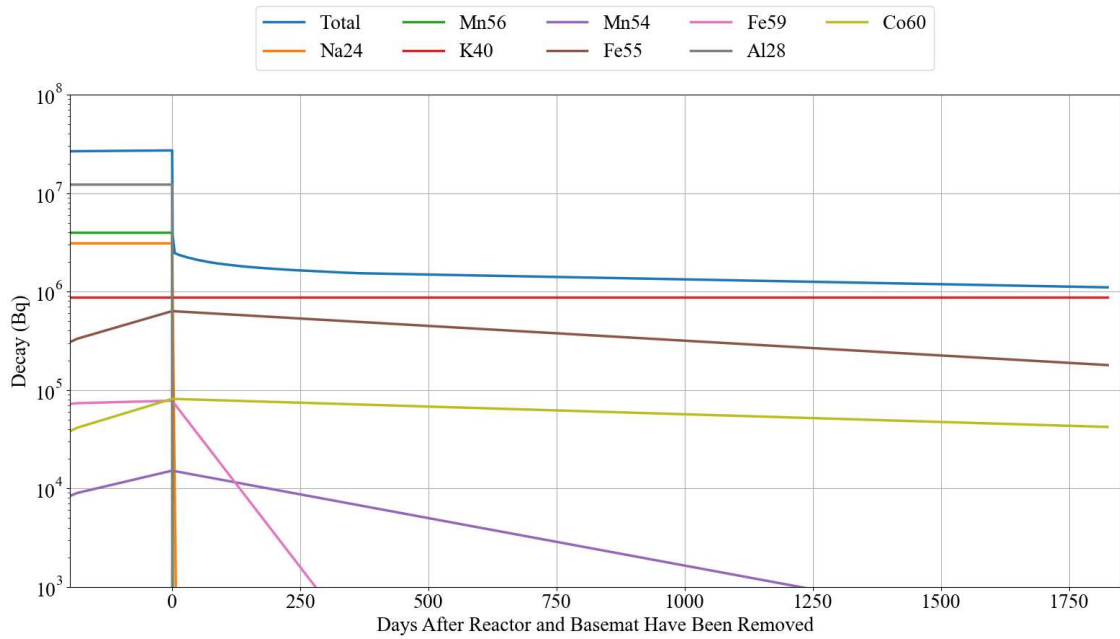


Figure 3.18: Top contributing isotopes to the dose rate from the 2-foot thick cobalt-doped soil using HDPE and borated polyethylene simulation over the time the reactor was running, to after the reactor and basemat were removed (where the negative days represent when the reactor was running) in Becquerels. Total represents the total decay rate of all isotopes.

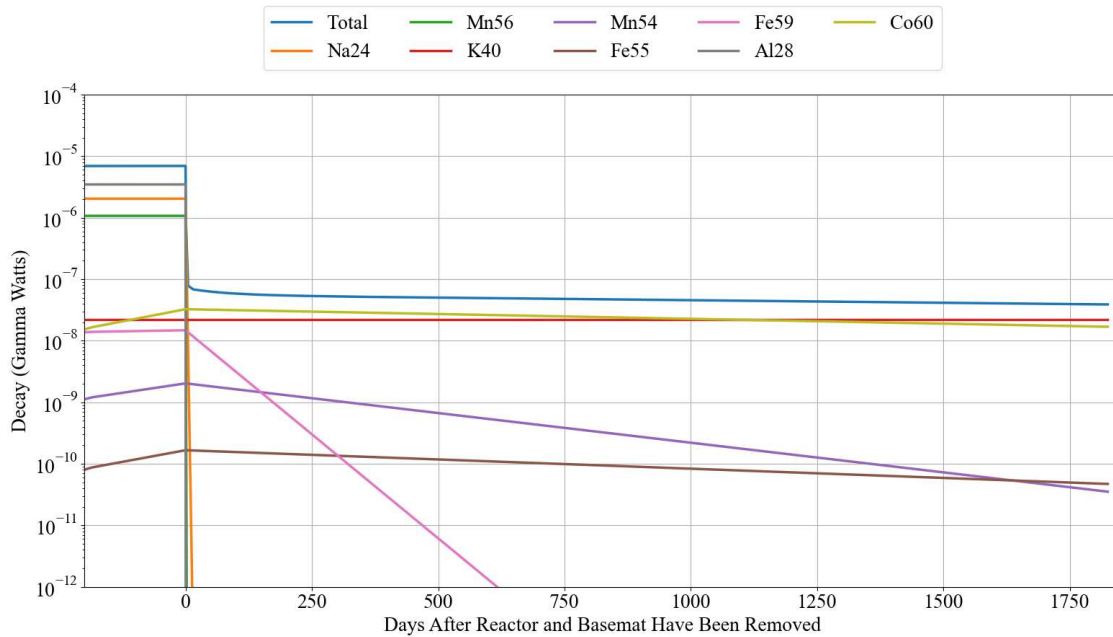


Figure 3.19: Top contributing isotopes to the dose rate from the 2-foot thick cobalt-doped soil using HDPE and borated polyethylene simulation over the time the reactor was running, to after the reactor and basemat were removed (where the negative days represent when the reactor was running) in Gamma-Watts. Total represents the total decay rate of all isotopes.

### 3.2.4 Radioisotope Decay Paths

To understand the source of radioisotopes that contribute to the dose rate, the decay paths for some of the high contributors to the total decay were explored. Sodium-24 and aluminum-28 are strong contributors to the total decay rate for the first couple of days and hours, respectively. The U.S. average soil composition used in the simulations contains 0.614% of sodium-23 by weight ( $2.44 \times 10^{-4}$  atoms per barn-cm) [26]. While the reactor runs, sodium-23 captures a neutron and becomes sodium-24, which beta decays into manganese-24, a stable isotope. The soil composition also contains 6.8564% of Al-27 ( $2.326076 \times 10^{-3}$  in atoms per barn-cm). Aluminum-27 will absorb a neutron while the reactor runs and becomes aluminum-28, a high contributor to the initial total decay value after the reactor and basemat are removed. Aluminum-28 beta decays into silicon-28, which is stable, as

seen in Figure 3.20. The sodium-24 and aluminum-27 in the U.S. average soil composition produce two short-lived, but high-contributing radioisotopes to the initial overall decay rate after the reactor and basemat are removed. Therefore, areas with less sodium-23 and aluminum-27 will most likely decrease the initial overall decay rate, which will contribute to having a lower dose rate immediately after the reactor and basemat are removed.

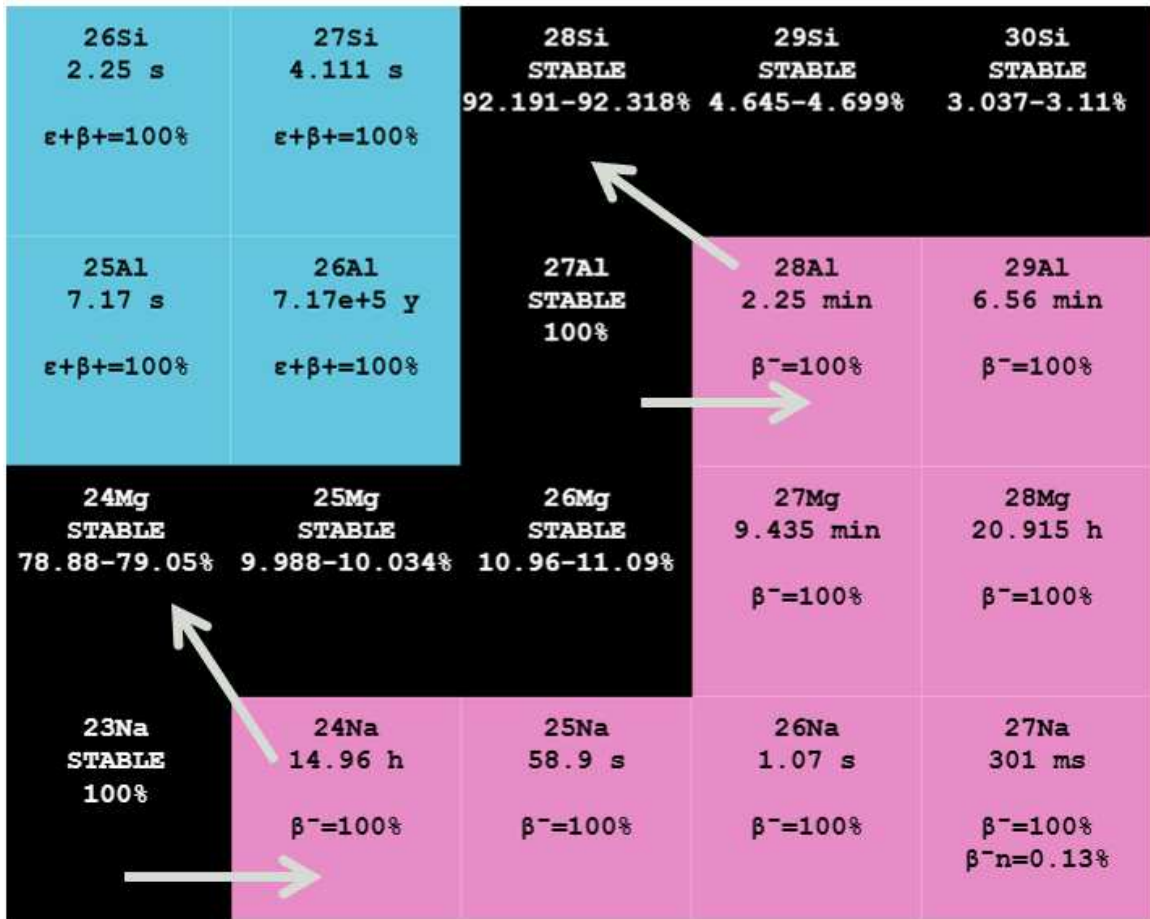


Figure 3.20: Decay path for sodium and aluminum based on the chart of nuclides [44].

Iron plays a strong role in the strength of the total decay after the first couple of days. The soil composition consisted of 5.629% of a combination of iron-54, iron-56, iron-57, and iron-58 (specifically in atoms per barn-cm  $5.392452 \times 10^{-5}$  of iron-54,  $8.464997 \times 10^{-4}$  of iron-56,  $1.954936 \times 10^{-5}$  of iron-57, and  $2.601658 \times 10^{-6}$  of iron-58) [26]. When iron-54 captures a neutron, it becomes iron-55, which has the lowest energy of the main contributors to the total decay. Iron-55 then goes through electron capture to become manganese-55.

On top of the manganese-55 that results from iron-55 decay, the U.S. average soil contains 0.0715% of manganese-55 ( $1.191317 \times 10^{-5}$  atoms-per-barn-cm)[26]. While the reactor is running, the manganese-55 can absorb a neutron to become manganese-56, another radioisotope with a short half-life that contributes to the higher initial overall decay rate after the reactor is removed. Manganese-56 then beta decays into iron-56, which is a stable isotope. Going back to the initial iron concentration in the soil, iron-57 can absorb neutrons to become iron-58, which is still stable. While the reactor runs, iron-58 absorbs a neutron and becomes iron-59, a larger contributor to the total dose for at least 40 days. Iron-59 then beta decays into cobalt-59, which is a stable isotope. In the simulation with soil doped with 40 ppm cobalt-59 ( $6.212902 \times 10^{-7}$  in atoms per barn-cm), the cobalt-59 absorbs a neutron while the reactor runs and becomes cobalt-60, which then beta decays to nickel-60. The produced cobalt-60 has a high gamma-watt value and a longer half-life, making it a large contributor to the total decay in the cobalt-doped soil case for years. The path explained above can be found in Figure 3.21.

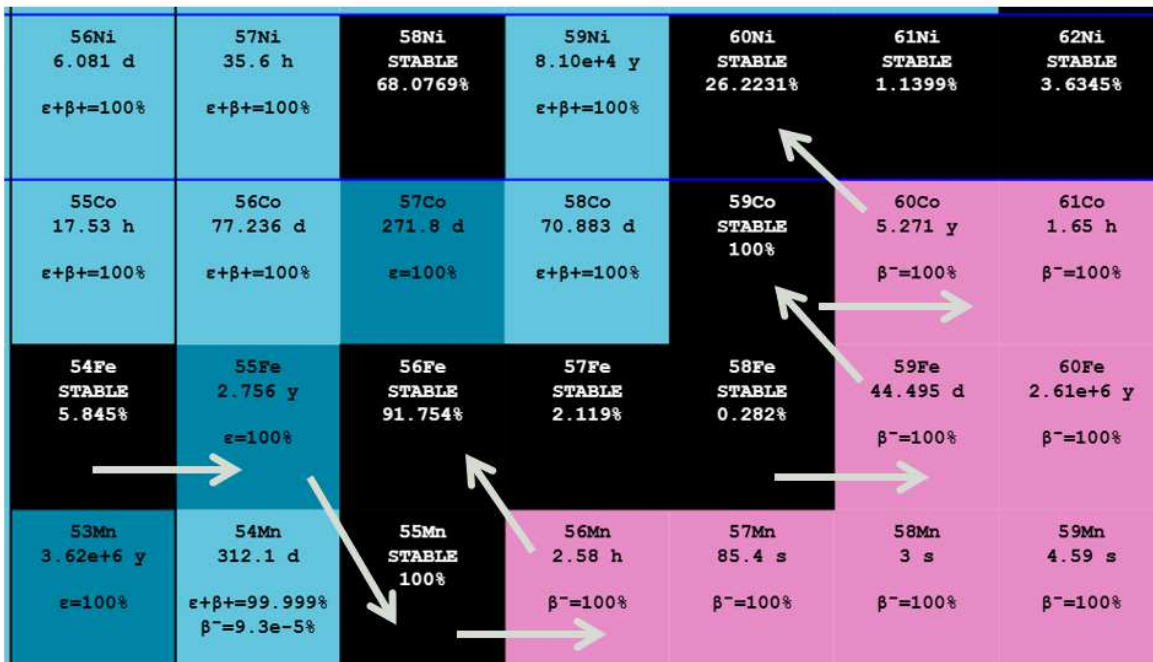


Figure 3.21: Decay path for iron, manganese, and cobalt based on the chart of nuclides [44].

In the soil doped with 2 ppm of europium ( $5.759722 \times 10^{-9}$  of Eu-151 and  $6.287385 \times 10^{-9}$  of E-153 in atoms per barn-cm), there were multiple forms of decay as seen in Figure 3.22. The half-life of europium-151 is  $4.6 \times 10^{18}$  years, which is longer than potassium-40's billion years, which allows it to be qualified as stable [38]. While the reactor runs, europium-151 can absorb a neutron to become europium-152, which has two modes of decay. Most of the time, it will beta decay to samarium-152, which is stable, or will go through electron capture to gadolinium-152, which will go through alpha decay and continue the chain. The long half-life of europium-152, and its decay energy and rate being high, give it a higher influence on the total decay value. Finally, when europium-153 absorbs a neutron while the reactor runs, it becomes europium-154, which most of the time beta decays to gadolinium-154, which is stable. While europium-154 is a strong contributor to the total dose, it has less of an impact than europium-152, which is mostly due to the difference in decay energy. Furthermore. Europium-152 decays to another unstable radioisotope 72% of the time, continuing the decay chain of events.

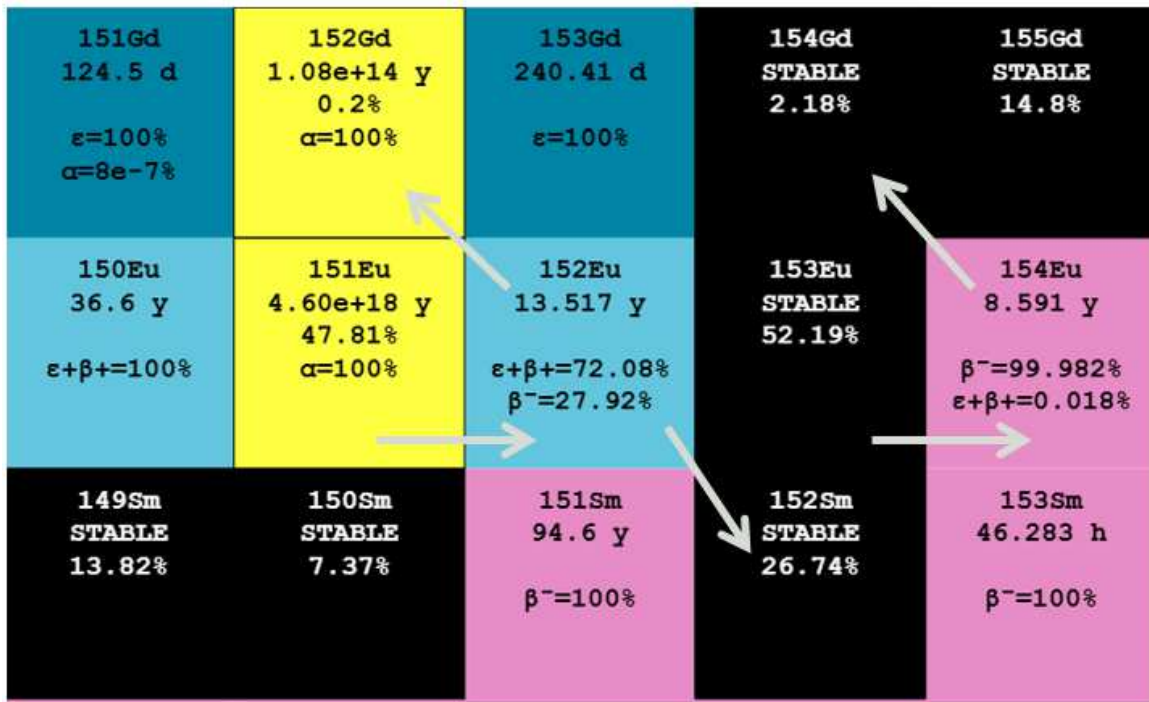


Figure 3.22: Decay path for europium based on the chart of nuclides [44].

### 3.3 Weight and Cost

The material combinations from Table 3.2 were compared by weight and cost. The weights calculated by equations 2.5 and 2.6 can be found in Table 3.4. Utilizing the weight or total volume for each material combination and the material cost from Table 2.1, the material cost for each basemat design is shown in Table 3.5

Table 3.4: List of weights for each basemat combination.

Material Combination (Structural Material & Shielding Material)	Weight (kg)
HDPE & Water	$4.13 * 10^4$
Concrete & Water	$5.98 * 10^4$
HDPE & Borated Polyethylene	$4.14 * 10^4$
Concrete & Borated Polyethylene	$5.99 * 10^4$
HDPE & Concrete	$7.76 * 10^4$
Concrete & Concrete	$1.44 * 10^5$
HDPE & WEP	$4.42 * 10^4$
Concrete & WEP	$9.40 * 10^4$

Table 3.5: Total material cost for each basemat combination.

Material Combination (Structural Material & Shielding Material)	Cost (USD)
HDPE & Water	\$21,891.49
Concrete & Water	\$14,558.75
HDPE & Borated Polyethylene	\$215,164.00
Concrete & Borated Polyethylene	\$294,298.06
HDPE & Concrete	\$24,577.03
Concrete & Concrete	\$12,976.86
HDPE & WEP	\$464,577.91
Concrete & WEP	\$962,102.82

The weight for all material combinations exceeds the maximum weight for common long-haul vehicles in the United States, 36.3 metric tonnes [45]. Despite the heavy load altogether, the basemat's hexagonal unit design allows it to be easily separated into smaller units and dispersed into two or more long-haul vehicles. The lighter material combinations, such as HDPE-water and HDPE-borated polyethylene, can be sent in two trucks, while the materials with concrete would need at least 3 trucks. More trucks increase the logistical difficulty of shipping the basemat to austere environments; therefore, the lighter basemat compositions are optimal.

Each basemat composition is capable of being an effective shield, so the factors that determine if the cost is reasonable are the weight and dose rate. Some of the higher costs may be justifiable if weight is a major concern and if the local area is deeply concerned about the timeline to reduce the dose rate to ALARA standards. Borated polyethylene and WEP are the largest drivers for the more expensive basemats. As seen in Figure 3.9, the structural materials combined with WEP perform worse than when combined with the other shielding materials. Therefore, WEP is not worth the extra cost. On the other hand, basemats containing borated polythene are one of the better-performing radiation shields, making the higher cost more justified. Beyond the basemats with WEP, the highest costing basemat is \$294,298, which is relatively small when compared to the millions of dollars a microreactor costs; ergo, all of the estimated basemat costs beyond the cases with WEP are relatively reasonable.

### **3.4 Decision Matrix**

To empirically determine which basemat composition is optimal, a decision matrix was used. The contributing factors were dose rate, basemat cost, and weight. The dose rate analysis was split into what the dose rate was at each time stamp (30 days, 90 days, 180 days, 1 year, 5 years). Because limiting dose rate is the most important factor, the dose rate section as a whole was weighted at 70%. The 70% was further subdivided into the

dose rate at each time stamp, where importance was placed on 30 and 90 days. The total weight and cost for the basemat were then placed at equal importance of 15%. Within each category, the eight material combinations were given a rank ranging from 1 to 8, where 8 is the best performing and 1 is the worst performing. Then the rank was multiplied by each corresponding weight factor and summed up to obtain the final performance score. The decision matrix, including the weights and individual performance, is shown in Table 3.6.

Table 3.6: Decision matrix to determine the optimum material combination and basemat thickness. The shortened names are concrete (con), water (H2O), and borated polyethylene (BPE).

Criterion	Weight	HDPE-H2O	Con-H2O	HDPE-BPE	Con-BPE	HDPE-Con	Con-Con	HDPE-WEP	Con-WEP
Dose Rate (30 Days)	0.2	8	2	6	5	7	3	4	1
Dose Rate (90 Days)	0.2	8	2	7	5	6	4	3	1
Dose Rate (180 Days)	0.15	7	2	8	5	6	4	3	1
Dose Rate (1 year)	0.1	7	3	8	4	5	6	1	2
Dose Rate (5 years)	0.05	6	2	7	4	5	8	1	3
Basemat Cost	0.15	5	6	1	3	2	7	4	8
Basemat Weight	0.15	8	5	7	4	3	1	6	2
Total Score	1	7.35	3.3	6.6	4.4	5.45	4.35	3.2	1.35

The decision matrix in Table 3.6 defined the 2-foot basemat using HDPE and water as the optimum basemat. The amount of hydrogen in both materials resulted in more neutron moderation, which lowered the overall dose rate. Furthermore, the hydrogen content yielded a lighter basemat. The low cost of high-purity water positioned the design among the more cost-effective material combinations. Despite this, one issue with HDPE and water that is not addressed by the decision matrix is water evaporation. PWRs use closed systems and water replacement to combat water evaporation. Because the basemat is not a closed system, continuously replacing water is not ideal, especially when being used in a post-disaster response. If water is to be used in the basemat design, then measures to prevent evaporation must be explored. Therefore, the next best basemat design is truly the optimal design, a 2-foot basemat consisting of HDPE and borated polyethylene. While this design is twice as expensive as the water and HDPE case, it is one of the lightest designs and is an effective radiation shield. WEP is not a material to be used in the future; its poor shielding performance and its high cost prevent it from being a viable lightweight shielding solution. The HDPE and concrete basemat provide a more reasonable alternative solution, with the pre-cured concrete acting as a compromised solution, for as long as weight is not a concern. However, the cost difference between the two is around \$190,000, which may be a cost that is worthwhile to reduce the dose rate in the long run. The concrete-concrete basemat is in the bottom half of the total score of the decision matrix. This exemplifies how lightweight shielding materials can outperform concrete as a radiation shield for the price of a higher total cost. The optimal design will vary based on what criteria are of higher concern. Changes to the importance values (referred to as weight in Table 3.6) may change which material combination is optimal. For the importance values used in this and including the evaporation issue with water, the HDPE and borated polyethylene with a thickness of 2 feet is the optimal basemat design.

d in this paper, the HDPE and borated polyethylene with a thickness of 2 feet is the optimum basemat design.

## CHAPTER 4

### CONCLUSION

Deployable microreactors have the potential to provide consistent energy after a natural disaster to speed up recovery. A rapidly deployable external shielding application is required to maintain the logistical requirements of a deployable microreactor responding to a natural disaster. Typical shielding applications, such as layers of concrete (that are poured on site), impede the timeline to reactor setup, creating the need for the application of transportable lightweight shielding materials, defined as a basemat. This paper explored a design consisting of two different materials, a lightweight radiation shielding material and a lightweight structural material, to provide an apparatus that holds the weight of the reactor and acts as an effective radiation shield. Concrete was also explored to see if using pre-cured concrete and transporting it to the site is a worthwhile solution. The basemat design consisted of a hexagonal mesh for strength and to allow a shielding material to structural material ratio of 2:1. 12 different material combinations were explored with 6 different overall thicknesses to determine the optimum material combination and basemat thickness.

A SCALE model was developed to evaluate all 72 different material and thickness combinations. From the simulations, the combinations with concrete, water, WEP, HDPE, and borated polyethylene met the NRC standard, assuming 24/7 exposure year-round with a thickness of 2 to 3 feet. The combinations with aluminum did not meet the NRC requirement and were excluded from further analysis. Of the eight remaining material combinations, the radioisotopes were explored. The material combinations with HDPE, Water, or borated polyethylene acted as better shields and were able to limit the main contributor to the decay rate to potassium-40 in a couple of days, which is considered background radiation. The cases with concrete and WEP did not perform as well and needed around 200 days to have potassium-40 as the main contributor to the total decay. The extra time needed

is a result of iron-59 dominating the total decay value for about 200 days, indicating that Concrete and WEP have difficulty in shielding against iron-59. However, the combinations without aluminum all attenuated the radiation to background radiation within one year, effectively meeting the ALARA requirement.

After the shielding was tested, the material cost and overall weight were obtained to help determine which shielding combination is optimal. The basemats containing concrete were heavier and required more trucks for transportation than the other materials. In turn for lighter weight, the cost was generally increased. The decision matrix placed the highest importance on shielding ability (0.7), and weight and cost were weighted equally (0.15 each). In this weighting scheme, the HDPE-water 2-foot combination won. However, evaporation is a high concern, so the HDPE-borated polyethylene 2-foot basemat was defined as the optimal basemat. WEP was determined to be too expensive and was one of the worst shielding performers; therefore, it is not recommended. The concrete-only basemat, while cheap, is too heavy, and it was in the bottom half of shielding performance; hence, it is also not recommended. However, other material combinations are viable solutions, depending on which criteria are important. If weight and how low the dose rate is under the NRC limit are less of a concern, while the budget is small, then pre-cured concrete and HDPE may be a good compromise choice. On the other hand, if weight and dose rate are a concern instead of cost, then the HDPE and borated polythene basemat is the best choice. Ultimately, combinations of HDPE, borated polyethylene, or concrete are the top-performing material combinations to use as a lightweight radiation shield for the soil directly underneath a rapidly deployed microreactor.

In the future, a more in-depth cost analysis needs to be done to include the cost of labor to build the basemat and the cost of transportation. Additionally, more research needs to be conducted to see if the complexity of the basemat design could be reduced. For example, is it reasonable to remove the inner hexagonal mesh for each hexagonal unit? Research is needed to see how long the basemat will stay irradiated before it can be reused at another

site. Finally, more research is needed to expand the shielding design to account for the radiation in all directions, not just the radiation sent directly below the reactor.

# **Appendices**

**APPENDIX A**  
**ADDITIONAL PLOTS**

The following plots are the energy vs neutron flux plots for the other basemat thicknesses not shown.

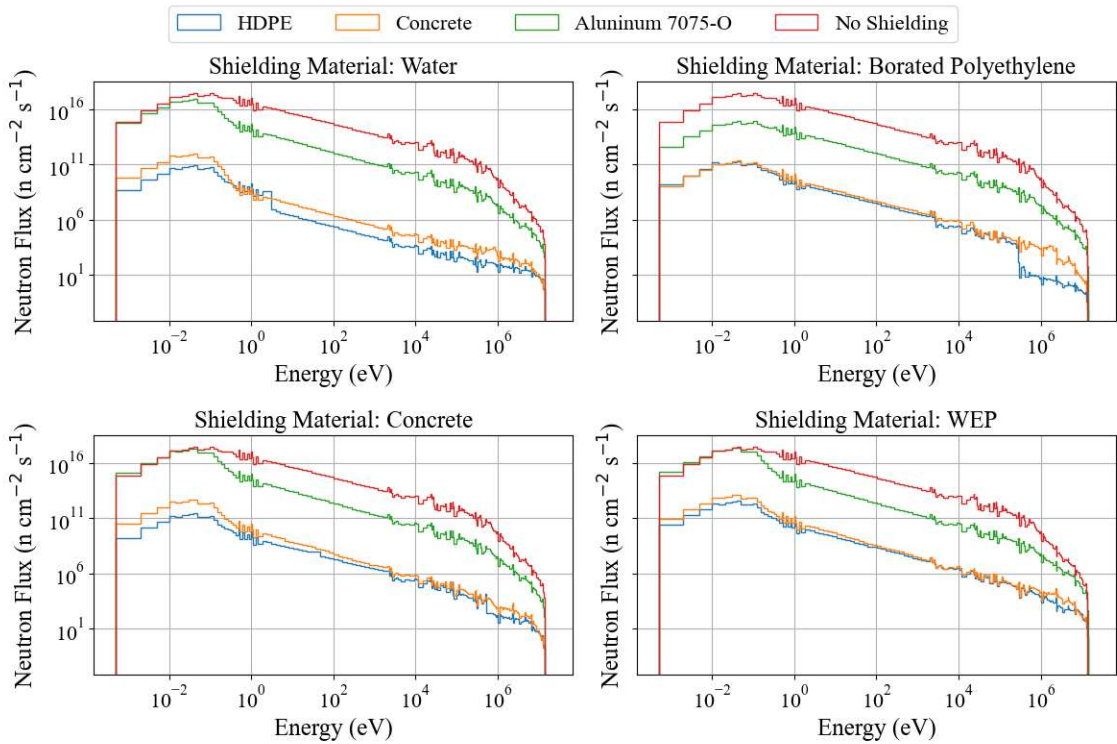


Figure A.1: Energy versus neutron flux plot for the 3-foot thick basemat separated by shielding material, and comparing the shielding material and its paired structural material.

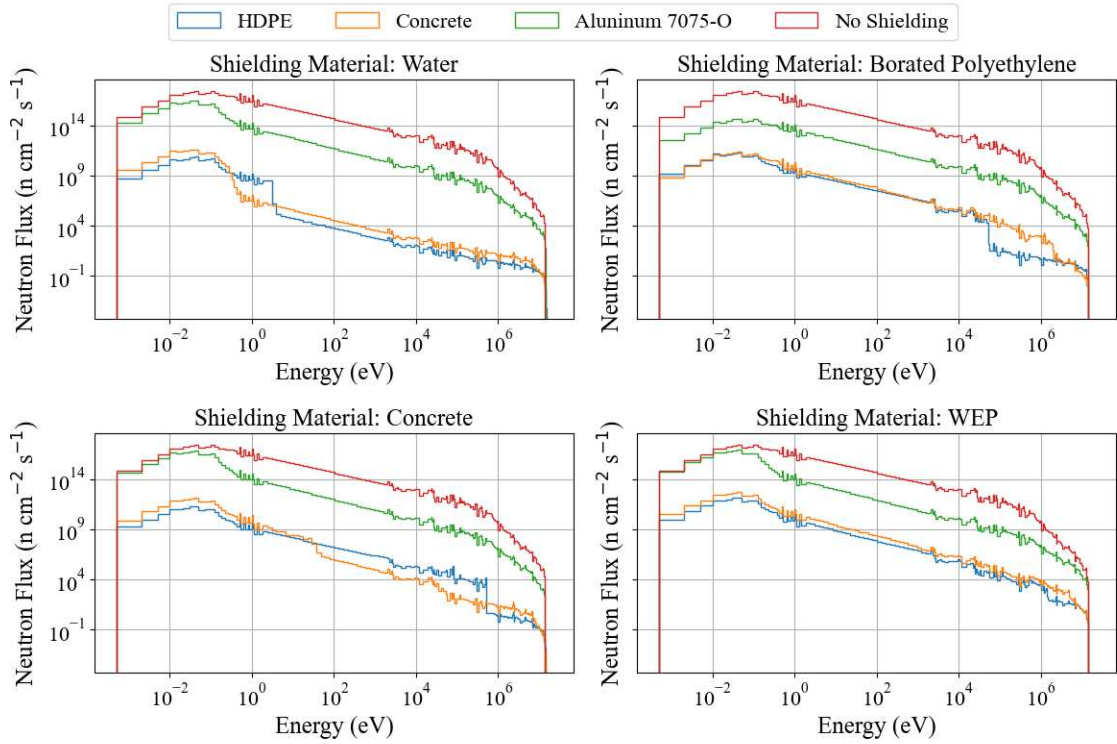


Figure A.2: Energy versus neutron flux plot for the 4-foot thick basemat separated by shielding material, and comparing the shielding material and its paired structural material.

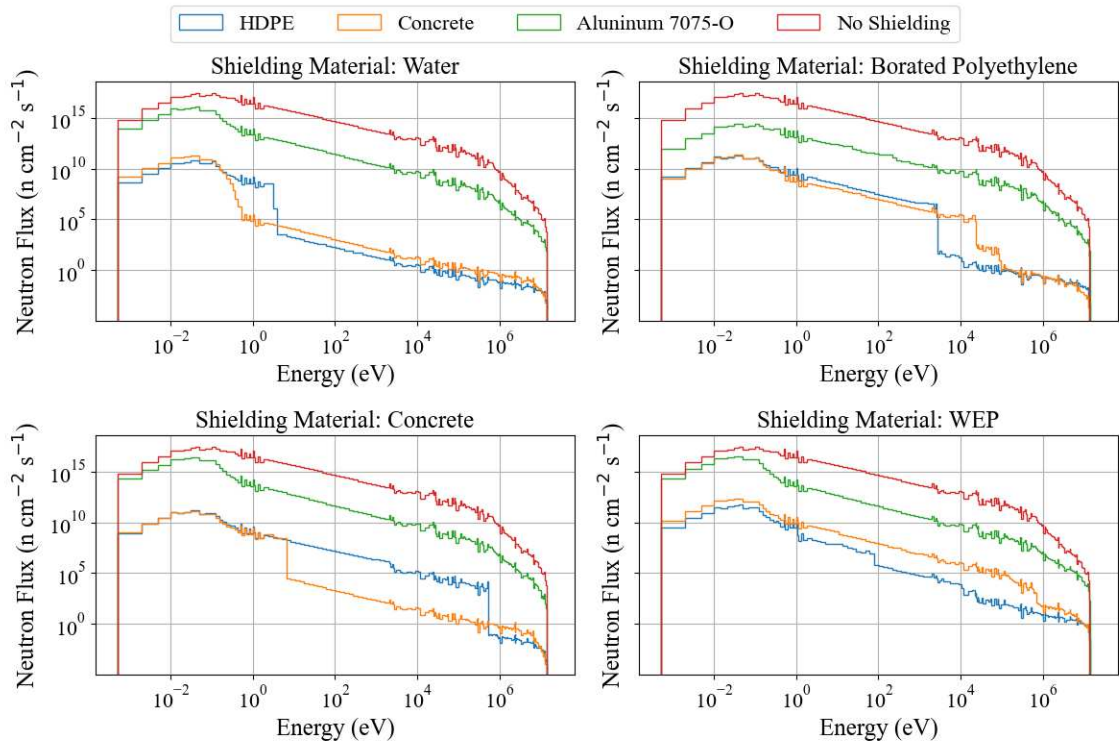


Figure A.3: Energy versus neutron flux plot for the 5-foot thick basemat separated by shielding material, and comparing the shielding material and its paired structural material.

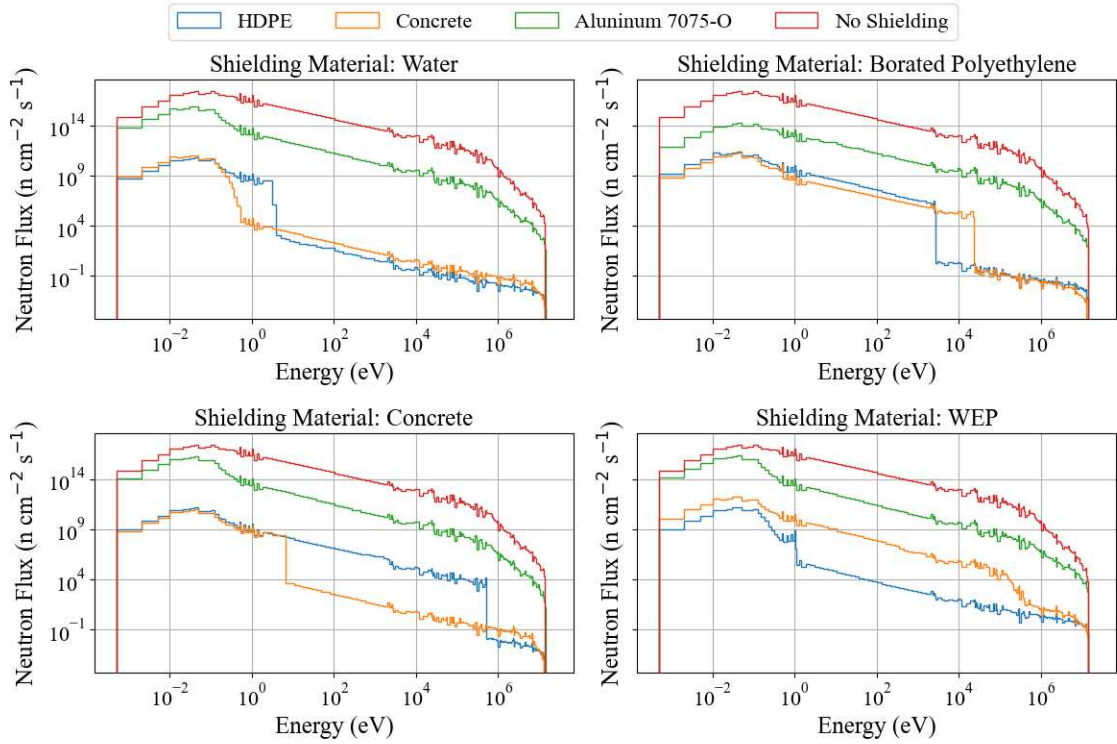


Figure A.4: Energy versus neutron flux plot for the 5.5-foot thick basemat separated by shielding material, and comparing the shielding material and its paired structural material.

The following plots are the decay plots containing the main contributing isotopes for the six other basemat material combinations in units of Becquerels and Gamma-Watts.

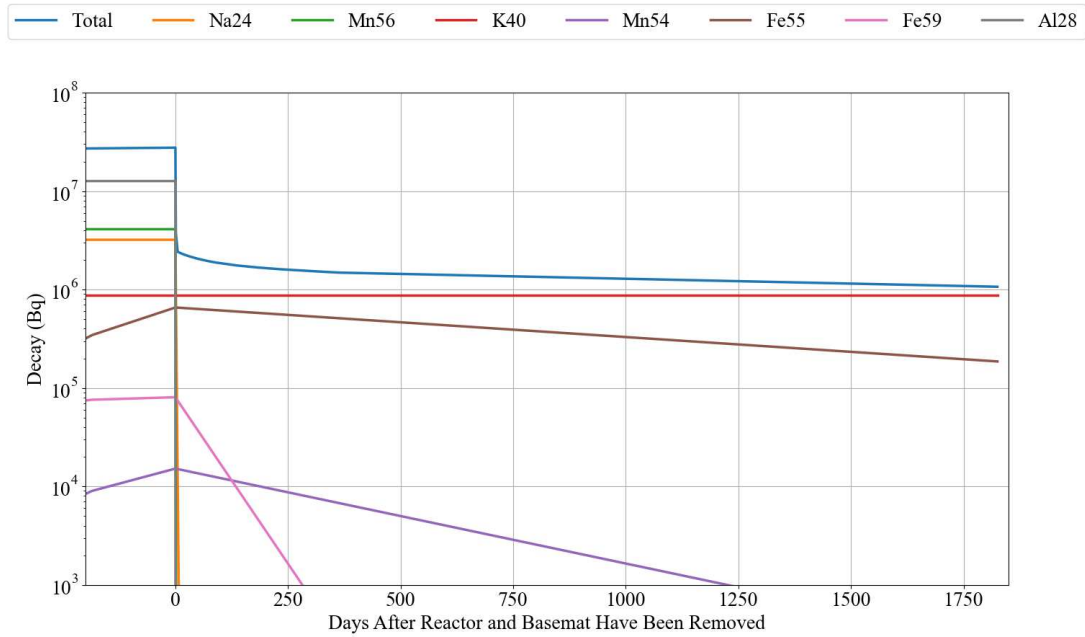


Figure A.5: Top contributing isotopes to the dose rate from U.S. average soil using 2-feet of HDPE and borated polyethylene simulation over the time the reactor was running to after the reactor and basemat were removed (where the negative days represent when the reactor was running) in Becquerels. Total represents the total decay rate of all isotopes.

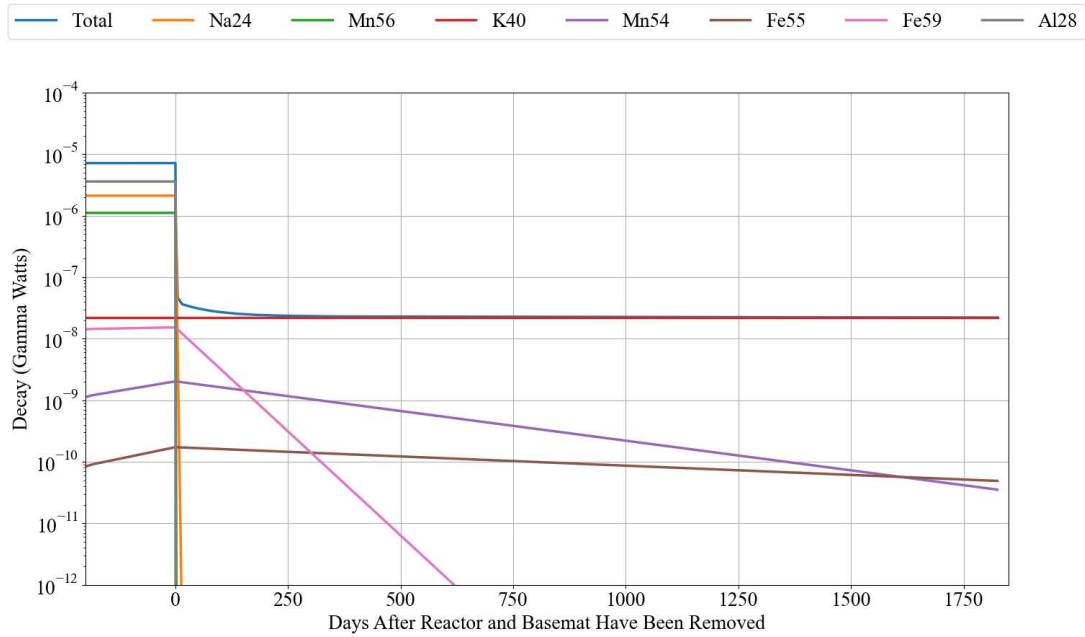


Figure A.6: Top contributing isotopes to the dose rate from U.S. average soil using 2-feet of HDPE and borated polyethylene simulation over the time the reactor was running to after the reactor and basemat were removed (where the negative days represent when the reactor was running) in Gamma-Watts. Total represents the total decay rate of all isotopes.

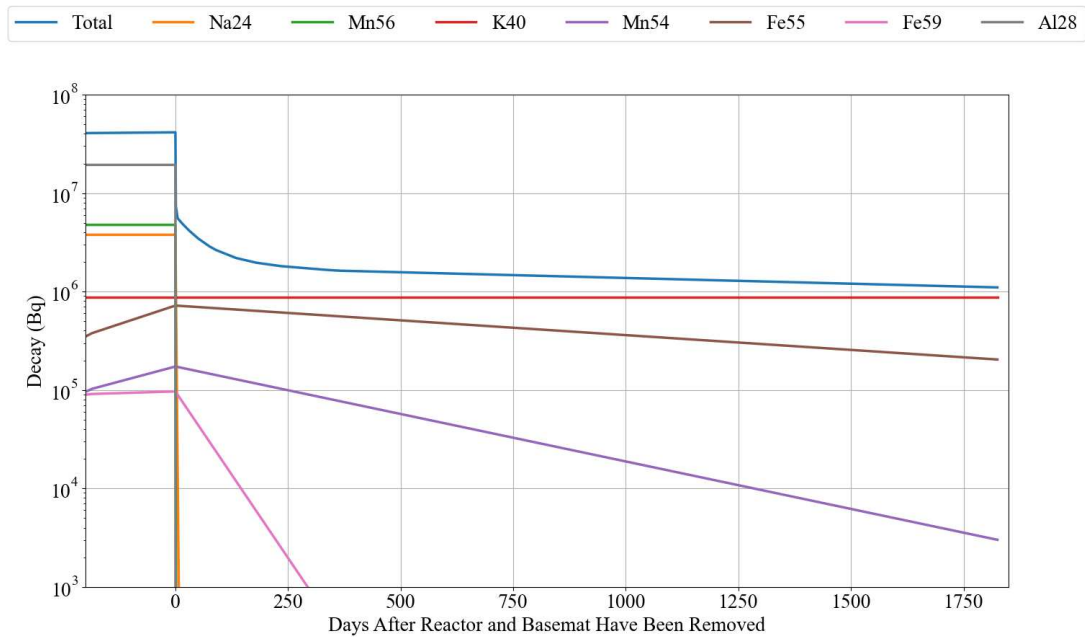


Figure A.7: Top contributing isotopes to the dose rate from U.S. average soil using 2-feet of concrete and borated polyethylene simulation over the time the reactor was running to after the reactor and basemat were removed (where the negative days represent when the reactor was running) in Becquerels. Total represents the total decay rate of all isotopes.

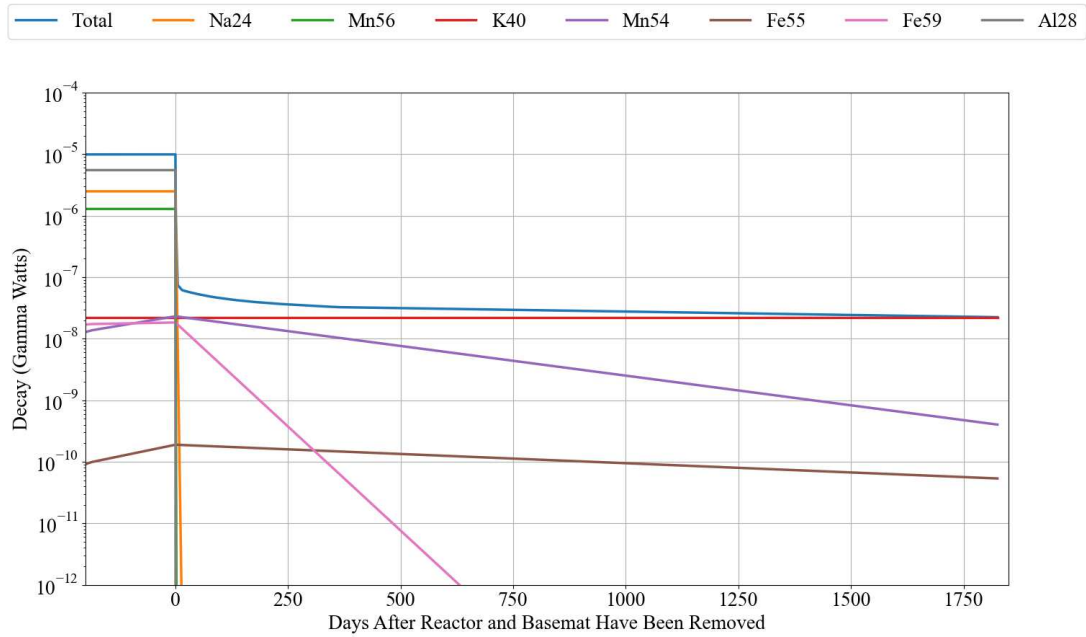


Figure A.8: Top contributing isotopes to the dose rate from U.S. average soil using 2-feet of concrete and borated polyethylene simulation over the time the reactor was running to after the reactor and basemat were removed (where the negative days represent when the reactor was running) in Gamma-Watts. Total represents the total decay rate of all isotopes.

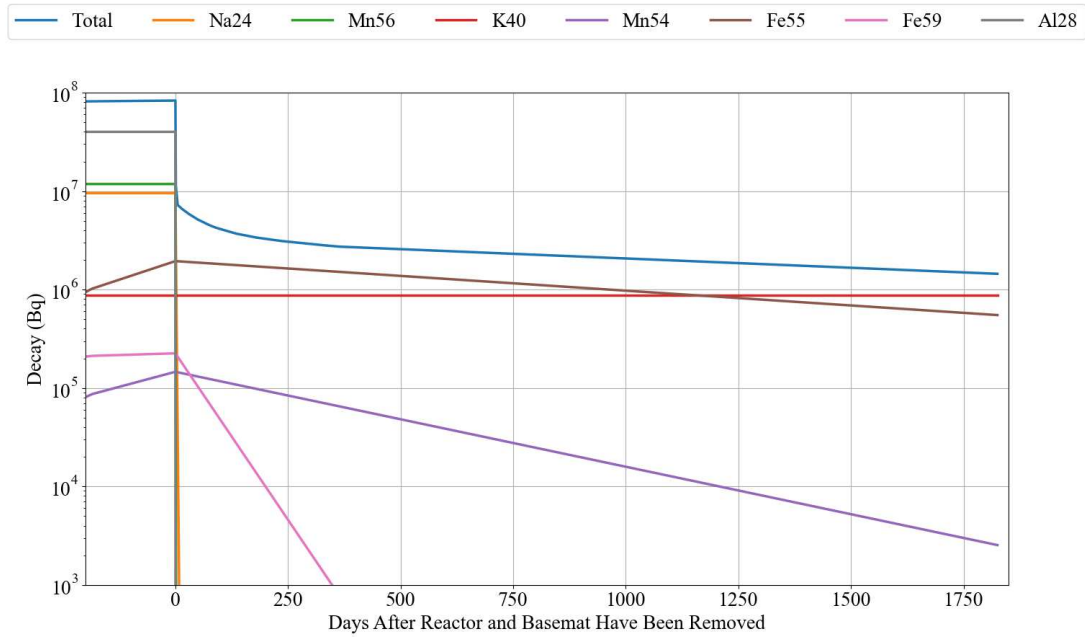


Figure A.9: Top contributing isotopes to the dose rate from U.S. average soil using 2-feet of HDPE and concrete simulation over the time the reactor was running to after the reactor and basemat were removed (where the negative days represent when the reactor was running) in Becquerels. Total represents the total decay rate of all isotopes.

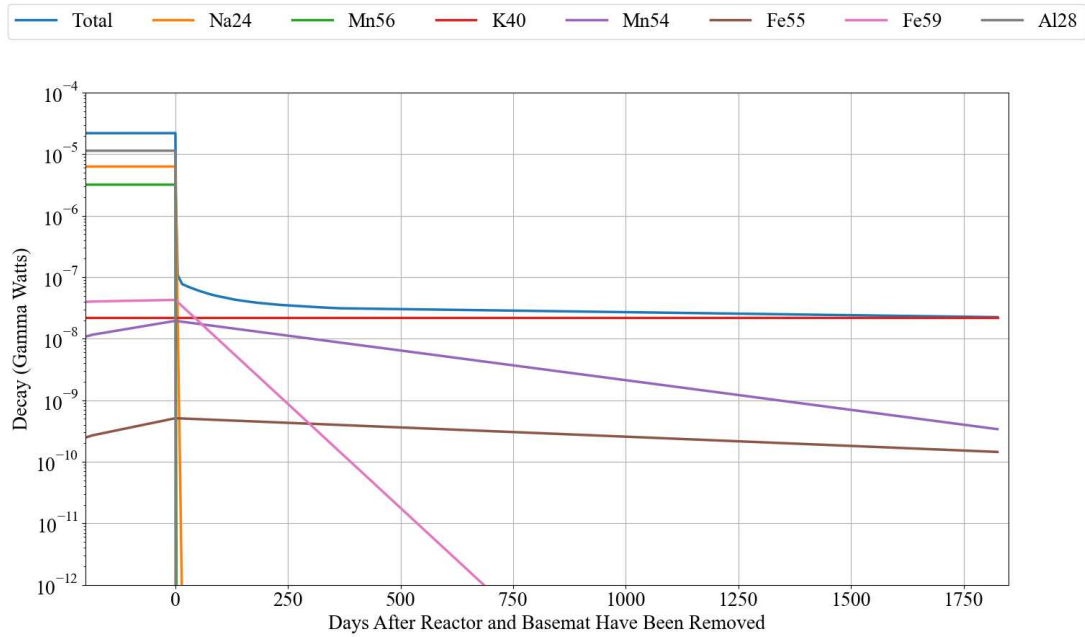


Figure A.10: Top contributing isotopes to the dose rate from U.S. average soil using 2-foot of HDPE and concrete simulation over the time the reactor was running to after the reactor and basemat were removed (where the negative days represent when the reactor was running) in Gamma-Watts. Total represents the total decay rate of all isotopes.

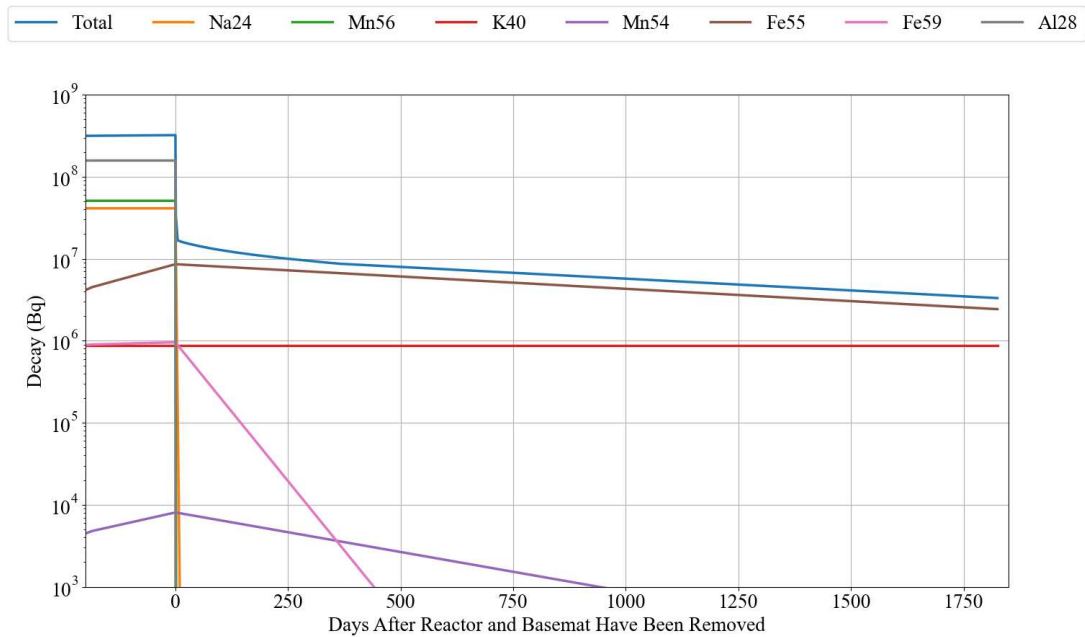


Figure A.11: Top contributing isotopes to the dose rate from U.S. average soil using 3-foot of concrete and concrete simulation over the time the reactor was running to after the reactor and basemat were removed (where the negative days represent when the reactor was running) in Becquerels. Total represents the total decay rate of all isotopes.

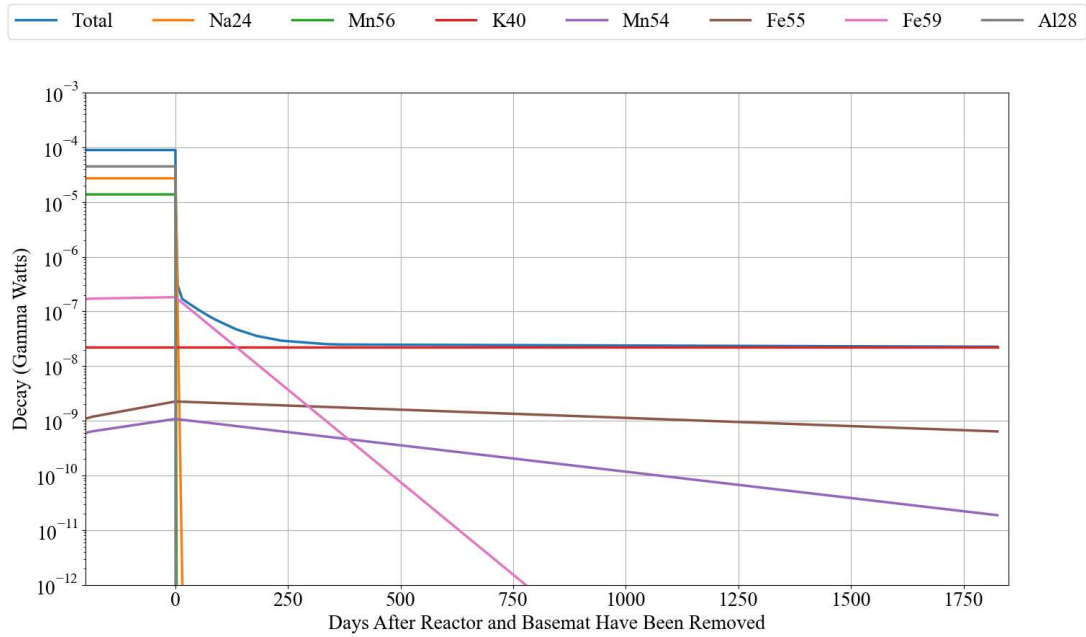


Figure A.12: Top contributing isotopes to the dose rate from U.S. average soil using 3-feet of concrete and concrete simulation over the time the reactor was running to after the reactor and basemat were removed (where the negative days represent when the reactor was running) in Gamma-Watts. Total represents the total decay rate of all isotopes.

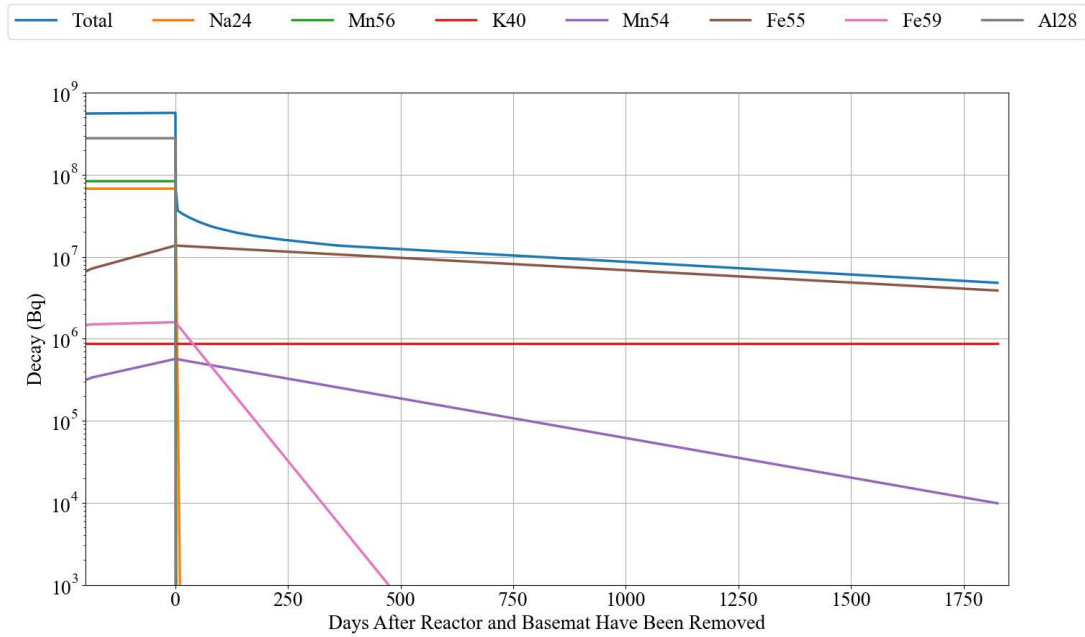


Figure A.13: Top contributing isotopes to the dose rate from U.S. average soil using 2-feet of HDPE and WEP simulation over the time the reactor was running to after the reactor and basemat were removed (where the negative days represent when the reactor was running) in Becquerels. Total represents the total decay rate of all isotopes.

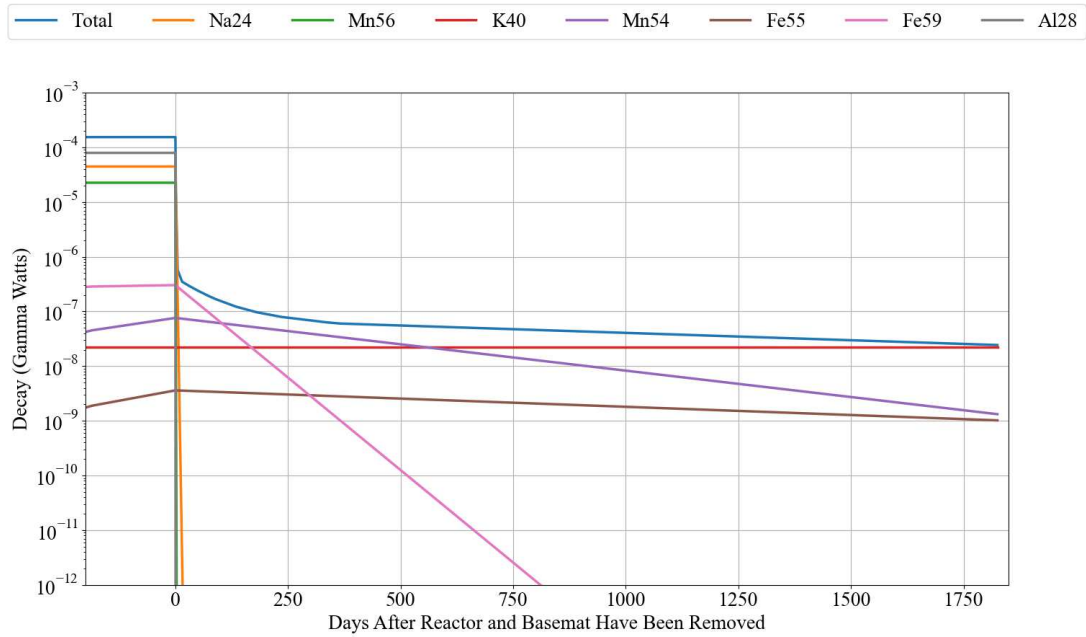


Figure A.14: Top contributing isotopes to the dose rate from U.S. average soil using 2-feet of HDPE and WEP simulation over the time the reactor was running to after the reactor and basemat were removed (where the negative days represent when the reactor was running) in Gamma-Watts. Total represents the total decay rate of all isotopes.

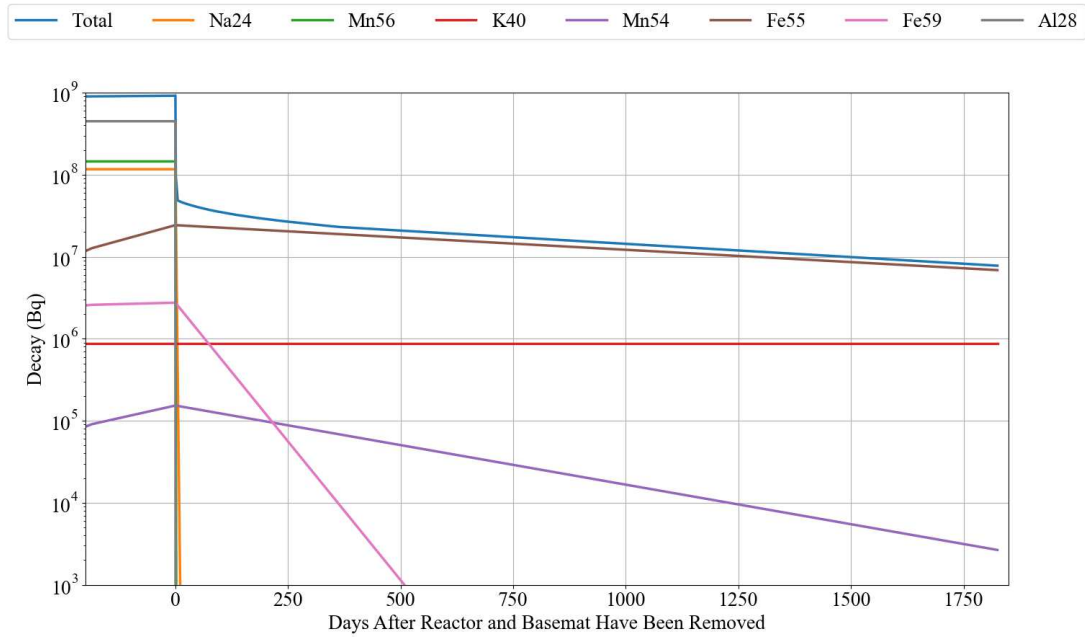


Figure A.15: Top contributing isotopes to the dose rate from U.S. average soil using 3-foot of concrete and WEP simulation over the time the reactor was running to after the reactor and basemat were removed (where the negative days represent when the reactor was running) in Becquerels. Total represents the total decay rate of all isotopes.

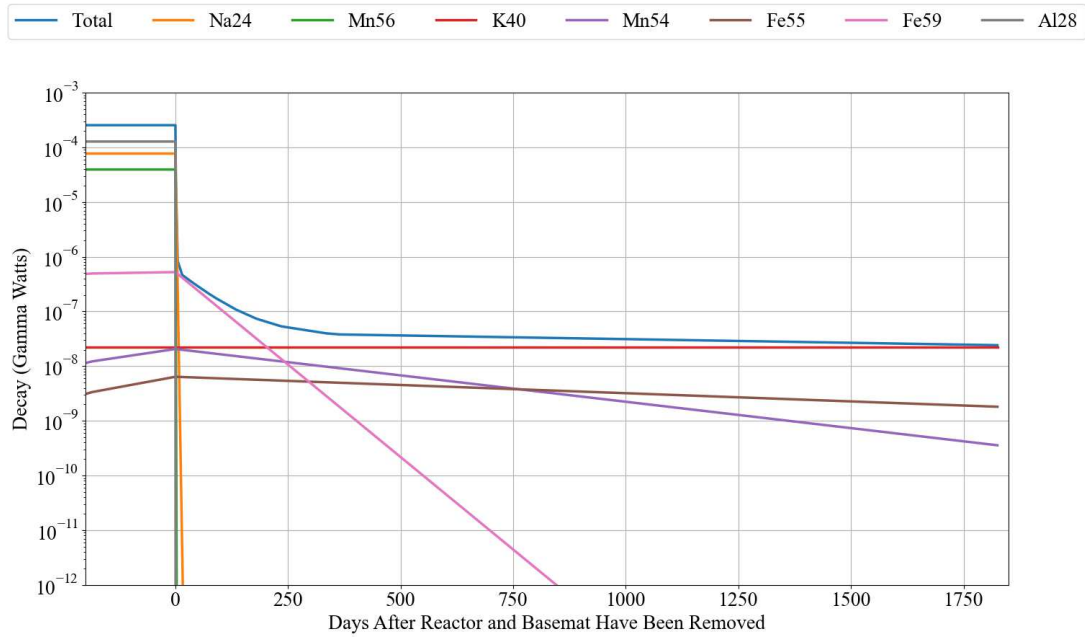


Figure A.16: Top contributing isotopes to the dose rate from U.S. average soil using 3-foot of concrete and WEP simulation over the time the reactor was running to after the reactor and basemat were removed (where the negative days represent when the reactor was running) in Gamma-Watts. Total represents the total decay rate of all isotopes.

## APPENDIX B

### SCALE CODE

Example of CSAS Code using the 2-foot of HDPE and water basemat. The material cards for all materials are included in the materials section.

```
=csas6 parm=( )
CSAS6 Basemat
v7.1-252

read parameters
npg=1000000
gen=550
nsk=50
flx=Yes
gfx=Yes
cds=Yes
nub=yes

end parameters

read gridGeometry 1
  xlinear 152 -381 381
  ylinear 55 -137.16 137.16
  zlinear 138 -363.83 304.8
end gridGeometry

read comp
'Mat1 = Air'
'Mat 2 =HDPE '
'Mat 3 = Water'
'Mat 20000s = U.S. Avg Soil'
'Mat 5 = Carbon Graphite 90%, UO2(U234-0.0267% U235-15% U236-0.0138% U238-94.9595%) 5%, Helium 5%'
'Mat 6 = Graphite'
'Mat 7 = Stainless Steel'
'Mat 10 = Borated Poly
'Mat 11 = Concrete
'Mat 12 = Water Extended Polyester
'Mat 13 = Aluminum

C-12 1 0 7.531249e-09 293.00 end
C-13 1 0 8.145595e-11 293.00 end
N-14 1 0 3.898657e-05 293.00 end
N-15 1 0 1.424234e-07 293.00 end
O-16 1 0 1.048711e-05 293.00 end
O-17 1 0 4.012723e-09 293.00 end
O-18 1 0 2.177106e-08 293.00 end
Ar-36 1 0 7.840725e-10 293.00 end
Ar-38 1 0 1.472621e-10 293.00 end
Ar-40 1 0 2.320771e-07 293.00 end

H-1 2 0 8.328176e-02 293.00 end
H-2 2 0 9.570963e-06 293.00 end
C-12 2 0 4.119978e-02 293.00 end
C-13 2 0 4.456057e-04 293.00 end

H-1 3 0 6.664754e-02 293.00 end
H-2 3 0 7.750656e-06 293.00 end
O-16 3 0 3.324666e-02 293.00 end
O-17 3 0 1.267984e-05 293.00 end
O-18 3 0 6.831622e-05 293.00 end
He-3 5 0 1.945879e-08 900.00 end
He-4 5 0 1.466252e-02 900.00 end
B-11 5 0 9.595416e-08 900.00 end
C-12 5 0 8.701254e-02 900.00 end
C-13 5 0 9.411041e-04 900.00 end
```

O-16 5 0 4.384330e-04 900.00 end  
O-17 5 0 2.761943e-07 900.00 end  
O-18 5 0 9.553593e-07 900.00 end  
U-234 5 0 5.804549e-08 900.00 end  
U-235 5 0 3.260983e-05 900.00 end  
U-238 5 0 1.847310e-04 900.00 end

B-11 6 0 9.299077e-08 273.00 end  
C-12 6 0 8.432530e-02 273.00 end  
C-13 6 0 9.120396e-04 273.00 end

C-12 7 0 3.174602e-04 273.00 end  
C-13 7 0 3.433564e-06 273.00 end  
Si-28 7 0 1.581969e-03 273.00 end  
Si-29 7 0 8.036526e-05 273.00 end  
Si-30 7 0 5.303936e-05 273.00 end  
P-31 7 0 6.999380e-05 273.00 end  
S-32 7 0 4.281655e-05 273.00 end  
S-33 7 0 3.380609e-07 273.00 end  
S-34 7 0 1.915680e-06 273.00 end  
S-36 7 0 4.507480e-09 273.00 end  
Cr-50 7 0 7.649153e-04 273.00 end  
Cr-52 7 0 1.475063e-02 273.00 end  
Cr-53 7 0 1.672603e-03 273.00 end  
Cr-54 7 0 4.163463e-04 273.00 end  
Mn-55 7 0 1.753871e-03 273.00 end  
Fe-54 7 0 3.446250e-03 273.00 end  
Fe-56 7 0 5.409876e-02 273.00 end  
Fe-57 7 0 1.249376e-03 273.00 end  
Fe-58 7 0 1.662688e-04 273.00 end  
Ni-58 7 0 5.308544e-03 273.00 end  
Ni-60 7 0 2.044842e-03 273.00 end  
Ni-61 7 0 8.888785e-05 273.00 end  
Ni-62 7 0 2.834134e-04 273.00 end  
Ni-64 7 0 7.217708e-05 273.00 end

C-12 8 0 3.819444e-04 293.00 end  
C-13 8 0 4.131007e-06 293.00 end  
P-31 8 0 2.245634e-04 293.00 end  
S-32 8 0 1.305309e-03 293.00 end  
Cr-52 8 0 4.463808e-04 293.00 end  
Mn-55 8 0 2.110127e-04 293.00 end  
Fe-56 8 0 8.066244e-02 293.00 end  
Ni-58 8 0 2.401151e-04 293.00 end  
Cu-63 8 0 3.684315e-04 293.00 end

H-1 10 0 7.488434e-02 293.00 end  
H-2 10 0 8.670975e-06 293.00 end  
B-10 10 0 1.108266e-03 293.00 end  
B-11 10 0 4.460821e-03 293.00 end  
C-12 10 0 3.842484e-02 293.00 end  
C-13 10 0 4.155927e-04 293.00 end

H-1 11 0 3.036448e-02 293.0 end  
H-2 11 0 3.438490e-06 293.0 end  
C-12 11 0 2.833928e-04 293.0 end  
C-13 11 0 3.065100e-06 293.0 end  
O-16 11 0 4.965171e-02 293.0 end  
O-17 11 0 1.890341e-05 293.0 end  
O-18 11 0 1.020399e-04 293.0 end  
Na-23 11 0 9.162548e-04 293.0 end  
Mg-24 11 0 5.698861e-05 293.0 end  
Mg-25 11 0 7.214662e-06 293.0 end  
Mg-26 11 0 7.943343e-06 293.0 end  
Al-27 11 0 1.024284e-03 293.0 end  
Si-28 11 0 1.385493e-02 293.0 end  
Si-29 11 0 7.038410e-04 293.0 end  
Si-30 11 0 4.645201e-04 293.0 end  
K-39 11 0 3.318619e-04 293.0 end  
K-40 11 0 4.163462e-08 293.0 end  
K-41 11 0 2.394963e-05 293.0 end  
Ca-40 11 0 1.438975e-03 293.0 end  
Ca-42 11 0 9.603948e-06 293.0 end

Ca-43 11 0 2.003922e-06 293.0 end  
Ca-44 11 0 3.096422e-05 293.0 end  
Ca-46 11 0 5.936982e-08 293.0 end  
Ca-48 11 0 2.775799e-06 293.0 end  
Fe-54 11 0 9.328814e-06 293.0 end  
Fe-56 11 0 1.464424e-04 293.0 end  
Fe-57 11 0 3.381994e-06 293.0 end  
Fe-58 11 0 4.500807e-07 293.0 end

H-1 12 7.011662e-02 293.0 end  
H-2 12 8.064493e-06 293.0 end  
C-12 12 1.518502e-02 293.0 end  
C-13 12 1.642370e-04 293.0 end  
O-16 12 2.953176e-02 293.0 end  
O-17 12 1.124928e-05 293.0 end  
O-18 12 6.068762e-05 293.0 end

Mg-24 13 1.374906e-03 293.00 end  
Mg-25 13 1.740607e-04 293.00 end  
Mg-26 13 1.916409e-04 293.00 end  
Al-27 13 5.597560e-02 293.00 end  
Si-28 13 1.301927e-04 293.00 end  
Si-29 13 6.613890e-06 293.00 end  
Si-30 13 4.365027e-06 293.00 end  
Ti-46 13 3.415342e-06 293.00 end  
Ti-47 13 3.080018e-06 293.00 end  
Ti-48 13 3.051867e-05 293.00 end  
Ti-49 13 2.239636e-06 293.00 end  
Ti-50 13 2.144421e-06 293.00 end  
Cr-50 13 3.252399e-06 293.00 end  
Cr-52 13 6.271929e-05 293.00 end  
Cr-53 13 7.111864e-06 293.00 end  
Cr-54 13 1.770293e-06 293.00 end  
Mn-55 13 5.411976e-05 293.00 end  
Fe-54 13 5.187710e-06 293.00 end  
Fe-56 13 8.143597e-05 293.00 end  
Fe-57 13 1.880711e-06 293.00 end  
Fe-58 13 2.502878e-07 293.00 end  
Cu-63 13 2.946327e-04 293.00 end  
Cu-65 13 1.314450e-04 293.00 end  
Zn-64 13 6.993087e-04 293.00 end  
Zn-66 13 4.053029e-04 293.00 end  
Zn-67 13 5.942994e-05 293.00 end  
Zn-68 13 2.756205e-04 293.00 end  
Zn-70 13 9.141958e-06 293.00 end

O-16 200001 0 2.931950e-02 293.00 end  
O-17 200001 0 1.114649e-05 293.00 end  
O-18 200001 0 6.026437e-05 293.00 end  
Na-23 200001 0 2.444715e-04 293.00 end  
Mg-24 200001 0 3.957787e-04 293.00 end  
Mg-25 200001 0 5.010491e-05 293.00 end  
Mg-26 200001 0 5.516551e-05 293.00 end  
Al-27 200001 0 2.326076e-03 293.00 end  
Si-28 200001 0 8.150971e-03 293.00 end  
Si-29 200001 0 4.140756e-04 293.00 end  
Si-30 200001 0 2.732811e-04 293.00 end  
K-39 200001 0 3.128084e-04 293.00 end  
K-40 200001 0 3.924422e-08 293.00 end  
K-41 200001 0 2.257459e-05 293.00 end  
Ca-40 200001 0 1.132863e-03 293.00 end  
Ca-42 200001 0 7.560904e-06 293.00 end  
Ca-43 200001 0 1.577628e-06 293.00 end  
Ca-44 200001 0 2.437722e-05 293.00 end  
Ca-46 200001 0 4.674011e-08 293.00 end  
Ca-48 200001 0 2.185305e-06 293.00 end  
Ti-46 200001 0 7.263565e-06 293.00 end  
Ti-47 200001 0 6.550416e-06 293.00 end  
Ti-48 200001 0 6.490546e-05 293.00 end  
Ti-49 200001 0 4.763137e-06 293.00 end  
Ti-50 200001 0 4.560639e-06 293.00 end  
Mn-55 200001 0 1.191317e-05 293.00 end  
Fe-54 200001 0 5.392452e-05 293.00 end

Fe-56 200001 0 8.464997e-04 293.00 end  
Fe-57 200001 0 1.954936e-05 293.00 end  
Fe-58 200001 0 2.601658e-06 293.00 end  
O-16 200002 0 2.931950e-02 293.00 end  
O-17 200002 0 1.114649e-05 293.00 end  
O-18 200002 0 6.026437e-05 293.00 end  
Na-23 200002 0 2.444715e-04 293.00 end  
Mg-24 200002 0 3.957787e-04 293.00 end  
Mg-25 200002 0 5.010491e-05 293.00 end  
Mg-26 200002 0 5.516551e-05 293.00 end  
Al-27 200002 0 2.326076e-03 293.00 end  
Si-28 200002 0 8.150971e-03 293.00 end  
Si-29 200002 0 4.140756e-04 293.00 end  
Si-30 200002 0 2.732811e-04 293.00 end  
K-39 200002 0 3.128084e-04 293.00 end  
K-40 200002 0 3.924422e-08 293.00 end  
K-41 200002 0 2.257459e-05 293.00 end  
Ca-40 200002 0 1.132863e-03 293.00 end  
Ca-42 200002 0 7.560904e-06 293.00 end  
Ca-43 200002 0 1.577628e-06 293.00 end  
Ca-44 200002 0 2.437722e-05 293.00 end  
Ca-46 200002 0 4.674011e-08 293.00 end  
Ca-48 200002 0 2.185305e-06 293.00 end  
Ti-46 200002 0 7.263565e-06 293.00 end  
Ti-47 200002 0 6.550416e-06 293.00 end  
Ti-48 200002 0 6.490546e-05 293.00 end  
Ti-49 200002 0 4.763137e-06 293.00 end  
Ti-50 200002 0 4.560639e-06 293.00 end  
Mn-55 200002 0 1.191317e-05 293.00 end  
Fe-54 200002 0 5.392452e-05 293.00 end  
Fe-56 200002 0 8.464997e-04 293.00 end  
Fe-57 200002 0 1.954936e-05 293.00 end  
Fe-58 200002 0 2.601658e-06 293.00 end  
O-16 200003 0 2.931950e-02 293.00 end  
O-17 200003 0 1.114649e-05 293.00 end  
O-18 200003 0 6.026437e-05 293.00 end  
Na-23 200003 0 2.444715e-04 293.00 end  
Mg-24 200003 0 3.957787e-04 293.00 end  
Mg-25 200003 0 5.010491e-05 293.00 end  
Mg-26 200003 0 5.516551e-05 293.00 end  
Al-27 200003 0 2.326076e-03 293.00 end  
Si-28 200003 0 8.150971e-03 293.00 end  
Si-29 200003 0 4.140756e-04 293.00 end  
Si-30 200003 0 2.732811e-04 293.00 end  
K-39 200003 0 3.128084e-04 293.00 end  
K-40 200003 0 3.924422e-08 293.00 end  
K-41 200003 0 2.257459e-05 293.00 end  
Ca-40 200003 0 1.132863e-03 293.00 end  
Ca-42 200003 0 7.560904e-06 293.00 end  
Ca-43 200003 0 1.577628e-06 293.00 end  
Ca-44 200003 0 2.437722e-05 293.00 end  
Ca-46 200003 0 4.674011e-08 293.00 end  
Ca-48 200003 0 2.185305e-06 293.00 end  
Ti-46 200003 0 7.263565e-06 293.00 end  
Ti-47 200003 0 6.550416e-06 293.00 end  
Ti-48 200003 0 6.490546e-05 293.00 end  
Ti-49 200003 0 4.763137e-06 293.00 end  
Ti-50 200003 0 4.560639e-06 293.00 end  
Mn-55 200003 0 1.191317e-05 293.00 end  
Fe-54 200003 0 5.392452e-05 293.00 end  
Fe-56 200003 0 8.464997e-04 293.00 end  
Fe-57 200003 0 1.954936e-05 293.00 end  
Fe-58 200003 0 2.601658e-06 293.00 end  
O-16 200004 0 2.931950e-02 293.00 end  
O-17 200004 0 1.114649e-05 293.00 end  
O-18 200004 0 6.026437e-05 293.00 end  
Na-23 200004 0 2.444715e-04 293.00 end  
Mg-24 200004 0 3.957787e-04 293.00 end  
Mg-25 200004 0 5.010491e-05 293.00 end  
Mg-26 200004 0 5.516551e-05 293.00 end  
Al-27 200004 0 2.326076e-03 293.00 end  
Si-28 200004 0 8.150971e-03 293.00 end  
Si-29 200004 0 4.140756e-04 293.00 end

Si-30 200004 0 2.732811e-04 293.00 end  
 K-39 200004 0 3.128084e-04 293.00 end  
 K-40 200004 0 3.924422e-08 293.00 end  
 K-41 200004 0 2.257459e-05 293.00 end  
 Ca-40 200004 0 1.132863e-03 293.00 end  
 Ca-42 200004 0 7.560904e-06 293.00 end  
 Ca-43 200004 0 1.577628e-06 293.00 end  
 Ca-44 200004 0 2.437722e-05 293.00 end  
 Ca-46 200004 0 4.674011e-08 293.00 end  
 Ca-48 200004 0 2.185305e-06 293.00 end  
 Ti-46 200004 0 7.263565e-06 293.00 end  
 Ti-47 200004 0 6.550416e-06 293.00 end  
 Ti-48 200004 0 6.490546e-05 293.00 end  
 Ti-49 200004 0 4.763137e-06 293.00 end  
 Ti-50 200004 0 4.560639e-06 293.00 end  
 Mn-55 200004 0 1.191317e-05 293.00 end  
 Fe-54 200004 0 5.392452e-05 293.00 end  
 Fe-56 200004 0 8.464997e-04 293.00 end  
 Fe-57 200004 0 1.954936e-05 293.00 end  
 Fe-58 200004 0 2.601658e-06 293.00 end  
 O-16 200005 0 2.931950e-02 293.00 end  
 O-17 200005 0 1.114649e-05 293.00 end  
 O-18 200005 0 6.026437e-05 293.00 end  
 Na-23 200005 0 2.444715e-04 293.00 end  
 Mg-24 200005 0 3.957787e-04 293.00 end  
 Mg-25 200005 0 5.010491e-05 293.00 end  
 Mg-26 200005 0 5.516551e-05 293.00 end  
 Al-27 200005 0 2.326076e-03 293.00 end  
 Si-28 200005 0 8.150971e-03 293.00 end  
 Si-29 200005 0 4.140756e-04 293.00 end  
 Si-30 200005 0 2.732811e-04 293.00 end  
 K-39 200005 0 3.128084e-04 293.00 end  
 K-40 200005 0 3.924422e-08 293.00 end  
 K-41 200005 0 2.257459e-05 293.00 end  
 Ca-40 200005 0 1.132863e-03 293.00 end  
 Ca-42 200005 0 7.560904e-06 293.00 end  
 Ca-43 200005 0 1.577628e-06 293.00 end  
 Ca-44 200005 0 2.437722e-05 293.00 end  
 Ca-46 200005 0 4.674011e-08 293.00 end  
 Ca-48 200005 0 2.185305e-06 293.00 end  
 Ti-46 200005 0 7.263565e-06 293.00 end  
 Ti-47 200005 0 6.550416e-06 293.00 end  
 Ti-48 200005 0 6.490546e-05 293.00 end  
 Ti-49 200005 0 4.763137e-06 293.00 end  
 Ti-50 200005 0 4.560639e-06 293.00 end  
 Mn-55 200005 0 1.191317e-05 293.00 end  
 Fe-54 200005 0 5.392452e-05 293.00 end  
 Fe-56 200005 0 8.464997e-04 293.00 end  
 Fe-57 200005 0 1.954936e-05 293.00 end  
 Fe-58 200005 0 2.601658e-06 293.00 end  
 O-16 200006 0 2.931950e-02 293.00 end  
 O-17 200006 0 1.114649e-05 293.00 end  
 O-18 200006 0 6.026437e-05 293.00 end  
 Na-23 200006 0 2.444715e-04 293.00 end  
 Mg-24 200006 0 3.957787e-04 293.00 end  
 Mg-25 200006 0 5.010491e-05 293.00 end  
 Mg-26 200006 0 5.516551e-05 293.00 end  
 Al-27 200006 0 2.326076e-03 293.00 end  
 Si-28 200006 0 8.150971e-03 293.00 end  
 Si-29 200006 0 4.140756e-04 293.00 end  
 Si-30 200006 0 2.732811e-04 293.00 end  
 K-39 200006 0 3.128084e-04 293.00 end  
 K-40 200006 0 3.924422e-08 293.00 end  
 K-41 200006 0 2.257459e-05 293.00 end  
 Ca-40 200006 0 1.132863e-03 293.00 end  
 Ca-42 200006 0 7.560904e-06 293.00 end  
 Ca-43 200006 0 1.577628e-06 293.00 end  
 Ca-44 200006 0 2.437722e-05 293.00 end  
 Ca-46 200006 0 4.674011e-08 293.00 end  
 Ca-48 200006 0 2.185305e-06 293.00 end  
 Ti-46 200006 0 7.263565e-06 293.00 end  
 Ti-47 200006 0 6.550416e-06 293.00 end  
 Ti-48 200006 0 6.490546e-05 293.00 end

Ti-49 200006 0 4.763137e-06 293.00 end  
Ti-50 200006 0 4.560639e-06 293.00 end  
Mn-55 200006 0 1.191317e-05 293.00 end  
Fe-54 200006 0 5.392452e-05 293.00 end  
Fe-56 200006 0 8.464997e-04 293.00 end  
Fe-57 200006 0 1.954936e-05 293.00 end  
Fe-58 200006 0 2.601658e-06 293.00 end  
O-16 200007 0 2.931950e-02 293.00 end  
O-17 200007 0 1.114649e-05 293.00 end  
O-18 200007 0 6.026437e-05 293.00 end  
Na-23 200007 0 2.444715e-04 293.00 end  
Mg-24 200007 0 3.957787e-04 293.00 end  
Mg-25 200007 0 5.010491e-05 293.00 end  
Mg-26 200007 0 5.516551e-05 293.00 end  
Al-27 200007 0 2.326076e-03 293.00 end  
Si-28 200007 0 8.150971e-03 293.00 end  
Si-29 200007 0 4.140756e-04 293.00 end  
Si-30 200007 0 2.732811e-04 293.00 end  
K-39 200007 0 3.128084e-04 293.00 end  
K-40 200007 0 3.924422e-08 293.00 end  
K-41 200007 0 2.257459e-05 293.00 end  
Ca-40 200007 0 1.132863e-03 293.00 end  
Ca-42 200007 0 7.560904e-06 293.00 end  
Ca-43 200007 0 1.577628e-06 293.00 end  
Ca-44 200007 0 2.437722e-05 293.00 end  
Ca-46 200007 0 4.674011e-08 293.00 end  
Ca-48 200007 0 2.185305e-06 293.00 end  
Ti-46 200007 0 7.263565e-06 293.00 end  
Ti-47 200007 0 6.550416e-06 293.00 end  
Ti-48 200007 0 6.490546e-05 293.00 end  
Ti-49 200007 0 4.763137e-06 293.00 end  
Ti-50 200007 0 4.560639e-06 293.00 end  
Mn-55 200007 0 1.191317e-05 293.00 end  
Fe-54 200007 0 5.392452e-05 293.00 end  
Fe-56 200007 0 8.464997e-04 293.00 end  
Fe-57 200007 0 1.954936e-05 293.00 end  
Fe-58 200007 0 2.601658e-06 293.00 end  
O-16 200008 0 2.931950e-02 293.00 end  
O-17 200008 0 1.114649e-05 293.00 end  
O-18 200008 0 6.026437e-05 293.00 end  
Na-23 200008 0 2.444715e-04 293.00 end  
Mg-24 200008 0 3.957787e-04 293.00 end  
Mg-25 200008 0 5.010491e-05 293.00 end  
Mg-26 200008 0 5.516551e-05 293.00 end  
Al-27 200008 0 2.326076e-03 293.00 end  
Si-28 200008 0 8.150971e-03 293.00 end  
Si-29 200008 0 4.140756e-04 293.00 end  
Si-30 200008 0 2.732811e-04 293.00 end  
K-39 200008 0 3.128084e-04 293.00 end  
K-40 200008 0 3.924422e-08 293.00 end  
K-41 200008 0 2.257459e-05 293.00 end  
Ca-40 200008 0 1.132863e-03 293.00 end  
Ca-42 200008 0 7.560904e-06 293.00 end  
Ca-43 200008 0 1.577628e-06 293.00 end  
Ca-44 200008 0 2.437722e-05 293.00 end  
Ca-46 200008 0 4.674011e-08 293.00 end  
Ca-48 200008 0 2.185305e-06 293.00 end  
Ti-46 200008 0 7.263565e-06 293.00 end  
Ti-47 200008 0 6.550416e-06 293.00 end  
Ti-48 200008 0 6.490546e-05 293.00 end  
Ti-49 200008 0 4.763137e-06 293.00 end  
Ti-50 200008 0 4.560639e-06 293.00 end  
Mn-55 200008 0 1.191317e-05 293.00 end  
Fe-54 200008 0 5.392452e-05 293.00 end  
Fe-56 200008 0 8.464997e-04 293.00 end  
Fe-57 200008 0 1.954936e-05 293.00 end  
Fe-58 200008 0 2.601658e-06 293.00 end  
O-16 200009 0 2.931950e-02 293.00 end  
O-17 200009 0 1.114649e-05 293.00 end  
O-18 200009 0 6.026437e-05 293.00 end  
Na-23 200009 0 2.444715e-04 293.00 end  
Mg-24 200009 0 3.957787e-04 293.00 end  
Mg-25 200009 0 5.010491e-05 293.00 end

Mg-26 200009 0 5.516551e-05 293.00 end  
Al-27 200009 0 2.326076e-03 293.00 end  
Si-28 200009 0 8.150971e-03 293.00 end  
Si-29 200009 0 4.140756e-04 293.00 end  
Si-30 200009 0 2.732811e-04 293.00 end  
K-39 200009 0 3.128084e-04 293.00 end  
K-40 200009 0 3.924422e-08 293.00 end  
K-41 200009 0 2.257459e-05 293.00 end  
Ca-40 200009 0 1.132863e-03 293.00 end  
Ca-42 200009 0 7.560904e-06 293.00 end  
Ca-43 200009 0 1.577628e-06 293.00 end  
Ca-44 200009 0 2.437722e-05 293.00 end  
Ca-46 200009 0 4.674011e-08 293.00 end  
Ca-48 200009 0 2.185305e-06 293.00 end  
Ti-46 200009 0 7.263565e-06 293.00 end  
Ti-47 200009 0 6.550416e-06 293.00 end  
Ti-48 200009 0 6.490546e-05 293.00 end  
Ti-49 200009 0 4.763137e-06 293.00 end  
Ti-50 200009 0 4.560639e-06 293.00 end  
Mn-55 200009 0 1.191317e-05 293.00 end  
Fe-54 200009 0 5.392452e-05 293.00 end  
Fe-56 200009 0 8.464997e-04 293.00 end  
Fe-57 200009 0 1.954936e-05 293.00 end  
Fe-58 200009 0 2.601658e-06 293.00 end  
O-16 200010 0 2.931950e-02 293.00 end  
O-17 200010 0 1.114649e-05 293.00 end  
O-18 200010 0 6.026437e-05 293.00 end  
Na-23 200010 0 2.444715e-04 293.00 end  
Mg-24 200010 0 3.957787e-04 293.00 end  
Mg-25 200010 0 5.010491e-05 293.00 end  
Mg-26 200010 0 5.516551e-05 293.00 end  
Al-27 200010 0 2.326076e-03 293.00 end  
Si-28 200010 0 8.150971e-03 293.00 end  
Si-29 200010 0 4.140756e-04 293.00 end  
Si-30 200010 0 2.732811e-04 293.00 end  
K-39 200010 0 3.128084e-04 293.00 end  
K-40 200010 0 3.924422e-08 293.00 end  
K-41 200010 0 2.257459e-05 293.00 end  
Ca-40 200010 0 1.132863e-03 293.00 end  
Ca-42 200010 0 7.560904e-06 293.00 end  
Ca-43 200010 0 1.577628e-06 293.00 end  
Ca-44 200010 0 2.437722e-05 293.00 end  
Ca-46 200010 0 4.674011e-08 293.00 end  
Ca-48 200010 0 2.185305e-06 293.00 end  
Ti-46 200010 0 7.263565e-06 293.00 end  
Ti-47 200010 0 6.550416e-06 293.00 end  
Ti-48 200010 0 6.490546e-05 293.00 end  
Ti-49 200010 0 4.763137e-06 293.00 end  
Ti-50 200010 0 4.560639e-06 293.00 end  
Mn-55 200010 0 1.191317e-05 293.00 end  
Fe-54 200010 0 5.392452e-05 293.00 end  
Fe-56 200010 0 8.464997e-04 293.00 end  
Fe-57 200010 0 1.954936e-05 293.00 end  
Fe-58 200010 0 2.601658e-06 293.00 end  
O-16 200011 0 2.931950e-02 293.00 end  
O-17 200011 0 1.114649e-05 293.00 end  
O-18 200011 0 6.026437e-05 293.00 end  
Na-23 200011 0 2.444715e-04 293.00 end  
Mg-24 200011 0 3.957787e-04 293.00 end  
Mg-25 200011 0 5.010491e-05 293.00 end  
Mg-26 200011 0 5.516551e-05 293.00 end  
Al-27 200011 0 2.326076e-03 293.00 end  
Si-28 200011 0 8.150971e-03 293.00 end  
Si-29 200011 0 4.140756e-04 293.00 end  
Si-30 200011 0 2.732811e-04 293.00 end  
K-39 200011 0 3.128084e-04 293.00 end  
K-40 200011 0 3.924422e-08 293.00 end  
K-41 200011 0 2.257459e-05 293.00 end  
Ca-40 200011 0 1.132863e-03 293.00 end  
Ca-42 200011 0 7.560904e-06 293.00 end  
Ca-43 200011 0 1.577628e-06 293.00 end  
Ca-44 200011 0 2.437722e-05 293.00 end  
Ca-46 200011 0 4.674011e-08 293.00 end

Ca-48 200011 0 2.185305e-06 293.00 end  
 Ti-46 200011 0 7.263565e-06 293.00 end  
 Ti-47 200011 0 6.550416e-06 293.00 end  
 Ti-48 200011 0 6.490546e-05 293.00 end  
 Ti-49 200011 0 4.763137e-06 293.00 end  
 Ti-50 200011 0 4.560639e-06 293.00 end  
 Mn-55 200011 0 1.191317e-05 293.00 end  
 Fe-54 200011 0 5.392452e-05 293.00 end  
 Fe-56 200011 0 8.464997e-04 293.00 end  
 Fe-57 200011 0 1.954936e-05 293.00 end  
 Fe-58 200011 0 2.601658e-06 293.00 end  
 O-16 200012 0 2.931950e-02 293.00 end  
 O-17 200012 0 1.114649e-05 293.00 end  
 O-18 200012 0 6.026437e-05 293.00 end  
 Na-23 200012 0 2.444715e-04 293.00 end  
 Mg-24 200012 0 3.957787e-04 293.00 end  
 Mg-25 200012 0 5.010491e-05 293.00 end  
 Mg-26 200012 0 5.516551e-05 293.00 end  
 Al-27 200012 0 2.326076e-03 293.00 end  
 Si-28 200012 0 8.150971e-03 293.00 end  
 Si-29 200012 0 4.140756e-04 293.00 end  
 Si-30 200012 0 2.732811e-04 293.00 end  
 K-39 200012 0 3.128084e-04 293.00 end  
 K-40 200012 0 3.924422e-08 293.00 end  
 K-41 200012 0 2.257459e-05 293.00 end  
 Ca-40 200012 0 1.132863e-03 293.00 end  
 Ca-42 200012 0 7.560904e-06 293.00 end  
 Ca-43 200012 0 1.577628e-06 293.00 end  
 Ca-44 200012 0 2.437722e-05 293.00 end  
 Ca-46 200012 0 4.674011e-08 293.00 end  
 Ca-48 200012 0 2.185305e-06 293.00 end  
 Ti-46 200012 0 7.263565e-06 293.00 end  
 Ti-47 200012 0 6.550416e-06 293.00 end  
 Ti-48 200012 0 6.490546e-05 293.00 end  
 Ti-49 200012 0 4.763137e-06 293.00 end  
 Ti-50 200012 0 4.560639e-06 293.00 end  
 Mn-55 200012 0 1.191317e-05 293.00 end  
 Fe-54 200012 0 5.392452e-05 293.00 end  
 Fe-56 200012 0 8.464997e-04 293.00 end  
 Fe-57 200012 0 1.954936e-05 293.00 end  
 Fe-58 200012 0 2.601658e-06 293.00 end  
 O-16 200013 0 2.931950e-02 293.00 end  
 O-17 200013 0 1.114649e-05 293.00 end  
 O-18 200013 0 6.026437e-05 293.00 end  
 Na-23 200013 0 2.444715e-04 293.00 end  
 Mg-24 200013 0 3.957787e-04 293.00 end  
 Mg-25 200013 0 5.010491e-05 293.00 end  
 Mg-26 200013 0 5.516551e-05 293.00 end  
 Al-27 200013 0 2.326076e-03 293.00 end  
 Si-28 200013 0 8.150971e-03 293.00 end  
 Si-29 200013 0 4.140756e-04 293.00 end  
 Si-30 200013 0 2.732811e-04 293.00 end  
 K-39 200013 0 3.128084e-04 293.00 end  
 K-40 200013 0 3.924422e-08 293.00 end  
 K-41 200013 0 2.257459e-05 293.00 end  
 Ca-40 200013 0 1.132863e-03 293.00 end  
 Ca-42 200013 0 7.560904e-06 293.00 end  
 Ca-43 200013 0 1.577628e-06 293.00 end  
 Ca-44 200013 0 2.437722e-05 293.00 end  
 Ca-46 200013 0 4.674011e-08 293.00 end  
 Ca-48 200013 0 2.185305e-06 293.00 end  
 Ti-46 200013 0 7.263565e-06 293.00 end  
 Ti-47 200013 0 6.550416e-06 293.00 end  
 Ti-48 200013 0 6.490546e-05 293.00 end  
 Ti-49 200013 0 4.763137e-06 293.00 end  
 Ti-50 200013 0 4.560639e-06 293.00 end  
 Mn-55 200013 0 1.191317e-05 293.00 end  
 Fe-54 200013 0 5.392452e-05 293.00 end  
 Fe-56 200013 0 8.464997e-04 293.00 end  
 Fe-57 200013 0 1.954936e-05 293.00 end  
 Fe-58 200013 0 2.601658e-06 293.00 end  
 O-16 200014 0 2.931950e-02 293.00 end  
 O-17 200014 0 1.114649e-05 293.00 end

O-18 200014 0 6.026437e-05 293.00 end  
Na-23 200014 0 2.444715e-04 293.00 end  
Mg-24 200014 0 3.957787e-04 293.00 end  
Mg-25 200014 0 5.010491e-05 293.00 end  
Mg-26 200014 0 5.516551e-05 293.00 end  
Al-27 200014 0 2.326076e-03 293.00 end  
Si-28 200014 0 8.150971e-03 293.00 end  
Si-29 200014 0 4.140756e-04 293.00 end  
Si-30 200014 0 2.732811e-04 293.00 end  
K-39 200014 0 3.128084e-04 293.00 end  
K-40 200014 0 3.924422e-08 293.00 end  
K-41 200014 0 2.257459e-05 293.00 end  
Ca-40 200014 0 1.132863e-03 293.00 end  
Ca-42 200014 0 7.560904e-06 293.00 end  
Ca-43 200014 0 1.577628e-06 293.00 end  
Ca-44 200014 0 2.437722e-05 293.00 end  
Ca-46 200014 0 4.674011e-08 293.00 end  
Ca-48 200014 0 2.185305e-06 293.00 end  
Ti-46 200014 0 7.263565e-06 293.00 end  
Ti-47 200014 0 6.550416e-06 293.00 end  
Ti-48 200014 0 6.490546e-05 293.00 end  
Ti-49 200014 0 4.763137e-06 293.00 end  
Ti-50 200014 0 4.560639e-06 293.00 end  
Mn-55 200014 0 1.191317e-05 293.00 end  
Fe-54 200014 0 5.392452e-05 293.00 end  
Fe-56 200014 0 8.464997e-04 293.00 end  
Fe-57 200014 0 1.954936e-05 293.00 end  
Fe-58 200014 0 2.601658e-06 293.00 end  
O-16 200015 0 2.931950e-02 293.00 end  
O-17 200015 0 1.114649e-05 293.00 end  
O-18 200015 0 6.026437e-05 293.00 end  
Na-23 200015 0 2.444715e-04 293.00 end  
Mg-24 200015 0 3.957787e-04 293.00 end  
Mg-25 200015 0 5.010491e-05 293.00 end  
Mg-26 200015 0 5.516551e-05 293.00 end  
Al-27 200015 0 2.326076e-03 293.00 end  
Si-28 200015 0 8.150971e-03 293.00 end  
Si-29 200015 0 4.140756e-04 293.00 end  
Si-30 200015 0 2.732811e-04 293.00 end  
K-39 200015 0 3.128084e-04 293.00 end  
K-40 200015 0 3.924422e-08 293.00 end  
K-41 200015 0 2.257459e-05 293.00 end  
Ca-40 200015 0 1.132863e-03 293.00 end  
Ca-42 200015 0 7.560904e-06 293.00 end  
Ca-43 200015 0 1.577628e-06 293.00 end  
Ca-44 200015 0 2.437722e-05 293.00 end  
Ca-46 200015 0 4.674011e-08 293.00 end  
Ca-48 200015 0 2.185305e-06 293.00 end  
Ti-46 200015 0 7.263565e-06 293.00 end  
Ti-47 200015 0 6.550416e-06 293.00 end  
Ti-48 200015 0 6.490546e-05 293.00 end  
Ti-49 200015 0 4.763137e-06 293.00 end  
Ti-50 200015 0 4.560639e-06 293.00 end  
Mn-55 200015 0 1.191317e-05 293.00 end  
Fe-54 200015 0 5.392452e-05 293.00 end  
Fe-56 200015 0 8.464997e-04 293.00 end  
Fe-57 200015 0 1.954936e-05 293.00 end  
Fe-58 200015 0 2.601658e-06 293.00 end  
O-16 200016 0 2.931950e-02 293.00 end  
O-17 200016 0 1.114649e-05 293.00 end  
O-18 200016 0 6.026437e-05 293.00 end  
Na-23 200016 0 2.444715e-04 293.00 end  
Mg-24 200016 0 3.957787e-04 293.00 end  
Mg-25 200016 0 5.010491e-05 293.00 end  
Mg-26 200016 0 5.516551e-05 293.00 end  
Al-27 200016 0 2.326076e-03 293.00 end  
Si-28 200016 0 8.150971e-03 293.00 end  
Si-29 200016 0 4.140756e-04 293.00 end  
Si-30 200016 0 2.732811e-04 293.00 end  
K-39 200016 0 3.128084e-04 293.00 end  
K-40 200016 0 3.924422e-08 293.00 end  
K-41 200016 0 2.257459e-05 293.00 end  
Ca-40 200016 0 1.132863e-03 293.00 end

Ca-42 200016 0 7.560904e-06 293.00 end  
Ca-43 200016 0 1.577628e-06 293.00 end  
Ca-44 200016 0 2.437722e-05 293.00 end  
Ca-46 200016 0 4.674011e-08 293.00 end  
Ca-48 200016 0 2.185305e-06 293.00 end  
Ti-46 200016 0 7.263565e-06 293.00 end  
Ti-47 200016 0 6.550416e-06 293.00 end  
Ti-48 200016 0 6.490546e-05 293.00 end  
Ti-49 200016 0 4.763137e-06 293.00 end  
Ti-50 200016 0 4.560639e-06 293.00 end  
Mn-55 200016 0 1.191317e-05 293.00 end  
Fe-54 200016 0 5.392452e-05 293.00 end  
Fe-56 200016 0 8.464997e-04 293.00 end  
Fe-57 200016 0 1.954936e-05 293.00 end  
Fe-58 200016 0 2.601658e-06 293.00 end  
O-16 200017 0 2.931950e-02 293.00 end  
O-17 200017 0 1.114649e-05 293.00 end  
O-18 200017 0 6.026437e-05 293.00 end  
Na-23 200017 0 2.444715e-04 293.00 end  
Mg-24 200017 0 3.957787e-04 293.00 end  
Mg-25 200017 0 5.010491e-05 293.00 end  
Mg-26 200017 0 5.516551e-05 293.00 end  
Al-27 200017 0 2.326076e-03 293.00 end  
Si-28 200017 0 8.150971e-03 293.00 end  
Si-29 200017 0 4.140756e-04 293.00 end  
Si-30 200017 0 2.732811e-04 293.00 end  
K-39 200017 0 3.128084e-04 293.00 end  
K-40 200017 0 3.924422e-08 293.00 end  
K-41 200017 0 2.257459e-05 293.00 end  
Ca-40 200017 0 1.132863e-03 293.00 end  
Ca-42 200017 0 7.560904e-06 293.00 end  
Ca-43 200017 0 1.577628e-06 293.00 end  
Ca-44 200017 0 2.437722e-05 293.00 end  
Ca-46 200017 0 4.674011e-08 293.00 end  
Ca-48 200017 0 2.185305e-06 293.00 end  
Ti-46 200017 0 7.263565e-06 293.00 end  
Ti-47 200017 0 6.550416e-06 293.00 end  
Ti-48 200017 0 6.490546e-05 293.00 end  
Ti-49 200017 0 4.763137e-06 293.00 end  
Ti-50 200017 0 4.560639e-06 293.00 end  
Mn-55 200017 0 1.191317e-05 293.00 end  
Fe-54 200017 0 5.392452e-05 293.00 end  
Fe-56 200017 0 8.464997e-04 293.00 end  
Fe-57 200017 0 1.954936e-05 293.00 end  
Fe-58 200017 0 2.601658e-06 293.00 end  
O-16 200018 0 2.931950e-02 293.00 end  
O-17 200018 0 1.114649e-05 293.00 end  
O-18 200018 0 6.026437e-05 293.00 end  
Na-23 200018 0 2.444715e-04 293.00 end  
Mg-24 200018 0 3.957787e-04 293.00 end  
Mg-25 200018 0 5.010491e-05 293.00 end  
Mg-26 200018 0 5.516551e-05 293.00 end  
Al-27 200018 0 2.326076e-03 293.00 end  
Si-28 200018 0 8.150971e-03 293.00 end  
Si-29 200018 0 4.140756e-04 293.00 end  
Si-30 200018 0 2.732811e-04 293.00 end  
K-39 200018 0 3.128084e-04 293.00 end  
K-40 200018 0 3.924422e-08 293.00 end  
K-41 200018 0 2.257459e-05 293.00 end  
Ca-40 200018 0 1.132863e-03 293.00 end  
Ca-42 200018 0 7.560904e-06 293.00 end  
Ca-43 200018 0 1.577628e-06 293.00 end  
Ca-44 200018 0 2.437722e-05 293.00 end  
Ca-46 200018 0 4.674011e-08 293.00 end  
Ca-48 200018 0 2.185305e-06 293.00 end  
Ti-46 200018 0 7.263565e-06 293.00 end  
Ti-47 200018 0 6.550416e-06 293.00 end  
Ti-48 200018 0 6.490546e-05 293.00 end  
Ti-49 200018 0 4.763137e-06 293.00 end  
Ti-50 200018 0 4.560639e-06 293.00 end  
Mn-55 200018 0 1.191317e-05 293.00 end  
Fe-54 200018 0 5.392452e-05 293.00 end  
Fe-56 200018 0 8.464997e-04 293.00 end

Fe-57 200018 0 1.954936e-05 293.00 end  
 Fe-58 200018 0 2.601658e-06 293.00 end  
 O-16 200019 0 2.931950e-02 293.00 end  
 O-17 200019 0 1.114649e-05 293.00 end  
 O-18 200019 0 6.026437e-05 293.00 end  
 Na-23 200019 0 2.444715e-04 293.00 end  
 Mg-24 200019 0 3.957787e-04 293.00 end  
 Mg-25 200019 0 5.010491e-05 293.00 end  
 Mg-26 200019 0 5.516551e-05 293.00 end  
 Al-27 200019 0 2.326076e-03 293.00 end  
 Si-28 200019 0 8.150971e-03 293.00 end  
 Si-29 200019 0 4.140756e-04 293.00 end  
 Si-30 200019 0 2.732811e-04 293.00 end  
 K-39 200019 0 3.128084e-04 293.00 end  
 K-40 200019 0 3.924422e-08 293.00 end  
 K-41 200019 0 2.257459e-05 293.00 end  
 Ca-40 200019 0 1.132863e-03 293.00 end  
 Ca-42 200019 0 7.560904e-06 293.00 end  
 Ca-43 200019 0 1.577628e-06 293.00 end  
 Ca-44 200019 0 2.437722e-05 293.00 end  
 Ca-46 200019 0 4.674011e-08 293.00 end  
 Ca-48 200019 0 2.185305e-06 293.00 end  
 Ti-46 200019 0 7.263565e-06 293.00 end  
 Ti-47 200019 0 6.550416e-06 293.00 end  
 Ti-48 200019 0 6.490546e-05 293.00 end  
 Ti-49 200019 0 4.763137e-06 293.00 end  
 Ti-50 200019 0 4.560639e-06 293.00 end  
 Mn-55 200019 0 1.191317e-05 293.00 end  
 Fe-54 200019 0 5.392452e-05 293.00 end  
 Fe-56 200019 0 8.464997e-04 293.00 end  
 Fe-57 200019 0 1.954936e-05 293.00 end  
 Fe-58 200019 0 2.601658e-06 293.00 end  
 O-16 200020 0 2.931950e-02 293.00 end  
 O-17 200020 0 1.114649e-05 293.00 end  
 O-18 200020 0 6.026437e-05 293.00 end  
 Na-23 200020 0 2.444715e-04 293.00 end  
 Mg-24 200020 0 3.957787e-04 293.00 end  
 Mg-25 200020 0 5.010491e-05 293.00 end  
 Mg-26 200020 0 5.516551e-05 293.00 end  
 Al-27 200020 0 2.326076e-03 293.00 end  
 Si-28 200020 0 8.150971e-03 293.00 end  
 Si-29 200020 0 4.140756e-04 293.00 end  
 Si-30 200020 0 2.732811e-04 293.00 end  
 K-39 200020 0 3.128084e-04 293.00 end  
 K-40 200020 0 3.924422e-08 293.00 end  
 K-41 200020 0 2.257459e-05 293.00 end  
 Ca-40 200020 0 1.132863e-03 293.00 end  
 Ca-42 200020 0 7.560904e-06 293.00 end  
 Ca-43 200020 0 1.577628e-06 293.00 end  
 Ca-44 200020 0 2.437722e-05 293.00 end  
 Ca-46 200020 0 4.674011e-08 293.00 end  
 Ca-48 200020 0 2.185305e-06 293.00 end  
 Ti-46 200020 0 7.263565e-06 293.00 end  
 Ti-47 200020 0 6.550416e-06 293.00 end  
 Ti-48 200020 0 6.490546e-05 293.00 end  
 Ti-49 200020 0 4.763137e-06 293.00 end  
 Ti-50 200020 0 4.560639e-06 293.00 end  
 Mn-55 200020 0 1.191317e-05 293.00 end  
 Fe-54 200020 0 5.392452e-05 293.00 end  
 Fe-56 200020 0 8.464997e-04 293.00 end  
 Fe-57 200020 0 1.954936e-05 293.00 end  
 Fe-58 200020 0 2.601658e-06 293.00 end  
 O-16 200021 0 2.931950e-02 293.00 end  
 O-17 200021 0 1.114649e-05 293.00 end  
 O-18 200021 0 6.026437e-05 293.00 end  
 Na-23 200021 0 2.444715e-04 293.00 end  
 Mg-24 200021 0 3.957787e-04 293.00 end  
 Mg-25 200021 0 5.010491e-05 293.00 end  
 Mg-26 200021 0 5.516551e-05 293.00 end  
 Al-27 200021 0 2.326076e-03 293.00 end  
 Si-28 200021 0 8.150971e-03 293.00 end  
 Si-29 200021 0 4.140756e-04 293.00 end  
 Si-30 200021 0 2.732811e-04 293.00 end

K-39 200021 0 3.128084e-04 293.00 end  
K-40 200021 0 3.924422e-08 293.00 end  
K-41 200021 0 2.257459e-05 293.00 end  
Ca-40 200021 0 1.132863e-03 293.00 end  
Ca-42 200021 0 7.560904e-06 293.00 end  
Ca-43 200021 0 1.577628e-06 293.00 end  
Ca-44 200021 0 2.437722e-05 293.00 end  
Ca-46 200021 0 4.674011e-08 293.00 end  
Ca-48 200021 0 2.185305e-06 293.00 end  
Ti-46 200021 0 7.263565e-06 293.00 end  
Ti-47 200021 0 6.550416e-06 293.00 end  
Ti-48 200021 0 6.490546e-05 293.00 end  
Ti-49 200021 0 4.763137e-06 293.00 end  
Ti-50 200021 0 4.560639e-06 293.00 end  
Mn-55 200021 0 1.191317e-05 293.00 end  
Fe-54 200021 0 5.392452e-05 293.00 end  
Fe-56 200021 0 8.464997e-04 293.00 end  
Fe-57 200021 0 1.954936e-05 293.00 end  
Fe-58 200021 0 2.601658e-06 293.00 end  
O-16 200022 0 2.931950e-02 293.00 end  
O-17 200022 0 1.114649e-05 293.00 end  
O-18 200022 0 6.026437e-05 293.00 end  
Na-23 200022 0 2.444715e-04 293.00 end  
Mg-24 200022 0 3.957787e-04 293.00 end  
Mg-25 200022 0 5.010491e-05 293.00 end  
Mg-26 200022 0 5.516551e-05 293.00 end  
Al-27 200022 0 2.326076e-03 293.00 end  
Si-28 200022 0 8.150971e-03 293.00 end  
Si-29 200022 0 4.140756e-04 293.00 end  
Si-30 200022 0 2.732811e-04 293.00 end  
K-39 200022 0 3.128084e-04 293.00 end  
K-40 200022 0 3.924422e-08 293.00 end  
K-41 200022 0 2.257459e-05 293.00 end  
Ca-40 200022 0 1.132863e-03 293.00 end  
Ca-42 200022 0 7.560904e-06 293.00 end  
Ca-43 200022 0 1.577628e-06 293.00 end  
Ca-44 200022 0 2.437722e-05 293.00 end  
Ca-46 200022 0 4.674011e-08 293.00 end  
Ca-48 200022 0 2.185305e-06 293.00 end  
Ti-46 200022 0 7.263565e-06 293.00 end  
Ti-47 200022 0 6.550416e-06 293.00 end  
Ti-48 200022 0 6.490546e-05 293.00 end  
Ti-49 200022 0 4.763137e-06 293.00 end  
Ti-50 200022 0 4.560639e-06 293.00 end  
Mn-55 200022 0 1.191317e-05 293.00 end  
Fe-54 200022 0 5.392452e-05 293.00 end  
Fe-56 200022 0 8.464997e-04 293.00 end  
Fe-57 200022 0 1.954936e-05 293.00 end  
Fe-58 200022 0 2.601658e-06 293.00 end  
O-16 200023 0 2.931950e-02 293.00 end  
O-17 200023 0 1.114649e-05 293.00 end  
O-18 200023 0 6.026437e-05 293.00 end  
Na-23 200023 0 2.444715e-04 293.00 end  
Mg-24 200023 0 3.957787e-04 293.00 end  
Mg-25 200023 0 5.010491e-05 293.00 end  
Mg-26 200023 0 5.516551e-05 293.00 end  
Al-27 200023 0 2.326076e-03 293.00 end  
Si-28 200023 0 8.150971e-03 293.00 end  
Si-29 200023 0 4.140756e-04 293.00 end  
Si-30 200023 0 2.732811e-04 293.00 end  
K-39 200023 0 3.128084e-04 293.00 end  
K-40 200023 0 3.924422e-08 293.00 end  
K-41 200023 0 2.257459e-05 293.00 end  
Ca-40 200023 0 1.132863e-03 293.00 end  
Ca-42 200023 0 7.560904e-06 293.00 end  
Ca-43 200023 0 1.577628e-06 293.00 end  
Ca-44 200023 0 2.437722e-05 293.00 end  
Ca-46 200023 0 4.674011e-08 293.00 end  
Ca-48 200023 0 2.185305e-06 293.00 end  
Ti-46 200023 0 7.263565e-06 293.00 end  
Ti-47 200023 0 6.550416e-06 293.00 end  
Ti-48 200023 0 6.490546e-05 293.00 end  
Ti-49 200023 0 4.763137e-06 293.00 end

Ti-50 200023 0 4.560639e-06 293.00 end  
Mn-55 200023 0 1.191317e-05 293.00 end  
Fe-54 200023 0 5.392452e-05 293.00 end  
Fe-56 200023 0 8.464997e-04 293.00 end  
Fe-57 200023 0 1.954936e-05 293.00 end  
Fe-58 200023 0 2.601658e-06 293.00 end  
O-16 200024 0 2.931950e-02 293.00 end  
O-17 200024 0 1.114649e-05 293.00 end  
O-18 200024 0 6.026437e-05 293.00 end  
Na-23 200024 0 2.444715e-04 293.00 end  
Mg-24 200024 0 3.957787e-04 293.00 end  
Mg-25 200024 0 5.010491e-05 293.00 end  
Mg-26 200024 0 5.516551e-05 293.00 end  
Al-27 200024 0 2.326076e-03 293.00 end  
Si-28 200024 0 8.150971e-03 293.00 end  
Si-29 200024 0 4.140756e-04 293.00 end  
Si-30 200024 0 2.732811e-04 293.00 end  
K-39 200024 0 3.128084e-04 293.00 end  
K-40 200024 0 3.924422e-08 293.00 end  
K-41 200024 0 2.257459e-05 293.00 end  
Ca-40 200024 0 1.132863e-03 293.00 end  
Ca-42 200024 0 7.560904e-06 293.00 end  
Ca-43 200024 0 1.577628e-06 293.00 end  
Ca-44 200024 0 2.437722e-05 293.00 end  
Ca-46 200024 0 4.674011e-08 293.00 end  
Ca-48 200024 0 2.185305e-06 293.00 end  
Ti-46 200024 0 7.263565e-06 293.00 end  
Ti-47 200024 0 6.550416e-06 293.00 end  
Ti-48 200024 0 6.490546e-05 293.00 end  
Ti-49 200024 0 4.763137e-06 293.00 end  
Ti-50 200024 0 4.560639e-06 293.00 end  
Mn-55 200024 0 1.191317e-05 293.00 end  
Fe-54 200024 0 5.392452e-05 293.00 end  
Fe-56 200024 0 8.464997e-04 293.00 end  
Fe-57 200024 0 1.954936e-05 293.00 end  
Fe-58 200024 0 2.601658e-06 293.00 end  
O-16 200025 0 2.931950e-02 293.00 end  
O-17 200025 0 1.114649e-05 293.00 end  
O-18 200025 0 6.026437e-05 293.00 end  
Na-23 200025 0 2.444715e-04 293.00 end  
Mg-24 200025 0 3.957787e-04 293.00 end  
Mg-25 200025 0 5.010491e-05 293.00 end  
Mg-26 200025 0 5.516551e-05 293.00 end  
Al-27 200025 0 2.326076e-03 293.00 end  
Si-28 200025 0 8.150971e-03 293.00 end  
Si-29 200025 0 4.140756e-04 293.00 end  
Si-30 200025 0 2.732811e-04 293.00 end  
K-39 200025 0 3.128084e-04 293.00 end  
K-40 200025 0 3.924422e-08 293.00 end  
K-41 200025 0 2.257459e-05 293.00 end  
Ca-40 200025 0 1.132863e-03 293.00 end  
Ca-42 200025 0 7.560904e-06 293.00 end  
Ca-43 200025 0 1.577628e-06 293.00 end  
Ca-44 200025 0 2.437722e-05 293.00 end  
Ca-46 200025 0 4.674011e-08 293.00 end  
Ca-48 200025 0 2.185305e-06 293.00 end  
Ti-46 200025 0 7.263565e-06 293.00 end  
Ti-47 200025 0 6.550416e-06 293.00 end  
Ti-48 200025 0 6.490546e-05 293.00 end  
Ti-49 200025 0 4.763137e-06 293.00 end  
Ti-50 200025 0 4.560639e-06 293.00 end  
Mn-55 200025 0 1.191317e-05 293.00 end  
Fe-54 200025 0 5.392452e-05 293.00 end  
Fe-56 200025 0 8.464997e-04 293.00 end  
Fe-57 200025 0 1.954936e-05 293.00 end  
Fe-58 200025 0 2.601658e-06 293.00 end  
O-16 200026 0 2.931950e-02 293.00 end  
O-17 200026 0 1.114649e-05 293.00 end  
O-18 200026 0 6.026437e-05 293.00 end  
Na-23 200026 0 2.444715e-04 293.00 end  
Mg-24 200026 0 3.957787e-04 293.00 end  
Mg-25 200026 0 5.010491e-05 293.00 end  
Mg-26 200026 0 5.516551e-05 293.00 end

Al-27 200026 0 2.326076e-03 293.00 end  
Si-28 200026 0 8.150971e-03 293.00 end  
Si-29 200026 0 4.140756e-04 293.00 end  
Si-30 200026 0 2.732811e-04 293.00 end  
K-39 200026 0 3.128084e-04 293.00 end  
K-40 200026 0 3.924422e-08 293.00 end  
K-41 200026 0 2.257459e-05 293.00 end  
Ca-40 200026 0 1.132863e-03 293.00 end  
Ca-42 200026 0 7.560904e-06 293.00 end  
Ca-43 200026 0 1.577628e-06 293.00 end  
Ca-44 200026 0 2.437722e-05 293.00 end  
Ca-46 200026 0 4.674011e-08 293.00 end  
Ca-48 200026 0 2.185305e-06 293.00 end  
Ti-46 200026 0 7.263565e-06 293.00 end  
Ti-47 200026 0 6.550416e-06 293.00 end  
Ti-48 200026 0 6.490546e-05 293.00 end  
Ti-49 200026 0 4.763137e-06 293.00 end  
Ti-50 200026 0 4.560639e-06 293.00 end  
Mn-55 200026 0 1.191317e-05 293.00 end  
Fe-54 200026 0 5.392452e-05 293.00 end  
Fe-56 200026 0 8.464997e-04 293.00 end  
Fe-57 200026 0 1.954936e-05 293.00 end  
Fe-58 200026 0 2.601658e-06 293.00 end  
O-16 200027 0 2.931950e-02 293.00 end  
O-17 200027 0 1.114649e-05 293.00 end  
O-18 200027 0 6.026437e-05 293.00 end  
Na-23 200027 0 2.444715e-04 293.00 end  
Mg-24 200027 0 3.957787e-04 293.00 end  
Mg-25 200027 0 5.010491e-05 293.00 end  
Mg-26 200027 0 5.516551e-05 293.00 end  
Al-27 200027 0 2.326076e-03 293.00 end  
Si-28 200027 0 8.150971e-03 293.00 end  
Si-29 200027 0 4.140756e-04 293.00 end  
Si-30 200027 0 2.732811e-04 293.00 end  
K-39 200027 0 3.128084e-04 293.00 end  
K-40 200027 0 3.924422e-08 293.00 end  
K-41 200027 0 2.257459e-05 293.00 end  
Ca-40 200027 0 1.132863e-03 293.00 end  
Ca-42 200027 0 7.560904e-06 293.00 end  
Ca-43 200027 0 1.577628e-06 293.00 end  
Ca-44 200027 0 2.437722e-05 293.00 end  
Ca-46 200027 0 4.674011e-08 293.00 end  
Ca-48 200027 0 2.185305e-06 293.00 end  
Ti-46 200027 0 7.263565e-06 293.00 end  
Ti-47 200027 0 6.550416e-06 293.00 end  
Ti-48 200027 0 6.490546e-05 293.00 end  
Ti-49 200027 0 4.763137e-06 293.00 end  
Ti-50 200027 0 4.560639e-06 293.00 end  
Mn-55 200027 0 1.191317e-05 293.00 end  
Fe-54 200027 0 5.392452e-05 293.00 end  
Fe-56 200027 0 8.464997e-04 293.00 end  
Fe-57 200027 0 1.954936e-05 293.00 end  
Fe-58 200027 0 2.601658e-06 293.00 end  
O-16 200028 0 2.931950e-02 293.00 end  
O-17 200028 0 1.114649e-05 293.00 end  
O-18 200028 0 6.026437e-05 293.00 end  
Na-23 200028 0 2.444715e-04 293.00 end  
Mg-24 200028 0 3.957787e-04 293.00 end  
Mg-25 200028 0 5.010491e-05 293.00 end  
Mg-26 200028 0 5.516551e-05 293.00 end  
Al-27 200028 0 2.326076e-03 293.00 end  
Si-28 200028 0 8.150971e-03 293.00 end  
Si-29 200028 0 4.140756e-04 293.00 end  
Si-30 200028 0 2.732811e-04 293.00 end  
K-39 200028 0 3.128084e-04 293.00 end  
K-40 200028 0 3.924422e-08 293.00 end  
K-41 200028 0 2.257459e-05 293.00 end  
Ca-40 200028 0 1.132863e-03 293.00 end  
Ca-42 200028 0 7.560904e-06 293.00 end  
Ca-43 200028 0 1.577628e-06 293.00 end  
Ca-44 200028 0 2.437722e-05 293.00 end  
Ca-46 200028 0 4.674011e-08 293.00 end  
Ca-48 200028 0 2.185305e-06 293.00 end

Ti-46 200028 0 7.263565e-06 293.00 end  
Ti-47 200028 0 6.550416e-06 293.00 end  
Ti-48 200028 0 6.490546e-05 293.00 end  
Ti-49 200028 0 4.763137e-06 293.00 end  
Ti-50 200028 0 4.560639e-06 293.00 end  
Mn-55 200028 0 1.191317e-05 293.00 end  
Fe-54 200028 0 5.392452e-05 293.00 end  
Fe-56 200028 0 8.464997e-04 293.00 end  
Fe-57 200028 0 1.954936e-05 293.00 end  
Fe-58 200028 0 2.601658e-06 293.00 end  
O-16 200029 0 2.931950e-02 293.00 end  
O-17 200029 0 1.114649e-05 293.00 end  
O-18 200029 0 6.026437e-05 293.00 end  
Na-23 200029 0 2.444715e-04 293.00 end  
Mg-24 200029 0 3.957787e-04 293.00 end  
Mg-25 200029 0 5.010491e-05 293.00 end  
Mg-26 200029 0 5.516551e-05 293.00 end  
Al-27 200029 0 2.326076e-03 293.00 end  
Si-28 200029 0 8.150971e-03 293.00 end  
Si-29 200029 0 4.140756e-04 293.00 end  
Si-30 200029 0 2.732811e-04 293.00 end  
K-39 200029 0 3.128084e-04 293.00 end  
K-40 200029 0 3.924422e-08 293.00 end  
K-41 200029 0 2.257459e-05 293.00 end  
Ca-40 200029 0 1.132863e-03 293.00 end  
Ca-42 200029 0 7.560904e-06 293.00 end  
Ca-43 200029 0 1.577628e-06 293.00 end  
Ca-44 200029 0 2.437722e-05 293.00 end  
Ca-46 200029 0 4.674011e-08 293.00 end  
Ca-48 200029 0 2.185305e-06 293.00 end  
Ti-46 200029 0 7.263565e-06 293.00 end  
Ti-47 200029 0 6.550416e-06 293.00 end  
Ti-48 200029 0 6.490546e-05 293.00 end  
Ti-49 200029 0 4.763137e-06 293.00 end  
Ti-50 200029 0 4.560639e-06 293.00 end  
Mn-55 200029 0 1.191317e-05 293.00 end  
Fe-54 200029 0 5.392452e-05 293.00 end  
Fe-56 200029 0 8.464997e-04 293.00 end  
Fe-57 200029 0 1.954936e-05 293.00 end  
Fe-58 200029 0 2.601658e-06 293.00 end  
O-16 200030 0 2.931950e-02 293.00 end  
O-17 200030 0 1.114649e-05 293.00 end  
O-18 200030 0 6.026437e-05 293.00 end  
Na-23 200030 0 2.444715e-04 293.00 end  
Mg-24 200030 0 3.957787e-04 293.00 end  
Mg-25 200030 0 5.010491e-05 293.00 end  
Mg-26 200030 0 5.516551e-05 293.00 end  
Al-27 200030 0 2.326076e-03 293.00 end  
Si-28 200030 0 8.150971e-03 293.00 end  
Si-29 200030 0 4.140756e-04 293.00 end  
Si-30 200030 0 2.732811e-04 293.00 end  
K-39 200030 0 3.128084e-04 293.00 end  
K-40 200030 0 3.924422e-08 293.00 end  
K-41 200030 0 2.257459e-05 293.00 end  
Ca-40 200030 0 1.132863e-03 293.00 end  
Ca-42 200030 0 7.560904e-06 293.00 end  
Ca-43 200030 0 1.577628e-06 293.00 end  
Ca-44 200030 0 2.437722e-05 293.00 end  
Ca-46 200030 0 4.674011e-08 293.00 end  
Ca-48 200030 0 2.185305e-06 293.00 end  
Ti-46 200030 0 7.263565e-06 293.00 end  
Ti-47 200030 0 6.550416e-06 293.00 end  
Ti-48 200030 0 6.490546e-05 293.00 end  
Ti-49 200030 0 4.763137e-06 293.00 end  
Ti-50 200030 0 4.560639e-06 293.00 end  
Mn-55 200030 0 1.191317e-05 293.00 end  
Fe-54 200030 0 5.392452e-05 293.00 end  
Fe-56 200030 0 8.464997e-04 293.00 end  
Fe-57 200030 0 1.954936e-05 293.00 end  
Fe-58 200030 0 2.601658e-06 293.00 end  
O-16 200031 0 2.931950e-02 293.00 end  
O-17 200031 0 1.114649e-05 293.00 end  
O-18 200031 0 6.026437e-05 293.00 end

Na-23 200031 0 2.444715e-04 293.00 end  
Mg-24 200031 0 3.957787e-04 293.00 end  
Mg-25 200031 0 5.010491e-05 293.00 end  
Mg-26 200031 0 5.516551e-05 293.00 end  
Al-27 200031 0 2.326076e-03 293.00 end  
Si-28 200031 0 8.150971e-03 293.00 end  
Si-29 200031 0 4.140756e-04 293.00 end  
Si-30 200031 0 2.732811e-04 293.00 end  
K-39 200031 0 3.128084e-04 293.00 end  
K-40 200031 0 3.924422e-08 293.00 end  
K-41 200031 0 2.257459e-05 293.00 end  
Ca-40 200031 0 1.132863e-03 293.00 end  
Ca-42 200031 0 7.560904e-06 293.00 end  
Ca-43 200031 0 1.577628e-06 293.00 end  
Ca-44 200031 0 2.437722e-05 293.00 end  
Ca-46 200031 0 4.674011e-08 293.00 end  
Ca-48 200031 0 2.185305e-06 293.00 end  
Ti-46 200031 0 7.263565e-06 293.00 end  
Ti-47 200031 0 6.550416e-06 293.00 end  
Ti-48 200031 0 6.490546e-05 293.00 end  
Ti-49 200031 0 4.763137e-06 293.00 end  
Ti-50 200031 0 4.560639e-06 293.00 end  
Mn-55 200031 0 1.191317e-05 293.00 end  
Fe-54 200031 0 5.392452e-05 293.00 end  
Fe-56 200031 0 8.464997e-04 293.00 end  
Fe-57 200031 0 1.954936e-05 293.00 end  
Fe-58 200031 0 2.601658e-06 293.00 end  
O-16 200032 0 2.931950e-02 293.00 end  
O-17 200032 0 1.114649e-05 293.00 end  
O-18 200032 0 6.026437e-05 293.00 end  
Na-23 200032 0 2.444715e-04 293.00 end  
Mg-24 200032 0 3.957787e-04 293.00 end  
Mg-25 200032 0 5.010491e-05 293.00 end  
Mg-26 200032 0 5.516551e-05 293.00 end  
Al-27 200032 0 2.326076e-03 293.00 end  
Si-28 200032 0 8.150971e-03 293.00 end  
Si-29 200032 0 4.140756e-04 293.00 end  
Si-30 200032 0 2.732811e-04 293.00 end  
K-39 200032 0 3.128084e-04 293.00 end  
K-40 200032 0 3.924422e-08 293.00 end  
K-41 200032 0 2.257459e-05 293.00 end  
Ca-40 200032 0 1.132863e-03 293.00 end  
Ca-42 200032 0 7.560904e-06 293.00 end  
Ca-43 200032 0 1.577628e-06 293.00 end  
Ca-44 200032 0 2.437722e-05 293.00 end  
Ca-46 200032 0 4.674011e-08 293.00 end  
Ca-48 200032 0 2.185305e-06 293.00 end  
Ti-46 200032 0 7.263565e-06 293.00 end  
Ti-47 200032 0 6.550416e-06 293.00 end  
Ti-48 200032 0 6.490546e-05 293.00 end  
Ti-49 200032 0 4.763137e-06 293.00 end  
Ti-50 200032 0 4.560639e-06 293.00 end  
Mn-55 200032 0 1.191317e-05 293.00 end  
Fe-54 200032 0 5.392452e-05 293.00 end  
Fe-56 200032 0 8.464997e-04 293.00 end  
Fe-57 200032 0 1.954936e-05 293.00 end  
Fe-58 200032 0 2.601658e-06 293.00 end  
O-16 200033 0 2.931950e-02 293.00 end  
O-17 200033 0 1.114649e-05 293.00 end  
O-18 200033 0 6.026437e-05 293.00 end  
Na-23 200033 0 2.444715e-04 293.00 end  
Mg-24 200033 0 3.957787e-04 293.00 end  
Mg-25 200033 0 5.010491e-05 293.00 end  
Mg-26 200033 0 5.516551e-05 293.00 end  
Al-27 200033 0 2.326076e-03 293.00 end  
Si-28 200033 0 8.150971e-03 293.00 end  
Si-29 200033 0 4.140756e-04 293.00 end  
Si-30 200033 0 2.732811e-04 293.00 end  
K-39 200033 0 3.128084e-04 293.00 end  
K-40 200033 0 3.924422e-08 293.00 end  
K-41 200033 0 2.257459e-05 293.00 end  
Ca-40 200033 0 1.132863e-03 293.00 end  
Ca-42 200033 0 7.560904e-06 293.00 end

Ca-43 200033 0 1.577628e-06 293.00 end  
Ca-44 200033 0 2.437722e-05 293.00 end  
Ca-46 200033 0 4.674011e-08 293.00 end  
Ca-48 200033 0 2.185305e-06 293.00 end  
Ti-46 200033 0 7.263565e-06 293.00 end  
Ti-47 200033 0 6.550416e-06 293.00 end  
Ti-48 200033 0 6.490546e-05 293.00 end  
Ti-49 200033 0 4.763137e-06 293.00 end  
Ti-50 200033 0 4.560639e-06 293.00 end  
Mn-55 200033 0 1.191317e-05 293.00 end  
Fe-54 200033 0 5.392452e-05 293.00 end  
Fe-56 200033 0 8.464997e-04 293.00 end  
Fe-57 200033 0 1.954936e-05 293.00 end  
Fe-58 200033 0 2.601658e-06 293.00 end  
O-16 200034 0 2.931950e-02 293.00 end  
O-17 200034 0 1.114649e-05 293.00 end  
O-18 200034 0 6.026437e-05 293.00 end  
Na-23 200034 0 2.444715e-04 293.00 end  
Mg-24 200034 0 3.957787e-04 293.00 end  
Mg-25 200034 0 5.010491e-05 293.00 end  
Mg-26 200034 0 5.516551e-05 293.00 end  
Al-27 200034 0 2.326076e-03 293.00 end  
Si-28 200034 0 8.150971e-03 293.00 end  
Si-29 200034 0 4.140756e-04 293.00 end  
Si-30 200034 0 2.732811e-04 293.00 end  
K-39 200034 0 3.128084e-04 293.00 end  
K-40 200034 0 3.924422e-08 293.00 end  
K-41 200034 0 2.257459e-05 293.00 end  
Ca-40 200034 0 1.132863e-03 293.00 end  
Ca-42 200034 0 7.560904e-06 293.00 end  
Ca-43 200034 0 1.577628e-06 293.00 end  
Ca-44 200034 0 2.437722e-05 293.00 end  
Ca-46 200034 0 4.674011e-08 293.00 end  
Ca-48 200034 0 2.185305e-06 293.00 end  
Ti-46 200034 0 7.263565e-06 293.00 end  
Ti-47 200034 0 6.550416e-06 293.00 end  
Ti-48 200034 0 6.490546e-05 293.00 end  
Ti-49 200034 0 4.763137e-06 293.00 end  
Ti-50 200034 0 4.560639e-06 293.00 end  
Mn-55 200034 0 1.191317e-05 293.00 end  
Fe-54 200034 0 5.392452e-05 293.00 end  
Fe-56 200034 0 8.464997e-04 293.00 end  
Fe-57 200034 0 1.954936e-05 293.00 end  
Fe-58 200034 0 2.601658e-06 293.00 end  
O-16 200035 0 2.931950e-02 293.00 end  
O-17 200035 0 1.114649e-05 293.00 end  
O-18 200035 0 6.026437e-05 293.00 end  
Na-23 200035 0 2.444715e-04 293.00 end  
Mg-24 200035 0 3.957787e-04 293.00 end  
Mg-25 200035 0 5.010491e-05 293.00 end  
Mg-26 200035 0 5.516551e-05 293.00 end  
Al-27 200035 0 2.326076e-03 293.00 end  
Si-28 200035 0 8.150971e-03 293.00 end  
Si-29 200035 0 4.140756e-04 293.00 end  
Si-30 200035 0 2.732811e-04 293.00 end  
K-39 200035 0 3.128084e-04 293.00 end  
K-40 200035 0 3.924422e-08 293.00 end  
K-41 200035 0 2.257459e-05 293.00 end  
Ca-40 200035 0 1.132863e-03 293.00 end  
Ca-42 200035 0 7.560904e-06 293.00 end  
Ca-43 200035 0 1.577628e-06 293.00 end  
Ca-44 200035 0 2.437722e-05 293.00 end  
Ca-46 200035 0 4.674011e-08 293.00 end  
Ca-48 200035 0 2.185305e-06 293.00 end  
Ti-46 200035 0 7.263565e-06 293.00 end  
Ti-47 200035 0 6.550416e-06 293.00 end  
Ti-48 200035 0 6.490546e-05 293.00 end  
Ti-49 200035 0 4.763137e-06 293.00 end  
Ti-50 200035 0 4.560639e-06 293.00 end  
Mn-55 200035 0 1.191317e-05 293.00 end  
Fe-54 200035 0 5.392452e-05 293.00 end  
Fe-56 200035 0 8.464997e-04 293.00 end  
Fe-57 200035 0 1.954936e-05 293.00 end

Fe-58 200035 0 2.601658e-06 293.00 end  
O-16 200036 0 2.931950e-02 293.00 end  
O-17 200036 0 1.114649e-05 293.00 end  
O-18 200036 0 6.026437e-05 293.00 end  
Na-23 200036 0 2.444715e-04 293.00 end  
Mg-24 200036 0 3.957787e-04 293.00 end  
Mg-25 200036 0 5.010491e-05 293.00 end  
Mg-26 200036 0 5.516551e-05 293.00 end  
Al-27 200036 0 2.326076e-03 293.00 end  
Si-28 200036 0 8.150971e-03 293.00 end  
Si-29 200036 0 4.140756e-04 293.00 end  
Si-30 200036 0 2.732811e-04 293.00 end  
K-39 200036 0 3.128084e-04 293.00 end  
K-40 200036 0 3.924422e-08 293.00 end  
K-41 200036 0 2.257459e-05 293.00 end  
Ca-40 200036 0 1.132863e-03 293.00 end  
Ca-42 200036 0 7.560904e-06 293.00 end  
Ca-43 200036 0 1.577628e-06 293.00 end  
Ca-44 200036 0 2.437722e-05 293.00 end  
Ca-46 200036 0 4.674011e-08 293.00 end  
Ca-48 200036 0 2.185305e-06 293.00 end  
Ti-46 200036 0 7.263565e-06 293.00 end  
Ti-47 200036 0 6.550416e-06 293.00 end  
Ti-48 200036 0 6.490546e-05 293.00 end  
Ti-49 200036 0 4.763137e-06 293.00 end  
Ti-50 200036 0 4.560639e-06 293.00 end  
Mn-55 200036 0 1.191317e-05 293.00 end  
Fe-54 200036 0 5.392452e-05 293.00 end  
Fe-56 200036 0 8.464997e-04 293.00 end  
Fe-57 200036 0 1.954936e-05 293.00 end  
Fe-58 200036 0 2.601658e-06 293.00 end  
O-16 200037 0 2.931950e-02 293.00 end  
O-17 200037 0 1.114649e-05 293.00 end  
O-18 200037 0 6.026437e-05 293.00 end  
Na-23 200037 0 2.444715e-04 293.00 end  
Mg-24 200037 0 3.957787e-04 293.00 end  
Mg-25 200037 0 5.010491e-05 293.00 end  
Mg-26 200037 0 5.516551e-05 293.00 end  
Al-27 200037 0 2.326076e-03 293.00 end  
Si-28 200037 0 8.150971e-03 293.00 end  
Si-29 200037 0 4.140756e-04 293.00 end  
Si-30 200037 0 2.732811e-04 293.00 end  
K-39 200037 0 3.128084e-04 293.00 end  
K-40 200037 0 3.924422e-08 293.00 end  
K-41 200037 0 2.257459e-05 293.00 end  
Ca-40 200037 0 1.132863e-03 293.00 end  
Ca-42 200037 0 7.560904e-06 293.00 end  
Ca-43 200037 0 1.577628e-06 293.00 end  
Ca-44 200037 0 2.437722e-05 293.00 end  
Ca-46 200037 0 4.674011e-08 293.00 end  
Ca-48 200037 0 2.185305e-06 293.00 end  
Ti-46 200037 0 7.263565e-06 293.00 end  
Ti-47 200037 0 6.550416e-06 293.00 end  
Ti-48 200037 0 6.490546e-05 293.00 end  
Ti-49 200037 0 4.763137e-06 293.00 end  
Ti-50 200037 0 4.560639e-06 293.00 end  
Mn-55 200037 0 1.191317e-05 293.00 end  
Fe-54 200037 0 5.392452e-05 293.00 end  
Fe-56 200037 0 8.464997e-04 293.00 end  
Fe-57 200037 0 1.954936e-05 293.00 end  
Fe-58 200037 0 2.601658e-06 293.00 end  
O-16 200038 0 2.931950e-02 293.00 end  
O-17 200038 0 1.114649e-05 293.00 end  
O-18 200038 0 6.026437e-05 293.00 end  
Na-23 200038 0 2.444715e-04 293.00 end  
Mg-24 200038 0 3.957787e-04 293.00 end  
Mg-25 200038 0 5.010491e-05 293.00 end  
Mg-26 200038 0 5.516551e-05 293.00 end  
Al-27 200038 0 2.326076e-03 293.00 end  
Si-28 200038 0 8.150971e-03 293.00 end  
Si-29 200038 0 4.140756e-04 293.00 end  
Si-30 200038 0 2.732811e-04 293.00 end  
K-39 200038 0 3.128084e-04 293.00 end

K-40 200038 0 3.924422e-08 293.00 end  
 K-41 200038 0 2.257459e-05 293.00 end  
 Ca-40 200038 0 1.132863e-03 293.00 end  
 Ca-42 200038 0 7.560904e-06 293.00 end  
 Ca-43 200038 0 1.577628e-06 293.00 end  
 Ca-44 200038 0 2.437722e-05 293.00 end  
 Ca-46 200038 0 4.674011e-08 293.00 end  
 Ca-48 200038 0 2.185305e-06 293.00 end  
 Ti-46 200038 0 7.263565e-06 293.00 end  
 Ti-47 200038 0 6.550416e-06 293.00 end  
 Ti-48 200038 0 6.490546e-05 293.00 end  
 Ti-49 200038 0 4.763137e-06 293.00 end  
 Ti-50 200038 0 4.560639e-06 293.00 end  
 Mn-55 200038 0 1.191317e-05 293.00 end  
 Fe-54 200038 0 5.392452e-05 293.00 end  
 Fe-56 200038 0 8.464997e-04 293.00 end  
 Fe-57 200038 0 1.954936e-05 293.00 end  
 Fe-58 200038 0 2.601658e-06 293.00 end  
 O-16 200039 0 2.931950e-02 293.00 end  
 O-17 200039 0 1.114649e-05 293.00 end  
 O-18 200039 0 6.026437e-05 293.00 end  
 Na-23 200039 0 2.444715e-04 293.00 end  
 Mg-24 200039 0 3.957787e-04 293.00 end  
 Mg-25 200039 0 5.010491e-05 293.00 end  
 Mg-26 200039 0 5.516551e-05 293.00 end  
 Al-27 200039 0 2.326076e-03 293.00 end  
 Si-28 200039 0 8.150971e-03 293.00 end  
 Si-29 200039 0 4.140756e-04 293.00 end  
 Si-30 200039 0 2.732811e-04 293.00 end  
 K-39 200039 0 3.128084e-04 293.00 end  
 K-40 200039 0 3.924422e-08 293.00 end  
 K-41 200039 0 2.257459e-05 293.00 end  
 Ca-40 200039 0 1.132863e-03 293.00 end  
 Ca-42 200039 0 7.560904e-06 293.00 end  
 Ca-43 200039 0 1.577628e-06 293.00 end  
 Ca-44 200039 0 2.437722e-05 293.00 end  
 Ca-46 200039 0 4.674011e-08 293.00 end  
 Ca-48 200039 0 2.185305e-06 293.00 end  
 Ti-46 200039 0 7.263565e-06 293.00 end  
 Ti-47 200039 0 6.550416e-06 293.00 end  
 Ti-48 200039 0 6.490546e-05 293.00 end  
 Ti-49 200039 0 4.763137e-06 293.00 end  
 Ti-50 200039 0 4.560639e-06 293.00 end  
 Mn-55 200039 0 1.191317e-05 293.00 end  
 Fe-54 200039 0 5.392452e-05 293.00 end  
 Fe-56 200039 0 8.464997e-04 293.00 end  
 Fe-57 200039 0 1.954936e-05 293.00 end  
 Fe-58 200039 0 2.601658e-06 293.00 end  
 O-16 200040 0 2.931950e-02 293.00 end  
 O-17 200040 0 1.114649e-05 293.00 end  
 O-18 200040 0 6.026437e-05 293.00 end  
 Na-23 200040 0 2.444715e-04 293.00 end  
 Mg-24 200040 0 3.957787e-04 293.00 end  
 Mg-25 200040 0 5.010491e-05 293.00 end  
 Mg-26 200040 0 5.516551e-05 293.00 end  
 Al-27 200040 0 2.326076e-03 293.00 end  
 Si-28 200040 0 8.150971e-03 293.00 end  
 Si-29 200040 0 4.140756e-04 293.00 end  
 Si-30 200040 0 2.732811e-04 293.00 end  
 K-39 200040 0 3.128084e-04 293.00 end  
 K-40 200040 0 3.924422e-08 293.00 end  
 K-41 200040 0 2.257459e-05 293.00 end  
 Ca-40 200040 0 1.132863e-03 293.00 end  
 Ca-42 200040 0 7.560904e-06 293.00 end  
 Ca-43 200040 0 1.577628e-06 293.00 end  
 Ca-44 200040 0 2.437722e-05 293.00 end  
 Ca-46 200040 0 4.674011e-08 293.00 end  
 Ca-48 200040 0 2.185305e-06 293.00 end  
 Ti-46 200040 0 7.263565e-06 293.00 end  
 Ti-47 200040 0 6.550416e-06 293.00 end  
 Ti-48 200040 0 6.490546e-05 293.00 end  
 Ti-49 200040 0 4.763137e-06 293.00 end  
 Ti-50 200040 0 4.560639e-06 293.00 end

Mn-55 200040 0 1.191317e-05 293.00 end  
Fe-54 200040 0 5.392452e-05 293.00 end  
Fe-56 200040 0 8.464997e-04 293.00 end  
Fe-57 200040 0 1.954936e-05 293.00 end  
Fe-58 200040 0 2.601658e-06 293.00 end  
O-16 200041 0 2.931950e-02 293.00 end  
O-17 200041 0 1.114649e-05 293.00 end  
O-18 200041 0 6.026437e-05 293.00 end  
Na-23 200041 0 2.444715e-04 293.00 end  
Mg-24 200041 0 3.957787e-04 293.00 end  
Mg-25 200041 0 5.010491e-05 293.00 end  
Mg-26 200041 0 5.516551e-05 293.00 end  
Al-27 200041 0 2.326076e-03 293.00 end  
Si-28 200041 0 8.150971e-03 293.00 end  
Si-29 200041 0 4.140756e-04 293.00 end  
Si-30 200041 0 2.732811e-04 293.00 end  
K-39 200041 0 3.128084e-04 293.00 end  
K-40 200041 0 3.924422e-08 293.00 end  
K-41 200041 0 2.257459e-05 293.00 end  
Ca-40 200041 0 1.132863e-03 293.00 end  
Ca-42 200041 0 7.560904e-06 293.00 end  
Ca-43 200041 0 1.577628e-06 293.00 end  
Ca-44 200041 0 2.437722e-05 293.00 end  
Ca-46 200041 0 4.674011e-08 293.00 end  
Ca-48 200041 0 2.185305e-06 293.00 end  
Ti-46 200041 0 7.263565e-06 293.00 end  
Ti-47 200041 0 6.550416e-06 293.00 end  
Ti-48 200041 0 6.490546e-05 293.00 end  
Ti-49 200041 0 4.763137e-06 293.00 end  
Ti-50 200041 0 4.560639e-06 293.00 end  
Mn-55 200041 0 1.191317e-05 293.00 end  
Fe-54 200041 0 5.392452e-05 293.00 end  
Fe-56 200041 0 8.464997e-04 293.00 end  
Fe-57 200041 0 1.954936e-05 293.00 end  
Fe-58 200041 0 2.601658e-06 293.00 end  
O-16 200042 0 2.931950e-02 293.00 end  
O-17 200042 0 1.114649e-05 293.00 end  
O-18 200042 0 6.026437e-05 293.00 end  
Na-23 200042 0 2.444715e-04 293.00 end  
Mg-24 200042 0 3.957787e-04 293.00 end  
Mg-25 200042 0 5.010491e-05 293.00 end  
Mg-26 200042 0 5.516551e-05 293.00 end  
Al-27 200042 0 2.326076e-03 293.00 end  
Si-28 200042 0 8.150971e-03 293.00 end  
Si-29 200042 0 4.140756e-04 293.00 end  
Si-30 200042 0 2.732811e-04 293.00 end  
K-39 200042 0 3.128084e-04 293.00 end  
K-40 200042 0 3.924422e-08 293.00 end  
K-41 200042 0 2.257459e-05 293.00 end  
Ca-40 200042 0 1.132863e-03 293.00 end  
Ca-42 200042 0 7.560904e-06 293.00 end  
Ca-43 200042 0 1.577628e-06 293.00 end  
Ca-44 200042 0 2.437722e-05 293.00 end  
Ca-46 200042 0 4.674011e-08 293.00 end  
Ca-48 200042 0 2.185305e-06 293.00 end  
Ti-46 200042 0 7.263565e-06 293.00 end  
Ti-47 200042 0 6.550416e-06 293.00 end  
Ti-48 200042 0 6.490546e-05 293.00 end  
Ti-49 200042 0 4.763137e-06 293.00 end  
Ti-50 200042 0 4.560639e-06 293.00 end  
Mn-55 200042 0 1.191317e-05 293.00 end  
Fe-54 200042 0 5.392452e-05 293.00 end  
Fe-56 200042 0 8.464997e-04 293.00 end  
Fe-57 200042 0 1.954936e-05 293.00 end  
Fe-58 200042 0 2.601658e-06 293.00 end  
O-16 200043 0 2.931950e-02 293.00 end  
O-17 200043 0 1.114649e-05 293.00 end  
O-18 200043 0 6.026437e-05 293.00 end  
Na-23 200043 0 2.444715e-04 293.00 end  
Mg-24 200043 0 3.957787e-04 293.00 end  
Mg-25 200043 0 5.010491e-05 293.00 end  
Mg-26 200043 0 5.516551e-05 293.00 end  
Al-27 200043 0 2.326076e-03 293.00 end

Si-28 200043 0 8.150971e-03 293.00 end  
Si-29 200043 0 4.140756e-04 293.00 end  
Si-30 200043 0 2.732811e-04 293.00 end  
K-39 200043 0 3.128084e-04 293.00 end  
K-40 200043 0 3.924422e-08 293.00 end  
K-41 200043 0 2.257459e-05 293.00 end  
Ca-40 200043 0 1.132863e-03 293.00 end  
Ca-42 200043 0 7.560904e-06 293.00 end  
Ca-43 200043 0 1.577628e-06 293.00 end  
Ca-44 200043 0 2.437722e-05 293.00 end  
Ca-46 200043 0 4.674011e-08 293.00 end  
Ca-48 200043 0 2.185305e-06 293.00 end  
Ti-46 200043 0 7.263565e-06 293.00 end  
Ti-47 200043 0 6.550416e-06 293.00 end  
Ti-48 200043 0 6.490546e-05 293.00 end  
Ti-49 200043 0 4.763137e-06 293.00 end  
Ti-50 200043 0 4.560639e-06 293.00 end  
Mn-55 200043 0 1.191317e-05 293.00 end  
Fe-54 200043 0 5.392452e-05 293.00 end  
Fe-56 200043 0 8.464997e-04 293.00 end  
Fe-57 200043 0 1.954936e-05 293.00 end  
Fe-58 200043 0 2.601658e-06 293.00 end  
O-16 200044 0 2.931950e-02 293.00 end  
O-17 200044 0 1.114649e-05 293.00 end  
O-18 200044 0 6.026437e-05 293.00 end  
Na-23 200044 0 2.444715e-04 293.00 end  
Mg-24 200044 0 3.957787e-04 293.00 end  
Mg-25 200044 0 5.010491e-05 293.00 end  
Mg-26 200044 0 5.516551e-05 293.00 end  
Al-27 200044 0 2.326076e-03 293.00 end  
Si-28 200044 0 8.150971e-03 293.00 end  
Si-29 200044 0 4.140756e-04 293.00 end  
Si-30 200044 0 2.732811e-04 293.00 end  
K-39 200044 0 3.128084e-04 293.00 end  
K-40 200044 0 3.924422e-08 293.00 end  
K-41 200044 0 2.257459e-05 293.00 end  
Ca-40 200044 0 1.132863e-03 293.00 end  
Ca-42 200044 0 7.560904e-06 293.00 end  
Ca-43 200044 0 1.577628e-06 293.00 end  
Ca-44 200044 0 2.437722e-05 293.00 end  
Ca-46 200044 0 4.674011e-08 293.00 end  
Ca-48 200044 0 2.185305e-06 293.00 end  
Ti-46 200044 0 7.263565e-06 293.00 end  
Ti-47 200044 0 6.550416e-06 293.00 end  
Ti-48 200044 0 6.490546e-05 293.00 end  
Ti-49 200044 0 4.763137e-06 293.00 end  
Ti-50 200044 0 4.560639e-06 293.00 end  
Mn-55 200044 0 1.191317e-05 293.00 end  
Fe-54 200044 0 5.392452e-05 293.00 end  
Fe-56 200044 0 8.464997e-04 293.00 end  
Fe-57 200044 0 1.954936e-05 293.00 end  
Fe-58 200044 0 2.601658e-06 293.00 end  
O-16 200045 0 2.931950e-02 293.00 end  
O-17 200045 0 1.114649e-05 293.00 end  
O-18 200045 0 6.026437e-05 293.00 end  
Na-23 200045 0 2.444715e-04 293.00 end  
Mg-24 200045 0 3.957787e-04 293.00 end  
Mg-25 200045 0 5.010491e-05 293.00 end  
Mg-26 200045 0 5.516551e-05 293.00 end  
Al-27 200045 0 2.326076e-03 293.00 end  
Si-28 200045 0 8.150971e-03 293.00 end  
Si-29 200045 0 4.140756e-04 293.00 end  
Si-30 200045 0 2.732811e-04 293.00 end  
K-39 200045 0 3.128084e-04 293.00 end  
K-40 200045 0 3.924422e-08 293.00 end  
K-41 200045 0 2.257459e-05 293.00 end  
Ca-40 200045 0 1.132863e-03 293.00 end  
Ca-42 200045 0 7.560904e-06 293.00 end  
Ca-43 200045 0 1.577628e-06 293.00 end  
Ca-44 200045 0 2.437722e-05 293.00 end  
Ca-46 200045 0 4.674011e-08 293.00 end  
Ca-48 200045 0 2.185305e-06 293.00 end  
Ti-46 200045 0 7.263565e-06 293.00 end

Ti-47 200045 0 6.550416e-06 293.00 end  
Ti-48 200045 0 6.490546e-05 293.00 end  
Ti-49 200045 0 4.763137e-06 293.00 end  
Ti-50 200045 0 4.560639e-06 293.00 end  
Mn-55 200045 0 1.191317e-05 293.00 end  
Fe-54 200045 0 5.392452e-05 293.00 end  
Fe-56 200045 0 8.464997e-04 293.00 end  
Fe-57 200045 0 1.954936e-05 293.00 end  
Fe-58 200045 0 2.601658e-06 293.00 end  
O-16 200046 0 2.931950e-02 293.00 end  
O-17 200046 0 1.114649e-05 293.00 end  
O-18 200046 0 6.026437e-05 293.00 end  
Na-23 200046 0 2.444715e-04 293.00 end  
Mg-24 200046 0 3.957787e-04 293.00 end  
Mg-25 200046 0 5.010491e-05 293.00 end  
Mg-26 200046 0 5.516551e-05 293.00 end  
Al-27 200046 0 2.326076e-03 293.00 end  
Si-28 200046 0 8.150971e-03 293.00 end  
Si-29 200046 0 4.140756e-04 293.00 end  
Si-30 200046 0 2.732811e-04 293.00 end  
K-39 200046 0 3.128084e-04 293.00 end  
K-40 200046 0 3.924422e-08 293.00 end  
K-41 200046 0 2.257459e-05 293.00 end  
Ca-40 200046 0 1.132863e-03 293.00 end  
Ca-42 200046 0 7.560904e-06 293.00 end  
Ca-43 200046 0 1.577628e-06 293.00 end  
Ca-44 200046 0 2.437722e-05 293.00 end  
Ca-46 200046 0 4.674011e-08 293.00 end  
Ca-48 200046 0 2.185305e-06 293.00 end  
Ti-46 200046 0 7.263565e-06 293.00 end  
Ti-47 200046 0 6.550416e-06 293.00 end  
Ti-48 200046 0 6.490546e-05 293.00 end  
Ti-49 200046 0 4.763137e-06 293.00 end  
Ti-50 200046 0 4.560639e-06 293.00 end  
Mn-55 200046 0 1.191317e-05 293.00 end  
Fe-54 200046 0 5.392452e-05 293.00 end  
Fe-56 200046 0 8.464997e-04 293.00 end  
Fe-57 200046 0 1.954936e-05 293.00 end  
Fe-58 200046 0 2.601658e-06 293.00 end  
O-16 200047 0 2.931950e-02 293.00 end  
O-17 200047 0 1.114649e-05 293.00 end  
O-18 200047 0 6.026437e-05 293.00 end  
Na-23 200047 0 2.444715e-04 293.00 end  
Mg-24 200047 0 3.957787e-04 293.00 end  
Mg-25 200047 0 5.010491e-05 293.00 end  
Mg-26 200047 0 5.516551e-05 293.00 end  
Al-27 200047 0 2.326076e-03 293.00 end  
Si-28 200047 0 8.150971e-03 293.00 end  
Si-29 200047 0 4.140756e-04 293.00 end  
Si-30 200047 0 2.732811e-04 293.00 end  
K-39 200047 0 3.128084e-04 293.00 end  
K-40 200047 0 3.924422e-08 293.00 end  
K-41 200047 0 2.257459e-05 293.00 end  
Ca-40 200047 0 1.132863e-03 293.00 end  
Ca-42 200047 0 7.560904e-06 293.00 end  
Ca-43 200047 0 1.577628e-06 293.00 end  
Ca-44 200047 0 2.437722e-05 293.00 end  
Ca-46 200047 0 4.674011e-08 293.00 end  
Ca-48 200047 0 2.185305e-06 293.00 end  
Ti-46 200047 0 7.263565e-06 293.00 end  
Ti-47 200047 0 6.550416e-06 293.00 end  
Ti-48 200047 0 6.490546e-05 293.00 end  
Ti-49 200047 0 4.763137e-06 293.00 end  
Ti-50 200047 0 4.560639e-06 293.00 end  
Mn-55 200047 0 1.191317e-05 293.00 end  
Fe-54 200047 0 5.392452e-05 293.00 end  
Fe-56 200047 0 8.464997e-04 293.00 end  
Fe-57 200047 0 1.954936e-05 293.00 end  
Fe-58 200047 0 2.601658e-06 293.00 end  
O-16 200048 0 2.931950e-02 293.00 end  
O-17 200048 0 1.114649e-05 293.00 end  
O-18 200048 0 6.026437e-05 293.00 end  
Na-23 200048 0 2.444715e-04 293.00 end

Mg-24 200048 0 3.957787e-04 293.00 end  
Mg-25 200048 0 5.010491e-05 293.00 end  
Mg-26 200048 0 5.516551e-05 293.00 end  
Al-27 200048 0 2.326076e-03 293.00 end  
Si-28 200048 0 8.150971e-03 293.00 end  
Si-29 200048 0 4.140756e-04 293.00 end  
Si-30 200048 0 2.732811e-04 293.00 end  
K-39 200048 0 3.128084e-04 293.00 end  
K-40 200048 0 3.924422e-08 293.00 end  
K-41 200048 0 2.257459e-05 293.00 end  
Ca-40 200048 0 1.132863e-03 293.00 end  
Ca-42 200048 0 7.560904e-06 293.00 end  
Ca-43 200048 0 1.577628e-06 293.00 end  
Ca-44 200048 0 2.437722e-05 293.00 end  
Ca-46 200048 0 4.674011e-08 293.00 end  
Ca-48 200048 0 2.185305e-06 293.00 end  
Ti-46 200048 0 7.263565e-06 293.00 end  
Ti-47 200048 0 6.550416e-06 293.00 end  
Ti-48 200048 0 6.490546e-05 293.00 end  
Ti-49 200048 0 4.763137e-06 293.00 end  
Ti-50 200048 0 4.560639e-06 293.00 end  
Mn-55 200048 0 1.191317e-05 293.00 end  
Fe-54 200048 0 5.392452e-05 293.00 end  
Fe-56 200048 0 8.464997e-04 293.00 end  
Fe-57 200048 0 1.954936e-05 293.00 end  
Fe-58 200048 0 2.601658e-06 293.00 end  
O-16 200049 0 2.931950e-02 293.00 end  
O-17 200049 0 1.114649e-05 293.00 end  
O-18 200049 0 6.026437e-05 293.00 end  
Na-23 200049 0 2.444715e-04 293.00 end  
Mg-24 200049 0 3.957787e-04 293.00 end  
Mg-25 200049 0 5.010491e-05 293.00 end  
Mg-26 200049 0 5.516551e-05 293.00 end  
Al-27 200049 0 2.326076e-03 293.00 end  
Si-28 200049 0 8.150971e-03 293.00 end  
Si-29 200049 0 4.140756e-04 293.00 end  
Si-30 200049 0 2.732811e-04 293.00 end  
K-39 200049 0 3.128084e-04 293.00 end  
K-40 200049 0 3.924422e-08 293.00 end  
K-41 200049 0 2.257459e-05 293.00 end  
Ca-40 200049 0 1.132863e-03 293.00 end  
Ca-42 200049 0 7.560904e-06 293.00 end  
Ca-43 200049 0 1.577628e-06 293.00 end  
Ca-44 200049 0 2.437722e-05 293.00 end  
Ca-46 200049 0 4.674011e-08 293.00 end  
Ca-48 200049 0 2.185305e-06 293.00 end  
Ti-46 200049 0 7.263565e-06 293.00 end  
Ti-47 200049 0 6.550416e-06 293.00 end  
Ti-48 200049 0 6.490546e-05 293.00 end  
Ti-49 200049 0 4.763137e-06 293.00 end  
Ti-50 200049 0 4.560639e-06 293.00 end  
Mn-55 200049 0 1.191317e-05 293.00 end  
Fe-54 200049 0 5.392452e-05 293.00 end  
Fe-56 200049 0 8.464997e-04 293.00 end  
Fe-57 200049 0 1.954936e-05 293.00 end  
Fe-58 200049 0 2.601658e-06 293.00 end  
O-16 200050 0 2.931950e-02 293.00 end  
O-17 200050 0 1.114649e-05 293.00 end  
O-18 200050 0 6.026437e-05 293.00 end  
Na-23 200050 0 2.444715e-04 293.00 end  
Mg-24 200050 0 3.957787e-04 293.00 end  
Mg-25 200050 0 5.010491e-05 293.00 end  
Mg-26 200050 0 5.516551e-05 293.00 end  
Al-27 200050 0 2.326076e-03 293.00 end  
Si-28 200050 0 8.150971e-03 293.00 end  
Si-29 200050 0 4.140756e-04 293.00 end  
Si-30 200050 0 2.732811e-04 293.00 end  
K-39 200050 0 3.128084e-04 293.00 end  
K-40 200050 0 3.924422e-08 293.00 end  
K-41 200050 0 2.257459e-05 293.00 end  
Ca-40 200050 0 1.132863e-03 293.00 end  
Ca-42 200050 0 7.560904e-06 293.00 end  
Ca-43 200050 0 1.577628e-06 293.00 end

```

Ca-44 200050 0 2.437722e-05 293.00 end
Ca-46 200050 0 4.674011e-08 293.00 end
Ca-48 200050 0 2.185305e-06 293.00 end
Ti-46 200050 0 7.263565e-06 293.00 end
Ti-47 200050 0 6.550416e-06 293.00 end
Ti-48 200050 0 6.490546e-05 293.00 end
Ti-49 200050 0 4.763137e-06 293.00 end
Ti-50 200050 0 4.560639e-06 293.00 end
Mn-55 200050 0 1.191317e-05 293.00 end
Fe-54 200050 0 5.392452e-05 293.00 end
Fe-56 200050 0 8.464997e-04 293.00 end
Fe-57 200050 0 1.954936e-05 293.00 end
Fe-58 200050 0 2.601658e-06 293.00 end

end comp

read geometry
'Outside Hexagonal Pattern dummy
  unit 3
  hexprism 1 3 0 -60.96
  media 2 1 1
  boundary 1
'Inner Hexagonal Pattern'
  unit 4
  hexprism 1 2 0 -60.96
  hexprism 2 3 0 -60.96
  media 3 1 1
  media 2 2 -1 2
  boundary 2
'Dummy Geogrid Block'
  unit 6
  hexprism 1 31 0 -60.96
  media 3 1 1
  boundary 1
'Inner Mesh Geogrid Block
'One Geogrid Block'
  unit 7
  hexprism 4 31 0 -60.96
  media 2 1 -3 4
  hexprism 3 29 0 -60.96
  cylinder 8 5 0 -60.96
  cylinder 9 6.5 0 -60.96
  media 3 1 8
  media 2 1 -8 9
  array 1 3 -8 -9 4 place 12 12 1 0 0 0
  boundary 4
'Reactor rod'
  unit 8
  xcylinder 13 80 -81 81 origin y=0 z=130
  xcylinder 14 95 -96 96 origin y=0 z=130
  xcylinder 15 100 -101 101 origin y=0 z=130
  media 5 1 13
  media 6 2 -13 14
  media 7 3 -13 -14 15
  boundary 15

global unit 10
'Geogrid Layer'
cuboid 10 -379 379 -135.16 135.16 -60.96 0
cuboid 11 -381 381 -137.16 137.16 -60.96 0
array 2 10 place 12 12 1 0 0 0
media 2 11 -10 11 17

'Soil Layer'
cuboid 12 -381 381 -137.16 137.16 -365.76 -60.96
'
=====
' THIS SECTION GENERATED BY SCALESlice
=====
'OLD LINE = media 4 1 12 17
plane 100001 xpl=1.0 ypl=0.0 zpl=0.0 con=381.0
plane 100002 xpl=1.0 ypl=0.0 zpl=0.0 con=-381.0
plane 100003 xpl=0.0 ypl=1.0 zpl=0.0 con=137.16
plane 100004 xpl=0.0 ypl=1.0 zpl=0.0 con=-137.16

```

plane	100005	xpl=0.0	ypl=0.0	zpl=1.0	con=365.76
plane	100006	xpl=0.0	ypl=0.0	zpl=1.0	con=359.664
plane	100007	xpl=0.0	ypl=0.0	zpl=1.0	con=353.568
plane	100008	xpl=0.0	ypl=0.0	zpl=1.0	con=347.472
plane	100009	xpl=0.0	ypl=0.0	zpl=1.0	con=341.376
plane	100010	xpl=0.0	ypl=0.0	zpl=1.0	con=335.28
plane	100011	xpl=0.0	ypl=0.0	zpl=1.0	con=329.184
plane	100012	xpl=0.0	ypl=0.0	zpl=1.0	con=323.088
plane	100013	xpl=0.0	ypl=0.0	zpl=1.0	con=316.992
plane	100014	xpl=0.0	ypl=0.0	zpl=1.0	con=310.896
plane	100015	xpl=0.0	ypl=0.0	zpl=1.0	con=304.8
plane	100016	xpl=0.0	ypl=0.0	zpl=1.0	con=298.704
plane	100017	xpl=0.0	ypl=0.0	zpl=1.0	con=292.608
plane	100018	xpl=0.0	ypl=0.0	zpl=1.0	con=286.512
plane	100019	xpl=0.0	ypl=0.0	zpl=1.0	con=280.416
plane	100020	xpl=0.0	ypl=0.0	zpl=1.0	con=274.32
plane	100021	xpl=0.0	ypl=0.0	zpl=1.0	con=268.224
plane	100022	xpl=0.0	ypl=0.0	zpl=1.0	con=262.128
plane	100023	xpl=0.0	ypl=0.0	zpl=1.0	con=256.032
plane	100024	xpl=0.0	ypl=0.0	zpl=1.0	con=249.936
plane	100025	xpl=0.0	ypl=0.0	zpl=1.0	con=243.84
plane	100026	xpl=0.0	ypl=0.0	zpl=1.0	con=237.744
plane	100027	xpl=0.0	ypl=0.0	zpl=1.0	con=231.648
plane	100028	xpl=0.0	ypl=0.0	zpl=1.0	con=225.552
plane	100029	xpl=0.0	ypl=0.0	zpl=1.0	con=219.456
plane	100030	xpl=0.0	ypl=0.0	zpl=1.0	con=213.36
plane	100031	xpl=0.0	ypl=0.0	zpl=1.0	con=207.264
plane	100032	xpl=0.0	ypl=0.0	zpl=1.0	con=201.168
plane	100033	xpl=0.0	ypl=0.0	zpl=1.0	con=195.072
plane	100034	xpl=0.0	ypl=0.0	zpl=1.0	con=188.976
plane	100035	xpl=0.0	ypl=0.0	zpl=1.0	con=182.88
plane	100036	xpl=0.0	ypl=0.0	zpl=1.0	con=176.784
plane	100037	xpl=0.0	ypl=0.0	zpl=1.0	con=170.688
plane	100038	xpl=0.0	ypl=0.0	zpl=1.0	con=164.592
plane	100039	xpl=0.0	ypl=0.0	zpl=1.0	con=158.496
plane	100040	xpl=0.0	ypl=0.0	zpl=1.0	con=152.4
plane	100041	xpl=0.0	ypl=0.0	zpl=1.0	con=146.304
plane	100042	xpl=0.0	ypl=0.0	zpl=1.0	con=140.208
plane	100043	xpl=0.0	ypl=0.0	zpl=1.0	con=134.112
plane	100044	xpl=0.0	ypl=0.0	zpl=1.0	con=128.016
plane	100045	xpl=0.0	ypl=0.0	zpl=1.0	con=121.92
plane	100046	xpl=0.0	ypl=0.0	zpl=1.0	con=115.824
plane	100047	xpl=0.0	ypl=0.0	zpl=1.0	con=109.728
plane	100048	xpl=0.0	ypl=0.0	zpl=1.0	con=103.632
plane	100049	xpl=0.0	ypl=0.0	zpl=1.0	con=97.536
plane	100050	xpl=0.0	ypl=0.0	zpl=1.0	con=91.44
plane	100051	xpl=0.0	ypl=0.0	zpl=1.0	con=85.344
plane	100052	xpl=0.0	ypl=0.0	zpl=1.0	con=79.248
plane	100053	xpl=0.0	ypl=0.0	zpl=1.0	con=73.152
plane	100054	xpl=0.0	ypl=0.0	zpl=1.0	con=67.056
plane	100055	xpl=0.0	ypl=0.0	zpl=1.0	con=60.96

'NOW TIME FOR MEDIA CARDS

media	200001	1	12	17	+100001	-100002	+100003	-100004	+100005	-100006
media	200002	1	12	17	+100001	-100002	+100003	-100004	+100006	-100007
media	200003	1	12	17	+100001	-100002	+100003	-100004	+100007	-100008
media	200004	1	12	17	+100001	-100002	+100003	-100004	+100008	-100009
media	200005	1	12	17	+100001	-100002	+100003	-100004	+100009	-100010
media	200006	1	12	17	+100001	-100002	+100003	-100004	+100010	-100011
media	200007	1	12	17	+100001	-100002	+100003	-100004	+100011	-100012
media	200008	1	12	17	+100001	-100002	+100003	-100004	+100012	-100013
media	200009	1	12	17	+100001	-100002	+100003	-100004	+100013	-100014
media	200010	1	12	17	+100001	-100002	+100003	-100004	+100014	-100015
media	200011	1	12	17	+100001	-100002	+100003	-100004	+100015	-100016
media	200012	1	12	17	+100001	-100002	+100003	-100004	+100016	-100017
media	200013	1	12	17	+100001	-100002	+100003	-100004	+100017	-100018
media	200014	1	12	17	+100001	-100002	+100003	-100004	+100018	-100019
media	200015	1	12	17	+100001	-100002	+100003	-100004	+100019	-100020
media	200016	1	12	17	+100001	-100002	+100003	-100004	+100020	-100021
media	200017	1	12	17	+100001	-100002	+100003	-100004	+100021	-100022
media	200018	1	12	17	+100001	-100002	+100003	-100004	+100022	-100023
media	200019	1	12	17	+100001	-100002	+100003	-100004	+100023	-100024



```

    3 3 3 3 3 3 4 4 4 4 4 4 4 4 4 4 3 3 3 3 3 3
    3 3 3 3 3 3 3 3 3 3 3 3 3 3 3 3 3 3 3 3 3 3
end fill
ara=2 typ=shexagonal nux=23 nuy=23 nuz=1
fill
  6 6 6 6 6 6 6 6 6 6 6 6 6 6 6 6 6 6 6 6 6 6
  6 6 6 6 6 6 7 7 7 7 7 7 7 7 7 7 7 6 6 6 6 6 6
6 6 6 6 6 6 7 7 7 7 7 7 7 7 7 7 7 7 6 6 6 6 6 6
  6 6 6 6 6 7 7 7 7 7 7 7 7 7 7 7 7 6 6 6 6 6 6
6 6 6 6 6 7 7 7 7 7 7 7 7 7 7 7 7 6 6 6 6 6 6
  6 6 6 6 7 7 7 7 7 7 7 7 7 7 7 7 7 6 6 6 6 6 6
6 6 6 7 7 7 7 7 7 7 7 7 7 7 7 7 7 7 6 6 6 6 6 6
  6 6 7 7 7 7 7 7 7 7 7 7 7 7 7 7 7 7 6 6 6 6 6 6
6 6 7 7 7 7 7 7 7 7 7 7 7 7 7 7 7 7 6 6 6 6 6 6
  6 7 7 7 7 7 7 7 7 7 7 7 7 7 7 7 7 7 6 6 6 6 6 6
6 6 7 7 7 7 7 7 7 7 7 7 7 7 7 7 7 7 6 6 6 6 6 6
  6 6 7 7 7 7 7 7 7 7 7 7 7 7 7 7 7 7 6 6 6 6 6 6
6 6 6 7 7 7 7 7 7 7 7 7 7 7 7 7 7 7 6 6 6 6 6 6
  6 6 6 7 7 7 7 7 7 7 7 7 7 7 7 7 7 7 6 6 6 6 6 6
6 6 6 6 7 7 7 7 7 7 7 7 7 7 7 7 7 7 6 6 6 6 6 6
  6 6 6 6 6 7 7 7 7 7 7 7 7 7 7 7 7 7 6 6 6 6 6 6
6 6 6 6 6 6 7 7 7 7 7 7 7 7 7 7 7 7 6 6 6 6 6 6
  6 6 6 6 6 6 6 6 6 6 6 6 6 6 6 6 6 6 6 6 6 6 6 6
end fill
end array
end data
end

```

Listing B.1: CSAS simulation script  
(CSAS.inp)

Example of MAVRIC Code (to obtain neutron flux) using the 2-foot HDPE and water basemat.

```
=mavric
1-1
v7.1-200n47g
read parameters
batches 250
perBatch=1000000
fissionMult=0
randomseed=7102537391082819
end parameters

read sources
  src 1
    title="KENO Fission Source"
    meshsourcefile="flux.msm"
    fissions=4.857513273E17
    edistributionid=1
  end src
end sources

read definitions
  response 1
    title="ANSI standard (1991) gamma flux-to-dose-rate factors (rem/h)"
    dosedata=9505
  end response

  response 2
    title="ANSI standard (1991) neutron flux-to-dose-rate factors (rem/h)"
    dosedata=9031
  end response

  gridGeometry 1
  ' 1.12M voxels total'
  title="Mesh to determine flux/dose rates over whole space (~5 cm voxels)"
  xlinear 152 -381 381
  ylinear 55 -137.16 137.16
  zlinear 138 -365.76 304.8
  end gridGeometry

  gridGeometry 2
  title="Adjoint Source Mesh (~5cm voxels)"
  xlinear 152 -381 381
  ylinear 30 -137.16 137.16
  zlinear 138 -365.76 304.8
  end gridGeometry

  distribution 1
    title="Watt Fission Spectrum for U-235"
    special="wattSpectrum"
    parameters 0.998 2.249 end
  end distribution

make3Dmaps

end definitions

read importancemap
  gridgeometryid=2
  adjointSource 1
  boundingbox=-381 381 -137.16 137.16 -365.76 304.8
  responseid=2
  end adjointSource
  respweighting
'adjointfluxes="Mav.adjoint.dff"
end importancemap
```

```

read tallies
  meshTally 2
  title="Neutron Dose Mesh Tally"
  neutron
  gridgeometryid=1
  responseID=2
  nogroupfluxes
  fromsource=1
  end meshTally

  regionTally 1
  neutron unit=10 mixture=200001
  end regionTally
  regionTally 2
  neutron unit=10 mixture=200002
  end regionTally
  regionTally 3
  neutron unit=10 mixture=200003
  end regionTally
  regionTally 4
  neutron unit=10 mixture=200004
  end regionTally
  regionTally 5
  neutron unit=10 mixture=200005
  end regionTally
  regionTally 6
  neutron unit=10 mixture=200006
  end regionTally
  regionTally 7
  neutron unit=10 mixture=200007
  end regionTally
  regionTally 8
  neutron unit=10 mixture=200008
  end regionTally
  regionTally 9
  neutron unit=10 mixture=200009
  end regionTally
  regionTally 10
  neutron unit=10 mixture=200010
  end regionTally
  regionTally 11
  neutron unit=10 mixture=200011
  end regionTally
  regionTally 12
  neutron unit=10 mixture=200012
  end regionTally
  regionTally 13
  neutron unit=10 mixture=200013
  end regionTally
  regionTally 14
  neutron unit=10 mixture=200014
  end regionTally
  regionTally 15
  neutron unit=10 mixture=200015
  end regionTally
  regionTally 16
  neutron unit=10 mixture=200016
  end regionTally
  regionTally 17
  neutron unit=10 mixture=200017
  end regionTally
  regionTally 18
  neutron unit=10 mixture=200018
  end regionTally
  regionTally 19
  neutron unit=10 mixture=200019
  end regionTally
  regionTally 20
  neutron unit=10 mixture=200020
  end regionTally
  regionTally 21
  neutron unit=10 mixture=200021
  end regionTally

```

```
regionTally 22
neutron unit=10 mixture=200022
end regionTally
regionTally 23
neutron unit=10 mixture=200023
end regionTally
regionTally 24
neutron unit=10 mixture=200024
end regionTally
regionTally 25
neutron unit=10 mixture=200025
end regionTally
regionTally 26
neutron unit=10 mixture=200026
end regionTally
regionTally 27
neutron unit=10 mixture=200027
end regionTally
regionTally 28
neutron unit=10 mixture=200028
end regionTally
regionTally 29
neutron unit=10 mixture=200029
end regionTally
regionTally 30
neutron unit=10 mixture=200030
end regionTally
regionTally 31
neutron unit=10 mixture=200031
end regionTally
regionTally 32
neutron unit=10 mixture=200032
end regionTally
regionTally 33
neutron unit=10 mixture=200033
end regionTally
regionTally 34
neutron unit=10 mixture=200034
end regionTally
regionTally 35
neutron unit=10 mixture=200035
end regionTally
regionTally 36
neutron unit=10 mixture=200036
end regionTally
regionTally 37
neutron unit=10 mixture=200037
end regionTally
regionTally 38
neutron unit=10 mixture=200038
end regionTally
regionTally 39
neutron unit=10 mixture=200039
end regionTally
regionTally 40
neutron unit=10 mixture=200040
end regionTally
regionTally 41
neutron unit=10 mixture=200041
end regionTally
regionTally 42
neutron unit=10 mixture=200042
end regionTally
regionTally 43
neutron unit=10 mixture=200043
end regionTally
regionTally 44
neutron unit=10 mixture=200044
end regionTally
regionTally 45
neutron unit=10 mixture=200045
end regionTally
regionTally 46
```

```

        neutron unit=10 mixture=200046
        end regionTally
        regionTally 47
        neutron unit=10 mixture=200047
        end regionTally
        regionTally 48
        neutron unit=10 mixture=200048
        end regionTally
        regionTally 49
        neutron unit=10 mixture=200049
        end regionTally
        regionTally 50
        neutron unit=10 mixture=200050
        end regionTally
end tallies

read comp
'INSERT SAME MATERIAL CARD THAT IS LISTED IN THE CSAS EXAMPLE'

end comp

read geometry
'Outside Hexagonal Pattern dummy
    unit 3
    hexprism 1 3 0 -60.96
    media 2 1 1
    boundary 1
'Inner Hexagonal Pattern'
    unit 4
    hexprism 1 2 0 -60.96
    hexprism 2 3 0 -60.96
    media 3 1 1
    media 2 2 -1 2
    boundary 2
'Dummy Geogrid Block'
    unit 6
    hexprism 1 31 0 -60.96
    media 3 1 1
    boundary 1
'Inner Mesh Geogrid Block
'One Geogrid Block'
    unit 7
    hexprism 4 31 0 -60.96
    media 2 1 -3 4
    hexprism 3 29 0 -60.96
    cylinder 8 5 0 -60.96
    cylinder 9 6.5 0 -60.96
    media 3 1 8
    media 2 1 -8 9
    array 1 3 -8 -9 4 place 12 12 1 0 0 0
    boundary 4
'Reactor rod'
    unit 8
    xcylinder 13 80 -81 81 origin y=0 z=130
    xcylinder 14 95 -96 96 origin y=0 z=130
    xcylinder 15 100 -101 101 origin y=0 z=130
    media 5 1 13
    media 6 2 -13 14
    media 7 3 -13 -14 15
    boundary 15

global unit 10
'Geogrid Layer'
cuboid 10 -379 379 -135.16 135.16 -60.96 0
cuboid 11 -381 381 -137.16 137.16 -60.96 0
array 2 10 place 12 12 1 0 0 0
media 2 11 -10 11 17

'Soil Layer'
cuboid 12 -381 381 -137.16 137.16 -365.76 -60.96
' =====
' THIS SECTION GENERATED BY SCALESlice
' =====

```

```

'OLD LINE = media 4 1 12 17
plane 100001 xpl=1.0 ypl=0.0 zpl=0.0 con=381.0
plane 100002 xpl=1.0 ypl=0.0 zpl=0.0 con=-381.0
plane 100003 xpl=0.0 ypl=1.0 zpl=0.0 con=137.16
plane 100004 xpl=0.0 ypl=1.0 zpl=0.0 con=-137.16
plane 100005 xpl=0.0 ypl=0.0 zpl=1.0 con=365.76
plane 100006 xpl=0.0 ypl=0.0 zpl=1.0 con=359.664
plane 100007 xpl=0.0 ypl=0.0 zpl=1.0 con=353.568
plane 100008 xpl=0.0 ypl=0.0 zpl=1.0 con=347.472
plane 100009 xpl=0.0 ypl=0.0 zpl=1.0 con=341.376
plane 100010 xpl=0.0 ypl=0.0 zpl=1.0 con=335.28
plane 100011 xpl=0.0 ypl=0.0 zpl=1.0 con=329.184
plane 100012 xpl=0.0 ypl=0.0 zpl=1.0 con=323.088
plane 100013 xpl=0.0 ypl=0.0 zpl=1.0 con=316.992
plane 100014 xpl=0.0 ypl=0.0 zpl=1.0 con=310.896
plane 100015 xpl=0.0 ypl=0.0 zpl=1.0 con=304.8
plane 100016 xpl=0.0 ypl=0.0 zpl=1.0 con=298.704
plane 100017 xpl=0.0 ypl=0.0 zpl=1.0 con=292.608
plane 100018 xpl=0.0 ypl=0.0 zpl=1.0 con=286.512
plane 100019 xpl=0.0 ypl=0.0 zpl=1.0 con=280.416
plane 100020 xpl=0.0 ypl=0.0 zpl=1.0 con=274.32
plane 100021 xpl=0.0 ypl=0.0 zpl=1.0 con=268.224
plane 100022 xpl=0.0 ypl=0.0 zpl=1.0 con=262.128
plane 100023 xpl=0.0 ypl=0.0 zpl=1.0 con=256.032
plane 100024 xpl=0.0 ypl=0.0 zpl=1.0 con=249.936
plane 100025 xpl=0.0 ypl=0.0 zpl=1.0 con=243.84
plane 100026 xpl=0.0 ypl=0.0 zpl=1.0 con=237.744
plane 100027 xpl=0.0 ypl=0.0 zpl=1.0 con=231.648
plane 100028 xpl=0.0 ypl=0.0 zpl=1.0 con=225.552
plane 100029 xpl=0.0 ypl=0.0 zpl=1.0 con=219.456
plane 100030 xpl=0.0 ypl=0.0 zpl=1.0 con=213.36
plane 100031 xpl=0.0 ypl=0.0 zpl=1.0 con=207.264
plane 100032 xpl=0.0 ypl=0.0 zpl=1.0 con=201.168
plane 100033 xpl=0.0 ypl=0.0 zpl=1.0 con=195.072
plane 100034 xpl=0.0 ypl=0.0 zpl=1.0 con=188.976
plane 100035 xpl=0.0 ypl=0.0 zpl=1.0 con=182.88
plane 100036 xpl=0.0 ypl=0.0 zpl=1.0 con=176.784
plane 100037 xpl=0.0 ypl=0.0 zpl=1.0 con=170.688
plane 100038 xpl=0.0 ypl=0.0 zpl=1.0 con=164.592
plane 100039 xpl=0.0 ypl=0.0 zpl=1.0 con=158.496
plane 100040 xpl=0.0 ypl=0.0 zpl=1.0 con=152.4
plane 100041 xpl=0.0 ypl=0.0 zpl=1.0 con=146.304
plane 100042 xpl=0.0 ypl=0.0 zpl=1.0 con=140.208
plane 100043 xpl=0.0 ypl=0.0 zpl=1.0 con=134.112
plane 100044 xpl=0.0 ypl=0.0 zpl=1.0 con=128.016
plane 100045 xpl=0.0 ypl=0.0 zpl=1.0 con=121.92
plane 100046 xpl=0.0 ypl=0.0 zpl=1.0 con=115.824
plane 100047 xpl=0.0 ypl=0.0 zpl=1.0 con=109.728
plane 100048 xpl=0.0 ypl=0.0 zpl=1.0 con=103.632
plane 100049 xpl=0.0 ypl=0.0 zpl=1.0 con=97.536
plane 100050 xpl=0.0 ypl=0.0 zpl=1.0 con=91.44
plane 100051 xpl=0.0 ypl=0.0 zpl=1.0 con=85.344
plane 100052 xpl=0.0 ypl=0.0 zpl=1.0 con=79.248
plane 100053 xpl=0.0 ypl=0.0 zpl=1.0 con=73.152
plane 100054 xpl=0.0 ypl=0.0 zpl=1.0 con=67.056
plane 100055 xpl=0.0 ypl=0.0 zpl=1.0 con=60.96

```

```
'NOW TIME FOR MEDIA CARDS
```

```

media 200001 1 12 17 +100001 -100002 +100003 -100004 +100005 -100006
media 200002 1 12 17 +100001 -100002 +100003 -100004 +100006 -100007
media 200003 1 12 17 +100001 -100002 +100003 -100004 +100007 -100008
media 200004 1 12 17 +100001 -100002 +100003 -100004 +100008 -100009
media 200005 1 12 17 +100001 -100002 +100003 -100004 +100009 -100010
media 200006 1 12 17 +100001 -100002 +100003 -100004 +100010 -100011
media 200007 1 12 17 +100001 -100002 +100003 -100004 +100011 -100012
media 200008 1 12 17 +100001 -100002 +100003 -100004 +100012 -100013
media 200009 1 12 17 +100001 -100002 +100003 -100004 +100013 -100014
media 200010 1 12 17 +100001 -100002 +100003 -100004 +100014 -100015
media 200011 1 12 17 +100001 -100002 +100003 -100004 +100015 -100016
media 200012 1 12 17 +100001 -100002 +100003 -100004 +100016 -100017
media 200013 1 12 17 +100001 -100002 +100003 -100004 +100017 -100018
media 200014 1 12 17 +100001 -100002 +100003 -100004 +100018 -100019

```

```

media 200015 1 12 17 +100001 -100002 +100003 -100004 +100019 -100020
media 200016 1 12 17 +100001 -100002 +100003 -100004 +100020 -100021
media 200017 1 12 17 +100001 -100002 +100003 -100004 +100021 -100022
media 200018 1 12 17 +100001 -100002 +100003 -100004 +100022 -100023
media 200019 1 12 17 +100001 -100002 +100003 -100004 +100023 -100024
media 200020 1 12 17 +100001 -100002 +100003 -100004 +100024 -100025
media 200021 1 12 17 +100001 -100002 +100003 -100004 +100025 -100026
media 200022 1 12 17 +100001 -100002 +100003 -100004 +100026 -100027
media 200023 1 12 17 +100001 -100002 +100003 -100004 +100027 -100028
media 200024 1 12 17 +100001 -100002 +100003 -100004 +100028 -100029
media 200025 1 12 17 +100001 -100002 +100003 -100004 +100029 -100030
media 200026 1 12 17 +100001 -100002 +100003 -100004 +100030 -100031
media 200027 1 12 17 +100001 -100002 +100003 -100004 +100031 -100032
media 200028 1 12 17 +100001 -100002 +100003 -100004 +100032 -100033
media 200029 1 12 17 +100001 -100002 +100003 -100004 +100033 -100034
media 200030 1 12 17 +100001 -100002 +100003 -100004 +100034 -100035
media 200031 1 12 17 +100001 -100002 +100003 -100004 +100035 -100036
media 200032 1 12 17 +100001 -100002 +100003 -100004 +100036 -100037
media 200033 1 12 17 +100001 -100002 +100003 -100004 +100037 -100038
media 200034 1 12 17 +100001 -100002 +100003 -100004 +100038 -100039
media 200035 1 12 17 +100001 -100002 +100003 -100004 +100039 -100040
media 200036 1 12 17 +100001 -100002 +100003 -100004 +100040 -100041
media 200037 1 12 17 +100001 -100002 +100003 -100004 +100041 -100042
media 200038 1 12 17 +100001 -100002 +100003 -100004 +100042 -100043
media 200039 1 12 17 +100001 -100002 +100003 -100004 +100043 -100044
media 200040 1 12 17 +100001 -100002 +100003 -100004 +100044 -100045
media 200041 1 12 17 +100001 -100002 +100003 -100004 +100045 -100046
media 200042 1 12 17 +100001 -100002 +100003 -100004 +100046 -100047
media 200043 1 12 17 +100001 -100002 +100003 -100004 +100047 -100048
media 200044 1 12 17 +100001 -100002 +100003 -100004 +100048 -100049
media 200045 1 12 17 +100001 -100002 +100003 -100004 +100049 -100050
media 200046 1 12 17 +100001 -100002 +100003 -100004 +100050 -100051
media 200047 1 12 17 +100001 -100002 +100003 -100004 +100051 -100052
media 200048 1 12 17 +100001 -100002 +100003 -100004 +100052 -100053
media 200049 1 12 17 +100001 -100002 +100003 -100004 +100053 -100054
media 200050 1 12 17 +100001 -100002 +100003 -100004 +100054 -100055

```

```

' =====
' END OF SCALESlice GENERATED SECTION
' =====

```

```

'Air Layer'/Connex Box'
cuboid 16 -381 381 -137.16 137.16 0 304.8
cuboid 18 -284 284 -102.92 102.92 19 240
cuboid 19 -303 303 -121.92 121.92 0 259.08
media 1 1 16 17 -18 -19
media 8 1 16 17 -18 19
media 1 1 16 17 18 19
hole 8
'Outer Region'
cuboid 17 -381 381 -137.16 137.16 -363.83 304.8
boundary 17

```

```

end geometry
read array
ara=1 typ=shexagonal nux=23 nuy=23 nuz=1
fill
3 3 3 3 3 3 3 3 3 3 3 3 3 3 3 3 3 3 3 3 3 3 3 3 3
3 3 3 3 3 3 4 4 4 4 4 4 4 4 4 4 4 4 3 3 3 3 3 3 3
3 3 3 3 3 3 4 4 4 4 4 4 4 4 4 4 4 4 4 4 3 3 3 3 3
3 3 3 3 3 3 4 4 4 4 4 4 4 4 4 4 4 4 4 4 4 3 3 3 3 3
3 3 3 3 3 3 4 4 4 4 4 4 4 4 4 4 4 4 4 4 4 4 3 3 3 3
3 3 3 4 4 4 4 4 4 4 4 4 4 4 4 4 4 4 4 4 4 4 4 3 3 3
3 3 3 4 4 4 4 4 4 4 4 4 4 4 4 4 4 4 4 4 4 4 4 3 3
3 3 4 4 4 4 4 4 4 4 4 4 4 4 4 4 4 4 4 4 4 4 4 3 3
3 3 4 4 4 4 4 4 4 4 4 4 4 4 4 4 4 4 4 4 4 4 4 3
3 4 4 4 4 4 4 4 4 4 4 4 4 4 4 4 4 4 4 4 4 4 4 4 3
3 3 4 4 4 4 4 4 4 4 4 4 4 4 4 4 4 4 4 4 4 4 4 3
3 3 4 4 4 4 4 4 4 4 4 4 4 4 4 4 4 4 4 4 4 4 4 3 3
3 3 3 4 4 4 4 4 4 4 4 4 4 4 4 4 4 4 4 4 4 4 4 3 3
3 3 3 4 4 4 4 4 4 4 4 4 4 4 4 4 4 4 4 4 4 4 4 3 3 3

```

```

3 3 3 3 4 4 4 4 4 4 4 4 4 4 4 4 4 4 4 4 3 3 3
3 3 3 3 4 4 4 4 4 4 4 4 4 4 4 4 4 4 4 4 3 3 3 3
3 3 3 3 3 4 4 4 4 4 4 4 4 4 4 4 4 4 4 4 3 3 3 3
3 3 3 3 3 3 4 4 4 4 4 4 4 4 4 4 4 4 4 3 3 3 3 3
3 3 3 3 3 3 4 4 4 4 4 4 4 4 4 4 4 4 3 3 3 3 3 3
3 3 3 3 3 3 3 3 3 3 3 3 3 3 3 3 3 3 3 3 3 3 3 3
end fill
ara=2 typ=shexagonal nux=23 nuy=23 nuz=1
fill
6 6 6 6 6 6 6 6 6 6 6 6 6 6 6 6 6 6 6 6 6 6 6
6 6 6 6 6 6 7 7 7 7 7 7 7 7 7 7 7 6 6 6 6 6 6
6 6 6 6 6 6 7 7 7 7 7 7 7 7 7 7 7 6 6 6 6 6 6
6 6 6 6 6 7 7 7 7 7 7 7 7 7 7 7 7 6 6 6 6 6 6
6 6 6 6 7 7 7 7 7 7 7 7 7 7 7 7 7 6 6 6 6 6 6
6 6 6 6 7 7 7 7 7 7 7 7 7 7 7 7 7 6 6 6 6 6 6
6 6 6 7 7 7 7 7 7 7 7 7 7 7 7 7 7 7 6 6 6 6 6
6 6 7 7 7 7 7 7 7 7 7 7 7 7 7 7 7 7 7 6 6 6 6
6 6 7 7 7 7 7 7 7 7 7 7 7 7 7 7 7 7 7 6 6 6 6
6 7 7 7 7 7 7 7 7 7 7 7 7 7 7 7 7 7 7 7 6 6 6 6
6 7 7 7 7 7 7 7 7 7 7 7 7 7 7 7 7 7 7 7 6 6 6 6
6 6 7 7 7 7 7 7 7 7 7 7 7 7 7 7 7 7 7 7 6 6 6 6
6 6 6 7 7 7 7 7 7 7 7 7 7 7 7 7 7 7 7 7 6 6 6 6
6 6 6 6 7 7 7 7 7 7 7 7 7 7 7 7 7 7 7 7 6 6 6 6
6 6 6 6 6 7 7 7 7 7 7 7 7 7 7 7 7 7 7 6 6 6 6 6
6 6 6 6 6 6 7 7 7 7 7 7 7 7 7 7 7 7 7 6 6 6 6 6
6 6 6 6 6 6 6 7 7 7 7 7 7 7 7 7 7 7 7 6 6 6 6 6 6
6 6 6 6 6 6 6 6 6 6 6 6 6 6 6 6 6 6 6 6 6 6 6 6
end fill
end array
end data
end

```

Listing B.2: MAVRIC (for neutron flux) simulation script (MAVRIC.inp)

Example of ORIGEN Code for one soil slice using the 2-foot HDPE and water basemat.

```
=origen
  bounds {
    neutron="scale.rev13.xn200g47v7.1"
    gamma=[ 999I 2.0e7 1.0e4 ]
  }
  build_lib("activation_source1.f33") {
    neutron(1) {
      type=ENDF_ENERGY_DEPENDENT
      reaction_resource="C:\file_path\origen.rev03.jeff200g"
      fp_yield_resource="C:\file_path\origen.rev05.yields.data"
      spectrum {
        type=MULTIGROUP
        flux=[0.00000E+00
0.00000E+00
0.00000E+00
0.00000E+00
0.00000E+00
0.00000E+00
0.00000E+00
0.00000E+00
0.00000E+00
0.00000E+00
0.00000E+00
0.00000E+00
0.00000E+00
2.39671E-01
1.71048E-01
2.27047E-01
4.45051E-01
2.30005E+00
1.66091E+00
4.37282E+00
1.35607E+01
7.46923E+00
7.08026E+00
1.01618E+01
1.17755E+01
1.05939E+01
4.13085E+01
1.96902E+01
1.16738E+02
1.80504E+02
9.99224E+01
1.02156E+02
1.60647E+02
1.08510E+02
1.33273E+02
1.30425E+02
2.61699E+02
2.27738E+02
1.60348E+02
9.41647E+01
1.64363E+02
2.14594E+02
2.93896E+02
3.42813E+02
3.87546E+02
7.26341E+02
4.20073E+02
1.27069E+03
2.31987E+03
2.49420E+03
2.14466E+03
1.59957E+03
1.16165E+03
9.02465E+02
```

1.41229E+03  
1.09814E+03  
8.96531E+02  
1.01662E+03  
1.16778E+03  
1.10882E+03  
7.46989E+02  
1.05376E+03  
9.61292E+02  
8.77216E+02  
1.02648E+03  
2.92136E+02  
5.78701E+02  
6.21377E+02  
7.07581E+02  
9.00099E+02  
1.10331E+03  
1.11546E+03  
1.10656E+03  
1.24175E+03  
1.17592E+03  
1.21241E+03  
1.07928E+03  
1.08787E+03  
1.24544E+03  
1.77765E+03  
8.11903E+02  
5.17573E+02  
4.27214E+02  
1.22551E+03  
1.55118E+03  
1.80510E+02  
5.20530E+01  
1.42539E+02  
3.10917E+02  
7.40974E+02  
1.55432E+03  
7.06301E+02  
7.23114E+02  
6.22808E+02  
6.02562E+02  
5.72294E+02  
6.31610E+02  
5.96871E+02  
8.56192E+02  
1.15176E+03  
9.04610E+02  
8.28990E+02  
1.08196E+03  
1.15528E+03  
1.20200E+03  
1.00305E+03  
1.10702E+03  
2.87459E+03  
2.27240E+03  
7.31560E+02  
7.97806E+02  
2.15188E+03  
1.72535E+03  
4.06541E+03  
1.69686E+03  
3.54582E+03  
3.43837E+03  
3.77738E+03  
2.14172E+03  
3.14817E+03  
1.17222E+03  
1.11420E+03  
1.52114E+03  
9.19187E+02  
9.20497E+02  
2.14561E+03  
3.97557E+03

8.21237E+03  
8.88902E+03  
3.52670E+03  
5.84089E+03  
1.02327E+04  
1.05813E+04  
1.20802E+04  
7.01338E+03  
4.50970E+03  
4.06404E+03  
3.18038E+03  
1.62212E+03  
2.12436E+03  
4.74295E+03  
4.89742E+03  
1.31583E+04  
1.38376E+04  
1.49628E+04  
1.66380E+04  
1.68417E+04  
1.85533E+04  
1.91033E+04  
2.14741E+04  
2.24588E+04  
2.47274E+04  
2.53464E+04  
2.71613E+04  
2.74112E+04  
2.89129E+04  
3.11909E+04  
3.22237E+04  
3.47011E+04  
3.77089E+04  
3.97956E+04  
4.00646E+04  
4.28955E+04  
4.46383E+04  
4.87625E+04  
4.69651E+04  
4.97966E+04  
5.47576E+04  
7.28519E+05  
1.49052E+08  
1.04592E+08  
3.85473E+07  
4.84223E+07  
1.29487E+07  
1.16342E+07  
1.18122E+07  
3.75708E+07  
2.44978E+07  
3.98973E+07  
2.11269E+07  
3.75343E+07  
1.36482E+07  
4.00869E+07  
2.47042E+07  
2.39355E+07  
3.17462E+07  
3.70531E+07  
3.64267E+07  
3.68102E+07  
3.28040E+07  
4.04671E+07  
6.33915E+07  
5.29659E+07  
2.87437E+07  
2.83034E+07  
2.35077E+07  
1.41224E+07  
7.76173E+06  
5.65626E+06  
1.62653E+06

```

2.91223E+05
1.53745E+04]
    }
  }
}
case(irradiation) {
title="Soil activation"
lib {
file="activation_source1.f33"
}
mat {
% elements in soil
units=atoms-per-barn-cm
iso=[O16=2.931950e-02, O17=1.114649e-05, O18=6.026437e-05,
Na23=2.444715e-04, Mg24=3.957787e-04, Mg25=5.010491e-05,
Mg26=5.516551e-05, Al27=2.326076e-03,
Si28=8.150971e-03, Si29=4.140756e-04, Si30=2.732811e-04,
K39=3.128084e-04, K40=3.924422e-08, K41=2.257459e-05, Ca40=1.132863e-
03, Ca42=7.560904e-06,
Ca43=1.577628e-06, Ca44=2.437722e-05, Ca46=4.674011e-08,
Ca48=2.185305e-06, Ti46=7.263565e-06, Ti47=6.550416e-06,
Ti48=6.490546e-05, Ti49=4.763137e-06
Ti50=4.560639e-06, Mn55=1.191317e-05, Fe54=5.392452e-05,
Fe56=8.464997e-04, Fe57=1.954936e-05, Fe58=2.601658e-06]
volume=1274258.097 %cm^3 of each soil slice
}

time {
units="days"
t=[1 2 5 10 20 30 40 80 120 160 180 365 366 370 380 395 415 440
455 500 545 600 700 730 2190]
}
flux = [12r 850.1652864129298 0 0 0 0 0 0 0 0 0 0 0 0 0]
neutron = yes
gamma{
sublib=ALL % LT, FP, or AC single sublib
% ALL = all sub-libraries
continuum=yes % expand continuum data stored as
% lines into proper continuua
immediate=yes % load lines for immediate gamma/x-rays
spont=yes % include photons from spont fiss
brem_medium=UO2 % include bremsstrahlung from betas
}
save{ file="DS01.f71" steps=all }
} % Bracket for case
end

=opus
title="Necutron Spectrum"
data="DS01.f71"
typarams=nspectrum
units=particles
end

=opus
title="Activation/Decay Source"
data="DS01.f71"
typarams=nuclides
units=grams
time=days
end

```

Listing B.3: ORIGEN simulation script (ORIGEN.inp)

Example of MAVRIC code (to generate photon dose rate map) using the 2-foot HDPE and water basemat.

```
=mavric
Mavric Basemat
v7.1-200n47g

read parameters
batches=200
perBatch=1000000
fissionMult=0
randomseed=7102537391082819
photons
pminenergy=1e-5
pmaxenergy=2e7
end parameters

read tallies
meshTally 17
title="Dose Tally"
photon
gridgeometryid=1
responseID=1
nogroupfluxes
end meshTally

end tallies

read definitions

response 1
  title="ANSI standard (1991) gamma flux-to-dose-rate factors (rem/h)"
  dosedata=9505
end response

response 2
  title="ANSI standard (1991) neutron flux-to-dose-rate factors (rem/h)"
  dosedata=9031
end response

gridGeometry 1
  ' 1.12M voxels total'
  title="Mesh to determine flux/dose rates over whole space (~5 cm voxels)"
  xlinear 1 -381 381
  ylinear 1 -137.16 137.16
  zlinear 121 -304.8 304.8
end gridGeometry

gridGeometry 2
  title="Adjoint Source Mesh (~5cm voxels)"
  xlinear 152 -381 381
  ylinear 30 -137.16 137.16
  zlinear 121 -304.8 304.8
end gridGeometry

distribution 1
  special="origensBinaryConcentrationFile"
  filename='DSO50.f71'
  parameters 17 5 end
end distribution

distribution 2
  special="origensBinaryConcentrationFile"
  filename='DSO49.f71'
  parameters 17 5 end
end distribution
```

```
distribution 3
  special="origensBinaryConcentrationFile"
  filename='DSO48.f71'
  parameters 17 5 end
end distribution

distribution 4
  special="origensBinaryConcentrationFile"
  filename='DSO47.f71'
  parameters 17 5 end
end distribution

distribution 5
  special="origensBinaryConcentrationFile"
  filename='DSO46.f71'
  parameters 17 5 end
end distribution

distribution 6
  special="origensBinaryConcentrationFile"
  filename='DSO45.f71'
  parameters 17 5 end
end distribution

distribution 7
  special="origensBinaryConcentrationFile"
  filename='DSO44.f71'
  parameters 17 5 end
end distribution

distribution 8
  special="origensBinaryConcentrationFile"
  filename='DSO43.f71'
  parameters 17 5 end
end distribution

distribution 9
  special="origensBinaryConcentrationFile"
  filename='DSO42.f71'
  parameters 17 5 end
end distribution

distribution 10
  special="origensBinaryConcentrationFile"
  filename='DSO41.f71'
  parameters 17 5 end
end distribution

distribution 11
  special="origensBinaryConcentrationFile"
  filename='DSO40.f71'
  parameters 17 5 end
end distribution

distribution 12
  special="origensBinaryConcentrationFile"
  filename='DSO39.f71'
  parameters 17 5 end
end distribution

distribution 17
  special="origensBinaryConcentrationFile"
  filename='DSO38.f71'
  parameters 17 5 end
end distribution

distribution 14
  special="origensBinaryConcentrationFile"
  filename='DSO37.f71'
  parameters 17 5 end
end distribution

distribution 15
```

```

        special="origensBinaryConcentrationFile"
        filename='DSO36.f71'
        parameters 17 5 end
end distribution

distribution 16
    special="origensBinaryConcentrationFile"
    filename='DSO35.f71'
    parameters 17 5 end
end distribution

distribution 13
    special="origensBinaryConcentrationFile"
    filename='DSO34.f71'
    parameters 17 5 end
end distribution

distribution 18
    special="origensBinaryConcentrationFile"
    filename='DSO33.f71'
    parameters 17 5 end
end distribution

distribution 19
    special="origensBinaryConcentrationFile"
    filename='DSO32.f71'
    parameters 17 5 end
end distribution

distribution 20
    special="origensBinaryConcentrationFile"
    filename='DSO31.f71'
    parameters 17 5 end
end distribution

distribution 21
    special="origensBinaryConcentrationFile"
    filename='DSO30.f71'
    parameters 17 5 end
end distribution

distribution 22
    special="origensBinaryConcentrationFile"
    filename='DSO29.f71'
    parameters 17 5 end
end distribution

distribution 23
    special="origensBinaryConcentrationFile"
    filename='DSO28.f71'
    parameters 17 5 end
end distribution

distribution 24
    special="origensBinaryConcentrationFile"
    filename='DSO27.f71'
    parameters 17 5 end
end distribution

distribution 25
    special="origensBinaryConcentrationFile"
    filename='DSO26.f71'
    parameters 17 5 end
end distribution

distribution 26
    special="origensBinaryConcentrationFile"
    filename='DSO25.f71'
    parameters 17 5 end
end distribution

distribution 27
    special="origensBinaryConcentrationFile"

```

```
        filename='DSO24.f71'  
        parameters 17 5 end  
end distribution  
  
distribution 28  
    special="origensBinaryConcentrationFile"  
    filename='DSO23.f71'  
    parameters 17 5 end  
end distribution  
  
distribution 29  
    special="origensBinaryConcentrationFile"  
    filename='DSO22.f71'  
    parameters 17 5 end  
end distribution  
  
distribution 30  
    special="origensBinaryConcentrationFile"  
    filename='DSO21.f71'  
    parameters 17 5 end  
end distribution  
  
distribution 31  
    special="origensBinaryConcentrationFile"  
    filename='DSO20.f71'  
    parameters 17 5 end  
end distribution  
  
distribution 32  
    special="origensBinaryConcentrationFile"  
    filename='DSO19.f71'  
    parameters 17 5 end  
end distribution  
  
distribution 33  
    special="origensBinaryConcentrationFile"  
    filename='DSO18.f71'  
    parameters 17 5 end  
end distribution  
  
distribution 34  
    special="origensBinaryConcentrationFile"  
    filename='DSO17.f71'  
    parameters 17 5 end  
end distribution  
  
distribution 35  
    special="origensBinaryConcentrationFile"  
    filename='DSO16.f71'  
    parameters 17 5 end  
end distribution  
  
distribution 36  
    special="origensBinaryConcentrationFile"  
    filename='DSO15.f71'  
    parameters 17 5 end  
end distribution  
  
distribution 37  
    special="origensBinaryConcentrationFile"  
    filename='DSO14.f71'  
    parameters 17 5 end  
end distribution  
  
distribution 38  
    special="origensBinaryConcentrationFile"  
    filename='DSO13.f71'  
    parameters 17 5 end  
end distribution  
  
distribution 39  
    special="origensBinaryConcentrationFile"  
    filename='DSO12.f71'
```

```

    parameters 17 5 end
end distribution

distribution 40
    special="origensBinaryConcentrationFile"
    filename='DSO11.f71'
    parameters 17 5 end
end distribution

distribution 41
    special="origensBinaryConcentrationFile"
    filename='DSO10.f71'
    parameters 17 5 end
end distribution

distribution 42
    special="origensBinaryConcentrationFile"
    filename='DSO9.f71'
    parameters 17 5 end
end distribution

distribution 43
    special="origensBinaryConcentrationFile"
    filename='DSO8.f71'
    parameters 17 5 end
end distribution

distribution 44
    special="origensBinaryConcentrationFile"
    filename='DSO7.f71'
    parameters 17 5 end
end distribution

distribution 45
    special="origensBinaryConcentrationFile"
    filename='DSO6.f71'
    parameters 17 5 end
end distribution

distribution 46
    special="origensBinaryConcentrationFile"
    filename='DSO5.f71'
    parameters 17 5 end
end distribution

distribution 47
    special="origensBinaryConcentrationFile"
    filename='DSO4.f71'
    parameters 17 5 end
end distribution

distribution 48
    special="origensBinaryConcentrationFile"
    filename='DSO3.f71'
    parameters 17 5 end
end distribution

distribution 49
    special="origensBinaryConcentrationFile"
    filename='DSO2.f71'
    parameters 17 5 end
end distribution

distribution 50
    special="origensBinaryConcentrationFile"
    filename='DSO1.f71'
    parameters 17 5 end
end distribution

end definitions
read sources

```

```
src 1
```

```

title="Gamma Sorce"
Photon
mixture=200050
cuboid -381 381 -137.16 137.16 -6.0959999999989 0.0
usenormconst
edistributionid=1
end src

src 2
title="Gamma Sorce"
Photon
mixture=200049
cuboid -381 381 -137.16 137.16 -12.1919999999978 -6.0959999999989
usenormconst
edistributionid=2
end src

src 3
title="Gamma Sorce"
Photon
mixture=200048
cuboid -381 381 -137.16 137.16 -18.2879999999967 -12.1919999999978
usenormconst
edistributionid=3
end src

src 4
title="Gamma Sorce"
Photon
mixture=200047
cuboid -381 381 -137.16 137.16 -24.3839999999956 -18.2879999999967
usenormconst
edistributionid=4
end src

src 5
title="Gamma Sorce"
Photon
mixture=200046
cuboid -381 381 -137.16 137.16 -30.4799999999945 -24.3839999999956
usenormconst
edistributionid=5
end src

src 6
title="Gamma Sorce"
Photon
mixture=200045
cuboid -381 381 -137.16 137.16 -36.5759999999934 -30.4799999999945
usenormconst
edistributionid=6
end src

src 7
title="Gamma Sorce"
Photon
mixture=200044
cuboid -381 381 -137.16 137.16 -42.6719999999923 -36.5759999999934
usenormconst
edistributionid=7
end src

src 8
title="Gamma Sorce"
Photon
mixture=200043
cuboid -381 381 -137.16 137.16 -48.7679999999912 -42.6719999999923
usenormconst
edistributionid=8
end src

src 9
title="Gamma Sorce"

```

```

Photon
mixture=200042
cuboid -381 381 -137.16 137.16 -54.86399999999901 -48.76799999999912
usenormconst
edistributionid=9
end src

src 10
title="Gamma Sorce"
Photon
mixture=200041
cuboid -381 381 -137.16 137.16 -60.95999999999989 -54.86399999999901
usenormconst
edistributionid=10
end src

src 11
title="Gamma Sorce"
Photon
mixture=200040
cuboid -381 381 -137.16 137.16 -67.055999999999879 -60.95999999999989
usenormconst
edistributionid=11
end src

src 12
title="Gamma Sorce"
Photon
mixture=200039
cuboid -381 381 -137.16 137.16 -73.151999999999868 -67.055999999999879
usenormconst
edistributionid=12
end src

src 13
title="Gamma Sorce"
Photon
mixture=200038
cuboid -381 381 -137.16 137.16 -79.247999999999857 -73.151999999999868
usenormconst
edistributionid=13
end src

src 14
title="Gamma Sorce"
Photon
mixture=200037
cuboid -381 381 -137.16 137.16 -85.343999999999846 -79.247999999999857
usenormconst
edistributionid=14
end src

src 15
title="Gamma Sorce"
Photon
mixture=200036
cuboid -381 381 -137.16 137.16 -91.439999999999835 -85.343999999999846
usenormconst
edistributionid=15
end src

src 16
title="Gamma Sorce"
Photon
mixture=200035
cuboid -381 381 -137.16 137.16 -97.535999999999824 -91.439999999999835
usenormconst
edistributionid=16
end src

src 17
title="Gamma Sorce"
Photon

```

```

mixture=200034
cuboid -381 381 -137.16 137.16 -103.63199999999813 -97.53599999999824
usenormconst
edistributionid=17
end src

src 18
title="Gamma Sorce"
Photon
mixture=200033
cuboid -381 381 -137.16 137.16 -109.72799999999802 -103.63199999999813
usenormconst
edistributionid=18
end src

src 19
title="Gamma Sorce"
Photon
mixture=200032
cuboid -381 381 -137.16 137.16 -115.82399999999791 -109.72799999999802
usenormconst
edistributionid=19
end src

src 20
title="Gamma Sorce"
Photon
mixture=200031
cuboid -381 381 -137.16 137.16 -121.9199999999978 -115.82399999999791
usenormconst
edistributionid=20
end src

src 21
title="Gamma Sorce"
Photon
mixture=200030
cuboid -381 381 -137.16 137.16 -128.0159999999977 -121.9199999999978
usenormconst
edistributionid=21
end src

src 22
title="Gamma Sorce"
Photon
mixture=200029
cuboid -381 381 -137.16 137.16 -134.11199999999758 -128.0159999999977
usenormconst
edistributionid=22
end src

src 23
title="Gamma Sorce"
Photon
mixture=200028
cuboid -381 381 -137.16 137.16 -140.20799999999747 -134.11199999999758
usenormconst
edistributionid=23
end src

src 24
title="Gamma Sorce"
Photon
mixture=200027
cuboid -381 381 -137.16 137.16 -146.30399999999736 -140.20799999999747
usenormconst
edistributionid=24
end src

src 25
title="Gamma Sorce"
Photon
mixture=200026

```

```

cuboid -381 381 -137.16 137.16 -152.3999999999725 -146.30399999999736
usenormconst
edistributionid=25
end src

src 26
title="Gamma Sorce"
Photon
mixture=200025
cuboid -381 381 -137.16 137.16 -158.49599999999714 -152.39999999999725
usenormconst
edistributionid=26
end src

src 27
title="Gamma Sorce"
Photon
mixture=200024
cuboid -381 381 -137.16 137.16 -164.59199999999703 -158.49599999999714
usenormconst
edistributionid=27
end src

src 28
title="Gamma Sorce"
Photon
mixture=200023
cuboid -381 381 -137.16 137.16 -170.68799999999692 -164.59199999999703
usenormconst
edistributionid=28
end src

src 29
title="Gamma Sorce"
Photon
mixture=200022
cuboid -381 381 -137.16 137.16 -176.7839999999968 -170.68799999999692
usenormconst
edistributionid=29
end src

src 30
title="Gamma Sorce"
Photon
mixture=200021
cuboid -381 381 -137.16 137.16 -182.8799999999967 -176.7839999999968
usenormconst
edistributionid=30
end src

src 31
title="Gamma Sorce"
Photon
mixture=200020
cuboid -381 381 -137.16 137.16 -188.9759999999966 -182.8799999999967
usenormconst
edistributionid=31
end src

src 32
title="Gamma Sorce"
Photon
mixture=200019
cuboid -381 381 -137.16 137.16 -195.07199999999648 -188.9759999999966
usenormconst
edistributionid=32
end src

src 33
title="Gamma Sorce"
Photon
mixture=200018
cuboid -381 381 -137.16 137.16 -201.16799999999637 -195.07199999999648

```

```

usenormconst
edistributionid=33
end src

src 34
title="Gamma Sorce"
Photon
mixture=200017
cuboid -381 381 -137.16 137.16 -207.2639999999626 -201.1679999999637
usenormconst
edistributionid=34
end src

src 35
title="Gamma Sorce"
Photon
mixture=200016
cuboid -381 381 -137.16 137.16 -213.3599999999615 -207.2639999999626
usenormconst
edistributionid=35
end src

src 36
title="Gamma Sorce"
Photon
mixture=200015
cuboid -381 381 -137.16 137.16 -219.4559999999604 -213.3599999999615
usenormconst
edistributionid=36
end src

src 37
title="Gamma Sorce"
Photon
mixture=200014
cuboid -381 381 -137.16 137.16 -225.5519999999593 -219.4559999999604
usenormconst
edistributionid=37
end src

src 38
title="Gamma Sorce"
Photon
mixture=200013
cuboid -381 381 -137.16 137.16 -231.6479999999582 -225.5519999999593
usenormconst
edistributionid=38
end src

src 39
title="Gamma Sorce"
Photon
mixture=200012
cuboid -381 381 -137.16 137.16 -237.743999999957 -231.6479999999582
usenormconst
edistributionid=39
end src

src 40
title="Gamma Sorce"
Photon
mixture=200011
cuboid -381 381 -137.16 137.16 -243.839999999956 -237.743999999957
usenormconst
edistributionid=40
end src

src 41
title="Gamma Sorce"
Photon
mixture=200010
cuboid -381 381 -137.16 137.16 -249.935999999955 -243.839999999956
usenormconst

```

```

edistributionid=41
end src

src 42
title="Gamma Sorce"
Photon
mixture=200009
cuboid -381 381 -137.16 137.16 -256.0319999999954 -249.9359999999955
usenormconst
edistributionid=42
end src

src 43
title="Gamma Sorce"
Photon
mixture=200008
cuboid -381 381 -137.16 137.16 -262.12799999999527 -256.0319999999954
usenormconst
edistributionid=43
end src

src 44
title="Gamma Sorce"
Photon
mixture=200007
cuboid -381 381 -137.16 137.16 -268.22399999999516 -262.12799999999527
usenormconst
edistributionid=44
end src

src 45
title="Gamma Sorce"
Photon
mixture=200006
cuboid -381 381 -137.16 137.16 -274.31999999999505 -268.22399999999516
usenormconst
edistributionid=45
end src

src 46
title="Gamma Sorce"
Photon
mixture=200005
cuboid -381 381 -137.16 137.16 -280.41599999999494 -274.31999999999505
usenormconst
edistributionid=46
end src

src 47
title="Gamma Sorce"
Photon
mixture=200004
cuboid -381 381 -137.16 137.16 -286.5119999999948 -280.41599999999494
usenormconst
edistributionid=47
end src

src 48
title="Gamma Sorce"
Photon
mixture=200003
cuboid -381 381 -137.16 137.16 -292.6079999999947 -286.5119999999948
usenormconst
edistributionid=48
end src

src 49
title="Gamma Sorce"
Photon
mixture=200002
cuboid -381 381 -137.16 137.16 -298.7039999999946 -292.6079999999947
usenormconst
edistributionid=49

```

```

end src

src 50
title="Gamma Sorce"
Photon
mixture=200001
cuboid -381 381 -137.16 137.16 -304.7999999999945 -298.7039999999946
usenormconst
edistributionid=50
end src

end sources

read comp
' INSERT SAME MATERIAL CARD AS LISTED IN CSAS EXAMPLE'

end comp

read geometry
global unit 10

'Soil Layer'
cuboid 12 -381 381 -137.16 137.16 -304.8 0
' =====
' THIS SECTION GENERATED BY SCALESlice
' =====
'OLD LINE = media 4 1 12 17
plane 100001 xpl=1.0 ypl=0.0 zpl=0.0 con=381.0
plane 100002 xpl=1.0 ypl=0.0 zpl=0.0 con=-381.0
plane 100003 xpl=0.0 ypl=1.0 zpl=0.0 con=137.16
plane 100004 xpl=0.0 ypl=1.0 zpl=0.0 con=-137.16
plane 100005 xpl=0.0 ypl=0.0 zpl=1.0 con=304.8
plane 100006 xpl=0.0 ypl=0.0 zpl=1.0 con=298.704
plane 100007 xpl=0.0 ypl=0.0 zpl=1.0 con=292.608
plane 100008 xpl=0.0 ypl=0.0 zpl=1.0 con=286.512
plane 100009 xpl=0.0 ypl=0.0 zpl=1.0 con=280.416
plane 100010 xpl=0.0 ypl=0.0 zpl=1.0 con=274.32
plane 100011 xpl=0.0 ypl=0.0 zpl=1.0 con=268.224
plane 100012 xpl=0.0 ypl=0.0 zpl=1.0 con=262.12800000000004
plane 100013 xpl=0.0 ypl=0.0 zpl=1.0 con=256.03200000000004
plane 100014 xpl=0.0 ypl=0.0 zpl=1.0 con=249.936
plane 100015 xpl=0.0 ypl=0.0 zpl=1.0 con=243.84
plane 100016 xpl=0.0 ypl=0.0 zpl=1.0 con=237.74400000000003
plane 100017 xpl=0.0 ypl=0.0 zpl=1.0 con=231.64800000000002
plane 100018 xpl=0.0 ypl=0.0 zpl=1.0 con=225.55200000000002
plane 100019 xpl=0.0 ypl=0.0 zpl=1.0 con=219.45600000000002
plane 100020 xpl=0.0 ypl=0.0 zpl=1.0 con=213.36
plane 100021 xpl=0.0 ypl=0.0 zpl=1.0 con=207.264
plane 100022 xpl=0.0 ypl=0.0 zpl=1.0 con=201.168
plane 100023 xpl=0.0 ypl=0.0 zpl=1.0 con=195.072
plane 100024 xpl=0.0 ypl=0.0 zpl=1.0 con=188.976
plane 100025 xpl=0.0 ypl=0.0 zpl=1.0 con=182.88
plane 100026 xpl=0.0 ypl=0.0 zpl=1.0 con=176.78400000000002
plane 100027 xpl=0.0 ypl=0.0 zpl=1.0 con=170.68800000000002
plane 100028 xpl=0.0 ypl=0.0 zpl=1.0 con=164.592
plane 100029 xpl=0.0 ypl=0.0 zpl=1.0 con=158.496
plane 100030 xpl=0.0 ypl=0.0 zpl=1.0 con=152.4
plane 100031 xpl=0.0 ypl=0.0 zpl=1.0 con=146.304
plane 100032 xpl=0.0 ypl=0.0 zpl=1.0 con=140.208
plane 100033 xpl=0.0 ypl=0.0 zpl=1.0 con=134.11200000000002
plane 100034 xpl=0.0 ypl=0.0 zpl=1.0 con=128.01600000000002
plane 100035 xpl=0.0 ypl=0.0 zpl=1.0 con=121.92000000000002
plane 100036 xpl=0.0 ypl=0.0 zpl=1.0 con=115.82400000000001
plane 100037 xpl=0.0 ypl=0.0 zpl=1.0 con=109.72800000000001
plane 100038 xpl=0.0 ypl=0.0 zpl=1.0 con=103.632
plane 100039 xpl=0.0 ypl=0.0 zpl=1.0 con=97.536
plane 100040 xpl=0.0 ypl=0.0 zpl=1.0 con=91.44
plane 100041 xpl=0.0 ypl=0.0 zpl=1.0 con=85.344
plane 100042 xpl=0.0 ypl=0.0 zpl=1.0 con=79.24800000000002
plane 100043 xpl=0.0 ypl=0.0 zpl=1.0 con=73.15200000000002

```

```

plane 100044 xpl=0.0 ypl=0.0 zpl=1.0 con=67.05600000000001
plane 100045 xpl=0.0 ypl=0.0 zpl=1.0 con=60.96000000000001
plane 100046 xpl=0.0 ypl=0.0 zpl=1.0 con=54.864000000000004
plane 100047 xpl=0.0 ypl=0.0 zpl=1.0 con=48.768000000000003
plane 100048 xpl=0.0 ypl=0.0 zpl=1.0 con=42.672000000000025
plane 100049 xpl=0.0 ypl=0.0 zpl=1.0 con=36.576000000000002
plane 100050 xpl=0.0 ypl=0.0 zpl=1.0 con=30.480000000000018
plane 100051 xpl=0.0 ypl=0.0 zpl=1.0 con=24.384000000000015
plane 100052 xpl=0.0 ypl=0.0 zpl=1.0 con=18.288000000000001
plane 100053 xpl=0.0 ypl=0.0 zpl=1.0 con=12.192000000000007
plane 100054 xpl=0.0 ypl=0.0 zpl=1.0 con=6.096000000000004
plane 100055 xpl=0.0 ypl=0.0 zpl=1.0 con=-0.0

```

'NOW TIME FOR MEDIA CARDS

```

media 200001 1 12 17 +100001 -100002 +100003 -100004 +100005 -100006
media 200002 1 12 17 +100001 -100002 +100003 -100004 +100006 -100007
media 200003 1 12 17 +100001 -100002 +100003 -100004 +100007 -100008
media 200004 1 12 17 +100001 -100002 +100003 -100004 +100008 -100009
media 200005 1 12 17 +100001 -100002 +100003 -100004 +100009 -100010
media 200006 1 12 17 +100001 -100002 +100003 -100004 +100010 -100011
media 200007 1 12 17 +100001 -100002 +100003 -100004 +100011 -100012
media 200008 1 12 17 +100001 -100002 +100003 -100004 +100012 -100013
media 200009 1 12 17 +100001 -100002 +100003 -100004 +100013 -100014
media 200010 1 12 17 +100001 -100002 +100003 -100004 +100014 -100015
media 200011 1 12 17 +100001 -100002 +100003 -100004 +100015 -100016
media 200012 1 12 17 +100001 -100002 +100003 -100004 +100016 -100017
media 200013 1 12 17 +100001 -100002 +100003 -100004 +100017 -100018
media 200014 1 12 17 +100001 -100002 +100003 -100004 +100018 -100019
media 200015 1 12 17 +100001 -100002 +100003 -100004 +100019 -100020
media 200016 1 12 17 +100001 -100002 +100003 -100004 +100020 -100021
media 200017 1 12 17 +100001 -100002 +100003 -100004 +100021 -100022
media 200018 1 12 17 +100001 -100002 +100003 -100004 +100022 -100023
media 200019 1 12 17 +100001 -100002 +100003 -100004 +100023 -100024
media 200020 1 12 17 +100001 -100002 +100003 -100004 +100024 -100025
media 200021 1 12 17 +100001 -100002 +100003 -100004 +100025 -100026
media 200022 1 12 17 +100001 -100002 +100003 -100004 +100026 -100027
media 200023 1 12 17 +100001 -100002 +100003 -100004 +100027 -100028
media 200024 1 12 17 +100001 -100002 +100003 -100004 +100028 -100029
media 200025 1 12 17 +100001 -100002 +100003 -100004 +100029 -100030
media 200026 1 12 17 +100001 -100002 +100003 -100004 +100030 -100031
media 200027 1 12 17 +100001 -100002 +100003 -100004 +100031 -100032
media 200028 1 12 17 +100001 -100002 +100003 -100004 +100032 -100033
media 200029 1 12 17 +100001 -100002 +100003 -100004 +100033 -100034
media 200030 1 12 17 +100001 -100002 +100003 -100004 +100034 -100035
media 200031 1 12 17 +100001 -100002 +100003 -100004 +100035 -100036
media 200032 1 12 17 +100001 -100002 +100003 -100004 +100036 -100037
media 200033 1 12 17 +100001 -100002 +100003 -100004 +100037 -100038
media 200034 1 12 17 +100001 -100002 +100003 -100004 +100038 -100039
media 200035 1 12 17 +100001 -100002 +100003 -100004 +100039 -100040
media 200036 1 12 17 +100001 -100002 +100003 -100004 +100040 -100041
media 200037 1 12 17 +100001 -100002 +100003 -100004 +100041 -100042
media 200038 1 12 17 +100001 -100002 +100003 -100004 +100042 -100043
media 200039 1 12 17 +100001 -100002 +100003 -100004 +100043 -100044
media 200040 1 12 17 +100001 -100002 +100003 -100004 +100044 -100045
media 200041 1 12 17 +100001 -100002 +100003 -100004 +100045 -100046
media 200042 1 12 17 +100001 -100002 +100003 -100004 +100046 -100047
media 200043 1 12 17 +100001 -100002 +100003 -100004 +100047 -100048
media 200044 1 12 17 +100001 -100002 +100003 -100004 +100048 -100049
media 200045 1 12 17 +100001 -100002 +100003 -100004 +100049 -100050
media 200046 1 12 17 +100001 -100002 +100003 -100004 +100050 -100051
media 200047 1 12 17 +100001 -100002 +100003 -100004 +100051 -100052
media 200048 1 12 17 +100001 -100002 +100003 -100004 +100052 -100053
media 200049 1 12 17 +100001 -100002 +100003 -100004 +100053 -100054
media 200050 1 12 17 +100001 -100002 +100003 -100004 +100054 -100055

```

```

' =====
' END OF SCALESlice GENERATED SECTION
' =====

```

'Air Layer'/Connex Box'  
cuboid 16 -381 381 -137.16 137.16 0 304.8

```
media 1 1 16 17
'Outer Region'
cuboid 17 -381 381 -137.16 137.16 -304.8 304.8
boundary 17

end geometry
end data
end

=mt2ascii
"file path" ! the mesh tally
"file path" ! output file name
end
```

Listing B.4: CSAS simulation script  
(MAVRIC-2.inp)

## APPENDIX C PYTHON CODE

Python code used to pull the neutron flux data out of the rt.txt files and generate the ORIGEN.inp file.

```
#Imports
import glob
import re
n = 1

#####Inputs#####
name="file name" #To change file in ORIGEN Directory
file_path = f"INSERT path for rt.txt file"
output_folder = f"INSERT output file path"
output_file = f"{output_folder}\\{name}.inp"
slice_volume = 1274258.097 #cm^3 of each slice
# The ORIGEN Format must be changed manually
#####

#Sort files numerically based on number in file name
file_list = glob.glob(file_path) # compile all files
file_list.sort(key=lambda x: [int(num) for num in re.findall(r'\d+', x)])

#Loop through all files
with open(output_file, "w") as file:
    for file_name in file_list:

        #Pull Data
        with open(file_name, "r") as file:
            data_section = False
            data_section2 = False
            data_section3 = False
            extracted_values = []
            dash_count = 0

            # Pull fluxes
            for line in file:
                if " uncertainty" in line: # finds the first iteration of uncertainty in a line and
                    goes to the next one
                    data_section = True
                    print(f"Processing data from {file_name}") # Debugging output
                    continue
                if data_section and line.strip(): # Process valid lines
                    parts = line.split() # Split based on whitespace
                    if "-----" in line: # Stop when the dashed line appears
                        dash_count+=1
                        if dash_count == 1:
                            continue
                        if dash_count == 2:
                            break # Stop when unrelated data appear
                    if len(parts) >= 7: # Ensure sufficient columns
                        extracted_values.append(parts[5]) # 6th column e in referenced line

            #Getting Total Track Length
            for line in file:
                if " Total Neutron Track-lengths - over all energy groups and time bins" in line:
                    data_section2 = True
                    continue
                if data_section2 and line.strip(): # Process valid line (not white space)
                    if "track-length estimator" in line:
                        continue
                    if "value" in line:
                        continue
```

```

        if "----" in line:
            continue
        parts = line.split() # Split based on whitespace
        if len(parts) >= 6: # Ensure sufficient columns exist
            total_track_length = float(parts[0]) # First value of the line
            # print(total_flux) to check for correct value
            break

#Generate new Origen Data
flux = '\n'.join(extracted_values)
origen_content = (
f'''=origen
bounds {{
neutron="scale.rev13.xn200g47v7.1"
gamma=[ 999I 2.0e7 1.0e4 ]
}}
build_lib("activation_source{n}.f33") {{
    neutron(1) {{
        type=ENDF_ENERGY_DEPENDENT
        reaction_resource="INSERT_path\origen.rev03.jeff200g"
        fp_yield_resource="INSERT_path\origen.rev05.yields.data"
        spectrum {{
            type=MULTIGROUP
            flux={{flux}}
        }}
    }}
}}
case(irradiation) {{
title="Soil activation"
lib {{
    file="activation_source{n}.f33"
}}
mat {{
    % elements in soil
    units=atoms-per-barn-cm
    iso=[O16=2.931950e-02, O17=1.114649e-05, O18=6.026437e-05, Na23=2.444715e-04, Mg24=3.957787e-04,
Mg25=5.010491e-05, Mg26=5.516551e-05, Al27=2.326076e-03,
    Si28=8.150971e-03, Si29=4.140756e-04, Si30=2.732811e-04, K39=3.128084e-04, K40=3.924422e-08,
K41=2.257459e-05, Ca40=1.132863e-03, Ca42=7.560904e-06,
    Ca43=1.577628e-06, Ca44=2.437722e-05, Ca46=4.674011e-08, Ca48=2.185305e-06, Ti46=7.263565e-
06, Ti47=6.550416e-06, Ti48=6.490546e-05, Ti49=4.763137e-06
    Ti50=4.560639e-06, Mn55=1.191317e-05, Fe54=5.392452e-05, Fe56=8.464997e-04, Fe57=1.954936e-
05, Fe58=2.601658e-06]
    volume={slice_volume} %cm^3 of each soil slice
}}

time {{
    units="days"
    t=[1 2 5 10 20 30 40 80 120 160 180 365 366 370 380 395 415 440 455 500 545 600 700 730 2190]
}}
flux = [12r {total_track_length/slice_volume} 0 0 0 0 0 0 0 0 0 0 0 0]
neutron = yes
gamma{{
    sublib=ALL          % LT, FP, or AC single sublib
                       % ALL = all sub-libraries
    continuum=yes      % expand continuum data stored as
                       % lines into proper continuua
    immediate=yes      % load lines for immediate gamma/x-rays
    spont=yes          % include photons from spont fiss
    brem_medium=UO2    % include bremsstrahlung from betas
}}
    save{{ file="DSO{n}.f71" steps=all }}
}} % Bracket for case
end

=opus
title="Necutron Spectrum"
data="DSO{n}.f71"
typarams=nspectrum
units=particles
end

```

```
=opus
title="Activation/Decay Source"
data="DSO{n}.f71"
typarams=nuclides
units=grams
time=days
end

'''

    with open(output_file, "a") as file: # appends each iteration to same origen file
        file.write(origen_content)

    n +=1 # Adds value for each iteration for naming convention purposes
```

Listing C.1: Neutron flux data parser  
(Flux-pull.py)

## REFERENCES

- [1] Z. U. Koreshi, “Chapter 3 - nuclear reactors and systems,” in *Nuclear Engineering Mathematical Modeling and Simulation*, Z. U. Koreshi, Ed., Academic Press, 2022, pp. 103–147, ISBN: 978-0-323-90618-0.
- [2] M. Ho, E. Obbard, P. A. Burr, and G. Yeoh, “A review on the development of nuclear power reactors,” *Energy Procedia*, vol. 160, pp. 459–466, 2019, 2nd International Conference on Energy and Power, ICEP2018, 13–15 December 2018, Sydney, Australia.
- [3] T. M. Persons, “Nuclear microreactors,” U.S. Government Accountability Office, Tech. Rep., 2020, <https://www.gao.gov/products/gao-20-380sp>.
- [4] *Westinghouse eVinci™ Heat Pipe Micro Reactor Technology Development*, vol. Volume 1: Operating Plant Challenges, Successes, and Lessons Learned; Nuclear Plant Engineering; Advanced Reactors and Fusion; Small Modular and Micro-Reactors Technologies and Applications, International Conference on Nuclear Engineering, Aug. 2021, V001T04A018. eprint: <https://asmedigitalcollection.asme.org/ICONE/proceedings-pdf/ICONE28/85246/V001T04A018/6774921/v001t04a018-icone28-67519.pdf>.
- [5] K. Stevens *et al.*, “Opportunities, challenges, and research needs for remote microreactor operations,” *Nuclear Technology*, vol. 210, no. 12, pp. 2257–2273, 2024. eprint: <https://doi.org/10.1080/00295450.2024.2344903>.
- [6] V. Iglesias *et al.*, “Risky development: Increasing exposure to natural hazards in the united states,” *Earth’s Future*, vol. 9, no. 7, e2020EF001795, 2021, e2020EF001795 2020EF001795. eprint: <https://agupubs.onlinelibrary.wiley.com/doi/pdf/10.1029/2020EF001795>.
- [7] *Electricity for hospitals, clinics, and medical facilities*, Electricity Plans, <https://electricityplans.com/landing/electricity-for-hospitals-clinics-medical-offices/>, Accessed-09/15/2025.
- [8] “Micro-reactor regulatory issues,” Nuclear Energy Institute, Tech. Rep., 2019, <https://www.nei.org/resources/reports-briefs/micro-reactor-regulatory-issues>.
- [9] B. Donalds, *National strategy to utilize microreactors for natural disaster response efforts act*, H.R. 8611, 117th Congress (2021-2022), <https://www.congress.gov/bill/117th-congress/house-bill/8611>, 2021.
- [10] U.S. Nuclear Regulatory Commission, *Radiation basics*, <https://www.nrc.gov/about-nrc/radiation/health-effects/radiation-basics.html>, Accessed 08/08/2025, 2020.

- [11] *Subpart d—radiation dose limits for individual members of the public*, <https://www.nrc.gov/reading-rm/doc-collections/cfr/part020/part020-1301.html>, Accessed 09/15/2025.
- [12] *Doses in our daily lives*, <https://www.nrc.gov/about-nrc/radiation/around-us/doses-daily-lives>, Accessed 09/20/2025.
- [13] Z. U. Koreshi, “Chapter 1 - the atom and nuclear radiation,” in *Nuclear Engineering Mathematical Modeling and Simulation*, Z. U. Koreshi, Ed., Academic Press, 2022, pp. 1–49, ISBN: 978-0-323-90618-0.
- [14] Hill and McCreary, *11.6: Penetrating power of radiation*, Sep. 2022.
- [15] A. M. Onaizi *et al.*, “Radiation-shielding concrete: A review of materials, performance, and the impact of radiation on concrete properties,” *Journal of Building Engineering*, vol. 97, p. 110 800, 2024.
- [16] J. K. Shultis and R. E. Faw, “Radiation shielding,” in *Nuclear Energy: A Volume in the Encyclopedia of Sustainability Science and Technology Series, Second Edition*, N. Tsoulfanidis, Ed. New York, NY: Springer New York, 2018, pp. 369–393, ISBN: 978-1-4939-6618-9.
- [17] A. S. Ouda, “Development of high-performance heavy density concrete using different aggregates for gamma-ray shielding,” *Progress in Nuclear Energy*, vol. 79, pp. 48–55, 2015.
- [18] R. H. Stewart, S. E. Bays, A. X. Zabriskie, J. N. Zelina, A. M.-E.-A. Ougouag, and R. C. O’Brien, “Preliminary analysis of a nuclear grade sandwich composite for transportable micro-reactor shielding,” Idaho National Laboratory (INL), Idaho Falls, ID (United States), 2024.
- [19] R. H. Stewart *et al.*, “Mass optimization of a multilayered shield for transportable microreactors,” *Nuclear Science and Engineering*, vol. 0, no. 0, pp. 1–14, 2024. eprint: <https://doi.org/10.1080/00295639.2024.2403899>.
- [20] M. Giménez and E. Lopasso, “Tungsten carbide compact primary shielding for small medium reactor,” *Annals of Nuclear Energy*, vol. 116, pp. 210–223, 2018.
- [21] A. E. Craft and J. C. King, “Radiation shielding options for a nuclear reactor power system landed on the lunar surface,” *Nuclear Technology*, vol. 172, no. 3, pp. 255–272, 2010. eprint: <https://doi.org/10.13182/NT10-A10934>.
- [22] S. Nambiar and J. T. W. Yeow, “Polymer-composite materials for radiation protection,” *ACS Applied Materials & Interfaces*, vol. 4, no. 11, pp. 5717–5726, 2012, PMID: 23009182. eprint: <https://doi.org/10.1021/am300783d>.

- [23] N. Cherkashina, V. Pavlenko, P. Rudnev, I. Cheshigin, D. Romanyuk, and A. Ruchiy, "Study of radiation-protective characteristics of polyethylene composites with b4c and bi2o3 to neutron and gamma radiation," *Nuclear Engineering and Design*, vol. 432, p. 113 732, 2025.
- [24] Z. Huo, Y. Lu, H. Zhang, and G. Zhong, "Sm2o3 micron plates/b4c/hdpe composites containing high specific surface area fillers for neutron and gamma-ray complex radiation shielding," *Composites Science and Technology*, vol. 251, p. 110 567, 2024.
- [25] H. Rene Vega Carrillo, E. Gallego, A. Lorente, E. Manzanares-Acuna, and V. Hernandez-Davila, "Neutron shielding performance of water-extended polyester," in *TA-3 Dosimetry and Instrumentation Poster Session 2*, 2006.
- [26] R. S. Detwiler, R. J. McConn, T. F. Grimes, S. A. Upton, and E. J. Engel, "Compendium of material composition data for radiation transport modeling," Pacific Northwest National Laboratory (PNNL), Richland, WA (United States), Tech. Rep., Apr. 2021.
- [27] W. A. Wieselquist and R. A. Lefebvre, "Scale 6.3.2 user manual," Oak Ridge National Laboratory (ORNL), Oak Ridge, TN (United States), Tech. Rep., Jan. 2024.
- [28] L. J. Fernandez de Losada, J. Buongiorno, and A. Manera, "Assessment of the life-cycle cost of nuclear-grade coolants for advanced reactors," *Progress in Nuclear Energy*, vol. 190, p. 105 888, 2026.
- [29] Y. E. P. Products, *Comprehensive guide to borated polyethylene price: Factors and cost insights*, <https://www.ysplastics.com/borated-polyethylene-price-guide/>.
- [30] ConcreteNetwork, *Concrete price considerations - cost of concrete*, <https://www.concretenetwork.com/concrete-prices.html>, Accessed 09/14/2025.
- [31] 3.-D. A. Inc, *Wep resin*, <https://threedart.com/product/wep/>, Accessed 09/14/205.
- [32] Mike, *Hdpe price index*, <https://businessanalytiq.com/procurementanalytics/index/hdpe-price-index/>, Accessed 10/15/2025.
- [33] J. Metal, *Aluminium 7075 sheet price list*, <https://www.jagdishmetalindia.com/aluminium-7075-sheet-bar-price-list.html>, Accessed 09/14/2025.
- [34] Ensigner Precision Components, *HDPE (High Density Polyethylene) High Performance Injection Molding & Plastic Manufacturing Ensigner Precision Components*, <https://www.ensinger-pc.com/injection-molding-materials/our-plastic-stock-shapes/hdpe-high-density-polyethylene/>, Accessed 09/10/2025.

- [35] Big D Ready Mix Concrete, *What is the standard strength of concrete?* <https://www.bigd-readymix.com/what-is-the-standard-strength-of-concrete/>, Accessed 09/10/2025.
- [36] Ferguson Perforating, *7075 Aluminium Alloy*, <https://www.fergusonperf.com/the-perforating-process/material-information/specialized-aluminum/7075-aluminium-alloy/>, Accessed 09/10/2025.
- [37] H. Xu *et al.*, “Ground radioactivity distribution reconstruction and dose rate estimation based on spectrum deconvolution,” *Sensors*, vol. 23, no. 12, 2023.
- [38] C.-K. C. Wang, *Atoms, Nuclei & Interactions of Ionizing Radiation With Matter*. Cognella Academic Publishing, 2018.
- [39] International Atomic Energy Agency (IAEA). “LiveChart of Nuclides.” (2025), (visited on 10/14/2025).
- [40] M. A. Wibowo, “Human health fact sheet radioactive properties of key europium isotopes,” Argonne National Laboratory, Tech. Rep., 2001.
- [41] H. E. A. Amer, H. AbdElgawad, M. M. Y. Madany, A. M. A. Khalil, and A. M. Saleh, “Soil contamination with europium induces reduced oxidative damage in hordeum vulgare grown in a CO<sub>2</sub>-enriched environment,” *Plants*, vol. 12, no. 17, 2023.
- [42] O. Pourret and M.-P. Faucon, “Cobalt,” in *Encyclopedia of Geochemistry*, 2018.
- [43] Agency for Toxic Substances and Disease Registry (US), *Toxicological Profile for Cobalt*. Atlanta (GA): U.S. Department of Health and Human Services, Oct. 2024.
- [44] National Nuclear Data Center, <https://www.nndc.bnl.gov/nudat/>, Information extracted from the NuDat database on 09/25/2025.
- [45] “Limits study: Volume 1 technical reports summary - chapter 1: Current truck size and weight regulations in the United States & other countries (2017),” *CTSW Limits Study: Volume 1 Technical Reports Summary - Chapter 1: Current Truck Size and Weight Regulations in the United States Other Countries*,